MODELING ANAEROBIC DIGESTION OF MICROALGAE

ANAEROBIC DIGESTION OF MICROALGAE: MODELING AND IDENTIFICATION FOR OPTIMIZATION AND CONTROL

by

Elliot T. Cameron, B.A.Sc. (Chem. Eng.)

A Thesis
Submitted to the School of Graduate Studies
in Partial Fulfillment of the Requirements
for the Degree
Master of Applied Science

McMaster University

MASTER OF ENGINEERING (2010) McMaster University

(Chemical Engineering) Hamilton, Ontario, Canada

TITLE:	Anaerobic Digestion of Microalgae
	Modeling and Identification for Optimization and Control
AUTHOR:	Elliot Cameron, B.A.Sc. (Chem. Eng.)
	(University of Ottawa, Canada)
SUPERVISOR:	Dr. Benoît Chachuat
NUMBER OF PAGES:	xv, 187

ABSTRACT

Owing to the rise in fossil fuel prices, overall energy security concerns, and the current push towards green engineering; renewable and green fuels have seen an increase in interest in recent years. Two notable technologies in this green movement are the production of biodiesel from microalgae and the production of biogas from anaerobic digestion of waste biomass. Production of biodiesel from microalgae was studied extensively in the 80s through the early 90s and found to be economically infeasible given the technology of the time. However, recent literature has suggested that one possible method to improve the feasability of the process would be to combine it with an anaerobic digestor to provide nutrient and biomass recycling. For such a system, having accurate models of each process would be highly advantageous for optimal design and control. To this end this thesis moves towards this overall goal by examining and modelling the anaerobic digestion of the microalgae *Chlorella vulgaris*.

Starting with a set of experimental data (anaerobic digestion of *Chlorella vulgaris*) provided by LBE-INRA, the minimum number of kinetic equations needed to predict the data are found using principal component style analysis. This number is found to be two to three reactions. Using this as a basis for model development, a mass balance model is developed around both two and three reaction cases. To date there is very little literature on the modelling of anaerobic digestion of microalgae and so kinetic laws are selected from the general anaerobic digestion models "Anaerobic Digestor Model 1" (ADM1) and "Acidogenesis/Methanogenisis Model" (AM2). Given that the kinetic laws were derived from general literature, model fitting is a must. To faciliate this process a novel systematic parameter identification procedure to locate identifiable parameter subsets within each model is presented. Applying this novel procedure to the provided data is seen to lead to promising

identification results. Through these identification trials it is shown that the three reaction model best captures the dynamics of the system. This three reaction model serves as the basis for subsequent steady state optimality and sensitivity analysis. From these efforts it is shown that the predicted optimal curves match literature data very well but uncertainty in certain key parameter estimates lead to highly sensitive model predictions (and therefore low confidence). This leads to the conclusion that the developed model is capable of predicting the kinetics of *Chlorella* digestion but additional trials are needed to further refine the model fitting results.

ACKNOWLEDGEMENTS

Elliot Cameron[*] is grateful for the help and contributions of Dr. Benoît Chachuat[**] (supervisor); Dr. Monique Ras[***], Dr. Jean-Philippe Steyer[***], and Dr. Laurent Lardon[***] of LBE-INRA (for supplying experimental data and theoretical support); Dr. Francis Mairet[****], and Dr. Olivier Bernard[****] of COMORE-INRIA (for supplying theoretical support); graduate scholarships from the Natural Sciences and Engineering Research Council (NSERC) and the Ontario Graduate Scholarship Program (OGS); and general support from the McMaster Advanced Control Consortium (MACC).

[*] Department of Chemical Engineering, McMaster University; Hamilton, Ontario, Canada
(Email: cameroet@mcmaster.ca)

[**] Department of Chemical Engineering, Imperial College London; London, United Kingdom
(Email: b.chachuat@imperial.ac.uk)

[***] Laboratoire de Biotechnologie de l'Environnement, Institut National de la Recherche Agronomique; Narbonne, France
(Email:{rasm,lardonl,jean-philippe.steyer}@supagro.inra.fr)

[****] Contrôle et Modélisation de Ressources Renouvelables, Institut National de Recherche en Informatique et en Automatique; Sophia-Antipolis, France
(Email:{francis.mairet,olivier.bernard}@inria.fr)

Table of Contents

List of Figures

List of Tables

Chapter 1

Introduction

This chapter provides the necessary background to understand the context with which this thesis was conducted as well as any background information necessary to understand the theory that follows. First, the motivation and scope of this thesis is discussed to provide the reader with an understanding of the context of this research as well the goals and hypothesized benefits. Following this a brief introduction to aquaculture and anaerobic digesters is provided. While the main focus of this thesis is on the development of process identification techniques, the applications of this theory are based in bioreactor design and so it is important that the history of this field be introduced. Directly following this is an introduction to how modelling currently factors in to bioreactor design and so begins to more firmly link the application side to the theoretical side of this thesis. Finally, this chapter concludes with concise statement of this thesis' objectives to provide the reader with a useful summary of the contents to be found in this report.

1.1 Motivation and Scope

Since the early 1980s, several studies have shown that certain strains of microalgae can build up high concentrations of lipids (in the range 30-86 %DW), from which oil can be extracted, processed and refined into biofuel [17; 18; 32]. Optimistic theoretical yields have placed potential algal biomass production at 470-510 tons/ha/year yet current technology places large scale achievable yields well below this value (40-190 tons/ha/year) [13; 17; 18; 32; 51]. Even under these lower yields, optimal predictions by [17; 18] and [32] estimate that it would take only 1 % of the United States' arable land to produce sufficient biodiesel to meet 50 % of the current U.S. annual transport fuel need of 0.53×10^9 m^3 and 23 % of global arable land to completely offset global fossil fuel demands respectively. Naturally, these optimal predictions take some liberties with oil yields, etc. but they are still an order of magnitude more efficient than terrestrial biomass production predictions (showing the obvious potential of the technology). Yet microalgal derived biodiesel currently has almost no large scale presence in the energy market. The reason for this is primarily economic (which can be attributed to current design, environmental, etc. factors). Despite the obvious potential of this technology, money talks and algal derived biodiesel is still prohibitively expensive when compared to fossil fuel sources ([17] estimated a 2006 cost of production of $2.80/L for microalgae derived biodiesel and $0.70/L for crude derived diesel). Obviously there is still a great deal of distance that needs to be covered, but it is not impossible.

It is primarily because of this economic gap, as well as the great potential of the technology as a whole, that microalgae are currently an area of great scientific research for biofuel production (although not a large component of industry and the energy sector). Once improvements in technology can crack the economic issues, the renewable energy potential

can be accessed. Microalgae already have a considerable advantage over terrestrial biofuel sources (e.g. corn ethanol) in that they do not require arable land (reactors can be constructed on waste lands) nor does it compete directly with agriculture (although the need for fertilizer supplements would arguably compete indirectly). However, it is because of the constant cost of nutrient supply and waste removal, along with the low overall oil yields (due to the difficulty of maintaining high biomass yields and oil content), that this technology still remains uncompetative with fossil fuels [17; 18; 51]. [51] argues that one of the key methods for making this technology feasible would be the use of anaerobic digestion to facilitate the reuse of waste biomass and the recycling of nutrients (this would reduce feed costs and provide the added bonus of abating nitrogen and phosphorus derived pollution that would arise from disposing of the waste algal biomass). The current consensus on the best way to achieve this is to couple algal photobioreactors and anaerobic digesters so that effluent organic nutrients can be broken down to their inorganic forms and recycled while organic carbon is converted to methane and collected (this would act as an additional energy source). A general flow diagram for this process is presented in Fig. 1.1.

In this process configuration, CO_2 gas is fed continuously into the algal reactor, which has been precharged with inorganic nitrogen, phosphorus, and all other required nutrients. This CO_2 gas is consumed by microalgae via photosynthesis and converted to biomass (a certain percentage of which being lipid biodiesel precursor). It has already been shown that several strains of microalgae can be forced into storing excess lipids through applying environmental stresses, such as nitrogen limitation or excess iron for examples [17; 18; 32; 33; 51]. The biomass is continuously harvested from the algal reactor and its lipid content is separated and cleaned before being sent to a separate tranesterification site. The remaining dead biomass is then passed to the anaerobic digester, where the organic constituents are

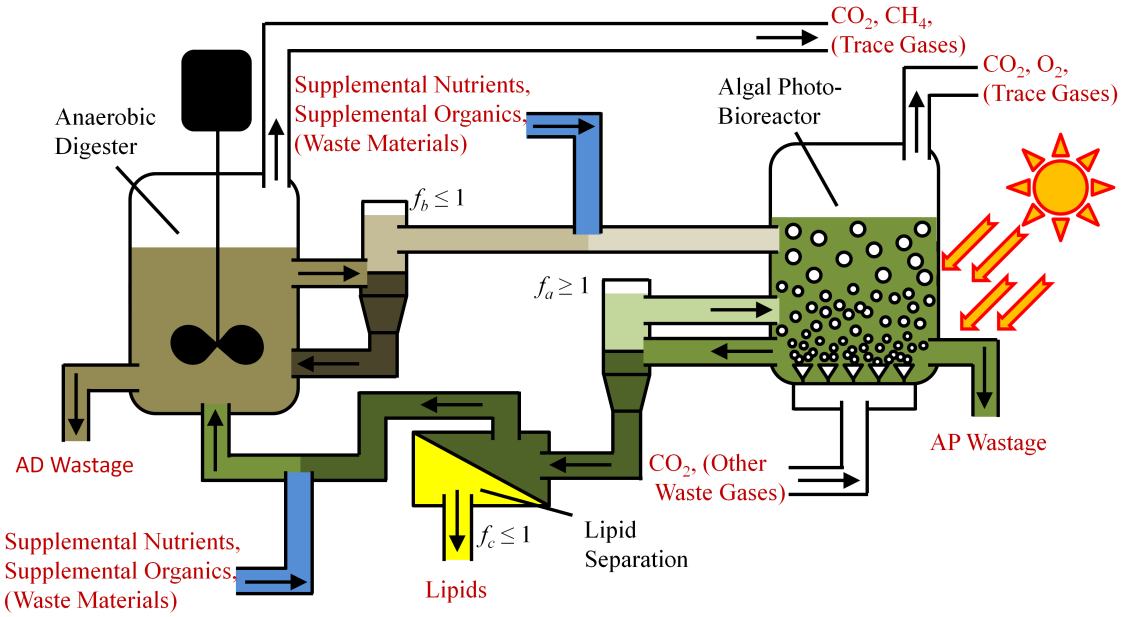

Figure 1.1: Conceptual Process Flow Diagram of Combined Algal Photobioreactor and Anaerobic Digester

converted to their inorganic forms and biogas is produced in the form of methane (as well as CO_2). The methane is harvested and purified, whereas the other nutrients are recycled back into the algal reactor to act as feed. Potentially, the CO_2 produced by the anaerobic digestion could be recycled back to the microalgal photobioreactor (a strategy investigated by [20]).

1.2 Brief History of Aquaculture and Anaerobic Digestion

The mass culturing of microalgae appears to have first come into the scientific spotlight during and immediately following World War II [6; 5; 32]. German scientists investigated the potential of microalgae as a protein source to alleviate a predicted gap in supplies [5].

High production costs as well as issues surrounding "social acceptance" of the food additive eventually tabled this particular application (although some microalgae species are available today as specialty foods). Research into other applications such as pharmaceuticals, specialty chemicals, and fuels continued. It was not until the seventies that the focus of mass culturing of microalgae shifted to renewable energy due to uncertainty over the long-term availability of petroleum [5]. This was especially true in the United States and Japan with large amounts of funding being allocated well into the early nineties [32]. At that point it was decided that economic mass production of microalgae for fuel purposes was infeasible given the technology of the time [32] and research tapered off. However, recent spikes in the price of oil along with a growing trend of "green engineering" has brought focus back to microalgae as a renewable energy source.

Large scale culturing of microalgae traditionally takes one of two forms depending on the end application (Fig. 1.2) [17]:

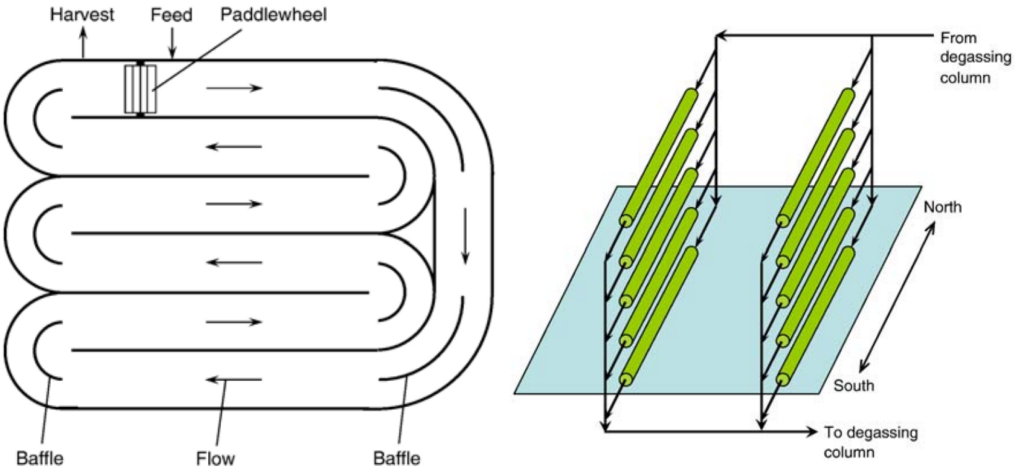

(a) Open Raceway Style Ponds [17] (b) Closed Tubular Photobioreactors [17]

Figure 1.2: General Large Scale Aquaculture Reactors

Raceway ponds are usually the cheaper of the two designs in terms of both initial instal-

lation and subsequent operation costs. However, since they normally rely on natural light for photosynthetic growth and some form of paddlewheel (or potentially an educter) to provide gas transfer and mixing (atmospheric CO_2 in and produced O_2 out) they normally suffer from a greater number of operational problems. Since they are using natural light as an energy source production is naturally subject to diurnal, seasonal, and random weather fluctuations in light level (as well as temperature). This can make operation quite unpredictable (although to be fair, any process for the production of biodiesel will need to use natural light, as any artificially lit process will be thermodynamically incapable of generating more energy/profit then what is put in). In addition, the open nature of most large scale ponds means that large water losses due to evaporation as well as poor CO_2 uptake efficiency (due to losses over a greater surface area and/or poor entrance dynamics due to the mixing strategy). Supplemental CO_2 can be provided through submerged spargers, etc. at an increased operational cost. The final major drawback of the raceway design is that with large open reactors the chances of contamination are increased over other reactor types, making it difficult to attack issues of optimization using some form of genetic engineering [17].

Tubular reactors on the other hand provide a closed environment with optimal reactor depth and surface area. Due to the enclosed nature evaporative and CO_2 losses are greatly reduced. Maintenance of pure cultures is also much more realistic [17]. The obvious drawbacks are the increased costs of operation and installation as well as fluctuations in pH and O_2 along the reactor that can lead to inhibition. Interestingly enough, [17] found that even though tubular reactors have higher initial and operational costs, the increased efficiency in lipid production resulted in a lower overall biodiesel production cost than raceway ponds ($1.40/L raw oil compared to $1.81/L raw oil for a 10,000 ton biomass/year facility).

Like most higher plants, microalgae require sources of carbon, nitrogen, phosphorus, sulfur, potassium, magnesium, and other trace elements to survive [5]. These can be provided in a variety of forms depending on the end application of the biomass. For example, waste streams can be used as nutrient sources for non-food related products such as biofuels, while pure nutrient streams are required for pharmaceutical and specialty food applications. Really the only limiting factor is how much control over the end product composition is desired/required [5]. In the case of *Chlorella vulgaris* the key macronutrients are carbon, oxygen, and nitrogen (Phosphorus is required to a lesser extent). Assuming fully autotrophic growth the carbon and oxygen source is naturally CO_2. This may be supplied either from a waste stream, synthetic feed stream, or from the atmosphere (although ambient CO_2 are normally insufficient to promote optimal growth). Nitrogen is commonly supplied in the form of nitrate or ammonium salt fertilizers (ammonium based salts being preferred since they are more readily utilized) [6], for instance $ClNH_4$.

The general composition of a microalgal cell depends both on the species of microalgae being cultivated as well as the nutrient medium being used. [6] provides a summary of the non-growth limited composition of several microalgal strains studied in the literature. This summary shows that protein, carbohydrate, and lipid concentrations can vary greatly, roughly between 30 - 70 %DW, 10 - 60 %DW, 2 - 20 %DW respectively to provide some context on strain specificity. It has also been well documented that several strains of microalgae can be forced to build up stores of carbohydrates and/or lipids through imposing nutrient stresses (nitrogen of iron for example) [5; 17; 18; 31; 32; 33; 37; 51]. This would naturally be advantageous for mass production of a desired component (lipids for biodiesel for example). While this is relevant to the larger idea of this project, of particular importance for this study is the non-growth limited composition of *Chlorella vulgaris*. This

value can be considered close to the composition of algal biomass after lipid extraction and so will be useful for analyzing feeds to the anaerobic digester in this thesis. According to the literature the average composition of non-growth limited *Chlorella vulgaris* is 60 %DW protein, 20 %DW carbohydrate, and 20 %DW lipids [6; 49]. We can further break these components into elemental values through the use of average constituent compositions [26; 28; 36; 39].

Table 1.1: Average Algal Substituent Compositions

Constituent	Composition	Molar Mass [g/mol]
Protein	$C_{4.43}H_7O_{1.44}N_{1.16}$	100.1
Carbohydrate	$C_6H_{12}O_6$	180.0
Lipid	$C_{40}H_{74}O_5$	634.0

Moving to the area of anaerobic digestion, when it comes to general heterotrophic microorganism growth there are three general growth regimes (Chemeotrophic processes are being omitted from this study) [41]:

Aerobic	(ex. Activated Sludge)	Obtains all organic carbon and nutrients from outside sources and uses oxygen to metabolize a portion of these organics to produce energy and facilitate growth
Anaerobic	(ex. Anaerobic Digestors)	Obtains all organic carbon and nutrients from outside sources and metabolizes a portion of these organics using an electron sink other then oxygen (ex. some intermediate organic compound) to produce energy and facilitate growth
Facultative		Any organism that prefers one form of growth but has some capability to grow in the other regime

Recall that one of the key issues surrounding microalgal growth is the removal of waste nutrients and biomass from the effluent stream. So why select anaerobic digestion? In the majority of Wastewater treatment facilities that operate using secondary or higher treatment levels, activated sludge is the go to process for organic and macronutrient removal. The reason for this is that it is robust, comparatively quick to start up, and a large number of process configurations exist that facilitate removal of Nitrogen and Phosphorus (two major pollution concerns as mentioned in the introduction), such as the Bardenpho and University of Cape Town designs [41]. This would certainly satisfy our organic and nutrient removal needs but activated sludge is a negative net profit process (i.e. it takes money to operate the required air pumps, etc. and no value added product is produced). In addition, while part of the algal biomass would be able to be converted into CO_2 (effectively removing it from the liquid resevoir), anaerobic digestion also offers the ability to degrade organics but provides the added benefit of breaking down organic macronutrients to their inorganic forms. Thus the anaerobic digester effluent can be fed back into the microalgal reactor to supplement the fertilizer input requirements. The break down of organics in an anaerobic digester also eventually leads to the production of methane, which adds a second profit generating energy source. While anaerobic digesters are much more finicky than activated sludge reactors, and start up is generally much slower, the added benefit of being able to supplement fertilizer input to the microalgal reactor as well as generate a secondary energy source (biomethane) is ideal for the desired end goal of making a combined biodiesel production system feasible.

The most common types of anaerobic digesters observed in industry and the literature are [38; 41]:

- Upflow Anaerobic Sludge Blanket (UASB) Digestor

- Expanded Granular Sludge Bed (EGSB) Digestor
- Continuous Stirred Tank Reactor (CSTR)
- Anaerobic Baffled Reactor (ABR)
- Two Stage High Rate (TSHR) Digestors

The UASB digestor would appear to be the most prominent design in use today. It uses the simple design principle of feeding waste in through the bottom of the reactor and allowing the clarified liquid to exit the top. Digestion within the reactor is facilitated by a blanket of sludge that is continuously settling under gravity (promoting mixing as well as retaining solids). UASB digestors are best applied to low to medium COD waste streams that contain a significant soluble component [38]. The fact that solids are retained allows for decoupling of solid and liquid retention times. This allows for high rates of digestion and liquid throughput due to the accumulated biomass.

The TSHR is a newer design receiving increasing interest in the literature [21]. Realizing that differing reactor conditions favour different populations, these types of designs split the anaerobic digestion process into its main base components, i.e. hydrolysis/acidogenesis/acetogenesis in reactor one and methanogenesis in reactor two. In doing so the conditions that favour each of these two broad stages can be manipulated to favour increased methane production and overall processing capacity.

Within any given reactor, however, the basic anaerobic process is fairly consistent. Anaerobic digestion starts with hydrolysis of biological polymers (proteins, long chain fatty acids, carbohydrates, DNA, cell membranes, etc.) through the use of local exogenous enzymes to soluble monomers (amino acids, lipids, simple sugars, etc.). These monomers are subse-

quently metabolized to various short chain organic acids (C_5 - C_2) along with CO_2, CH_4, and/or H_2. The short chain organic acids themselves are futher converted to acetic acid and eventually methane. Each of these steps is accomplished by colonies of specialized micro-organisms and the profile of the composition of a given feed will naturally dictate which organisms flourish and therefore which intermediates are observed [3; 27].

Combining these two processes (atleast in part) is also not new, although only experiments appear to have been conducted to date. The anaerobic digestion of algal biomass appears to have first been considered seriously by [30]. [30] observed *Chlorella sp.* and *Scenedesmus sp.* growing in waste stabilization ponds and wondered the potential energy available for harvest (the biomass also needed to be removed to prevent eutriphication). These first studies demonstrated the issues that would become hallmarks of microalgal digestion: difficult digestability [26; 30; 29] and low carbon to nitrogen ratios (leading to NH_3 inhibition) [30; 50]. The primary conclusion from Golueke's work was that the combined microalgal/digester resulted in low efficiency conversion of solar energy (2 %), although anaerobic digestion of algal biomass had an efficiency of 70 % on its own [29]. Since then there have been several studies showing both improved photobioreactor efficiency [32] and improved reactor combination concepts [27; 32; 45]. For example, studies have examined things such as the chemical and thermal pretreatment of algal biomass to improve biogas production [16], the combined production of H_2 from microalgae and CH_4 from decomposition of algal biomass [27], and multistage reactors to improved algal biomass yield and lipid content to name a few [32]. These studies show decent productivity results but the longevity of this technology will likely depend on proper modelling, to allow extensive system prediction, optimization, and control. This will allow a more thorough understanding of the underlying processes and therefore identify avenues for improvement perhaps not yet observed.

1.3 Modeling Paradigms in Bioprocesses

The modelling of bioprocesses is at best an approximatory field. What is meant by this is there is no theoretical basis for any of the reaction kinetics currently available in the literature and for the most part there is no universally accepted empirical model. Therefore models must be developed on a case by case basis to depict the relative phenomena under the expected reactor conditions. Naturally, a larger model attempting to encompass as many possible phenomena as possible should in theory result in the greatest predictive capability (i.e. increase robustness), but in practice this is usually not practical. As a phenomenoligical system, bioprocess models rely entirely on experimental data to both fit and validate a proposed kinetic mechanism. This problem is exacerbated by:

- Small number of observable quantities

  Common observable quantities:

  - Total Chemical Oxygen Demand
  - Soluble Chemical Oxygen Demand
  - Various Soluble Organics
  - Nitrogen
  - Ionic Species
  - pH
  - Gas Flow
  - Gas Composition

- Depending on the measurement technique, measurements can have a high degree of variability

What the above amounts to is a major difficulty in estimating large sets of parameters to a high degree of confidence [14]. Therefore the simplest feasible model is desirable to increase confidence in the fitted predictions. This reduction in model complexity is also desirable for carrying out mathematical analysis and implementing control strategies [52]. Of course, as with any experimental model, the predictive capability is generally only acceptable within the operating region studied and so model extrapolation can be quite dangerous. Therefore increased effort must be exerted during experimental design phases to generate sufficient information to both select/validate a model that is dynamically robust as well as confidently fit said model.

1.4 Thesis Objectives and Organization

While both algal photobioreactors and anaerobic digesters have been studied heavily in the literature, there remains little theoretical study on the combination of these two units as well as the specific anaerobic digestion of algal biomass. Theoretical in this project refers to the dynamic modelling of the process (as there have been a few empirical studies of these systems noted in the literature). Therefore the overarching goal of this project is to study such integrated systems in the hopes of generating the next generation of green fuel processes, the core idea being to use a model-based optimization methodology to gain knowledge leading to promising designs, operational strategies (i.e. control), and hopefully successful deployment. Central to this goal is the need for accurate models for each subsystem. As mentioned before, there remains little literature on the subject of modeling anaerobic digestion of algal biomass. As such, this thesis focuses on developing an accurate model for the anaerobic digestor subsystem. The focus will be on parsimony (gaining the

most information with the least amount of complexity to facilitate tractable optimization and control down the road).

Chapter 2, "Background", provides a comprehensive background on the modeling of anaerobic digestion, which is the core topic of this thesis, and is split into 2 sections. Section 2.1, "Gray-Box Modeling of Bioprocesses", provides a review of grey-box modelling and explains why most, if not all, traditional models use this approach. Section 2.2, "State-of-the-Art Modeling of Anaerobic Digestion", moves on to examine the two most up to date models on anaerobic digestion and describes them in detail. These two models are the Acidogenic-Methanogenic two reaction model (AM2) proposed by [12] and the Anaerobic Digester Model 1 (ADM1) generated by the International Water Association [3]. These models will serve as the basis for the model constructed in this thesis and so it is only natural to examine them in more detail.

Chapter 3, "Bioprocess Model Development and Identification", encompasses the bulk theoretical development of this thesis and is split into 3 sections. Section 3.1, "Determination of Reaction Complexity", provides a theoretical basis for determining the number of reactions required to explain a given experimental data set. This serves as a first step for developing a theoretical model to explain an observed phenomenon. Naturally, the model is only as good as the data and it is possible specifics of the "true" dynamics may be missed (this will be addressed in the "Future Work" section). Section 3.2, "Determination of Parameter Values", outlines the main theoretical contribution of this thesis. It contains the theoretical derivation of a local "progressive" identification algorithm (based on concepts originated by [48]) used to select "identifiable" subsets of parameters based on estimates of the Cramer-Rao lower bound. This section is further subdivided to delineate between the case of unconstrained and constrained parameter estimation problems (this will impact the

calculation of the solution covariance matrix used in the Cramer-Rao bound).

Chapter 4, "Application to Anaerobic Digestion of *Chlorella Vulgaris*", details the application of the theory in chapter 3 to a data set from the anaerobic digestion of the microalgae *Chlorella vulgaris*, and is split into 3 sections. Fortunately, a set of experimental data on the anaerobic digestion of *Chlorella vulgaris* was able to be acquired from the LBE-INRA. Section 4.1, "Description of Experimental Data", outlines all important details of LBE-INRA trial necessary to understand and use the data. Section 4.2, "Selection of Model Structure", contains the application of the theory in section 3.1 to the LBE-INRA data set to select a suitable model structure. Section 4.2 is split into 2 subsections, the first of which details the direct application of section 3.1 to determine the number of reactions required to describe the data set. The second subsection then details the selection of appropriate reaction schemes based on the results of the previous subsection and is based heavily on the theory discussed in the background section 2.2. The overall objective of this section is to develop a model that is capable of describing the *Chlorella vulgaris* data set and, if the data is dynamically robust enough, the digestion of *Chlorella vulgaris*/microalgae as a whole. Finally, section 4.3, "Systematic Parameter Identification", applies the algorithm developed in section 3.2 to fit the models developed in section 4.2.2 to the data. This furthers the goals of developing appropriate models for the digestion of microalgae.

Chapter 5, "Optima Studies", details the steady state optimization efforts conducted using the models developed in chapter 4 and is split into 2 sections. As detailed in the introduction, the long term objectives of this project is the combination of an algal photobioreactor to an anaerobic digestor to create a more symbiotic and efficient bioenergy production system. While the most revealing study would be of the the combined system, studying each system individually can provide insight into the maximum achievable yields of each reac-

tor (especially given that the feed was constructed to be representative of a microalgal feed after having had its oil content removed) as well as if any relevant literature data exists then comparing predictions can lead to further model validation. As such, section 5.1, "Steady State Optimization", explores the steady state predictions of the fitted models generated in chapter 4 and compares them to available steady state measurements on the digestion of *Chlorella/Scenedesmus* in the literature. Section 5.2, "Sensitivity Analysis", then assesses the sensitivity of these predictions (and therefore the model) to variations in the estimated parameters (this is done to account for the variability in the parameter predictions themselves).

Finally, Chapter 6, "Conclusions and Future Work", brings this thesis to a close and discusses the next logical steps for this research. Section 6.1, "Conclusion", acts as a bookend to this thesis, summarizing the main contributions and results. Section 6.2, "Future Work", is split into two subsections discussing the two major avenues to be pursued in the future. The first of these avenues addresses the problem in model sensitivity observed in chapter 5. It provides a theoretical method for determining best fit models based on the latest literature. The second subsection details the development of both an algal photobioreactor model and the resulting coupled system model and acts as a starting point for developing a model for such a system (naturally a similar procedure as chapter 3 and section 6.2.1 would need to be applied to determine a best fit reaction set, but the provided theory would act as a starting point).

Chapter 2

Background

This chapter delves into the current state of the art of bioprocess modelling. It starts with an introduction to the concept of bioprocess modelling as a whole, focusing on grey-box model and introducing the most common kinetic relations used in bioprocess modelling. From here two of the most state of the art models: Anaerobic Digester Model 1 (ADM1) and the Acidogenic-Methanogenic 2 Reaction Model (AM2) are discussed in detail (as these serve as the basis of our model to be identified).

2.1 Grey-Box Modeling of Bioprocesses

When one begins to talk about bioprocess modelling one is invariably talking about grey-box modelling (or in some cases black box modelling). The destinction here being that in classic white box models all information about the mechanics of the system is known a-priori. What this means in practice is that the model is formed from first principles. Black

box modelling is the logical opposite in that no system information is assumed a-priori and so the developed models are purely emperical. Naturally many models in engineering fall somewhere inbetween these two extremes and so are termed grey-box models. In the case of bioprocesses there is currently no such thing as a "fundamental reaction" for bioreactor systems in the literature. This is not to say that one does not exist, it just has not been discovered yet. Living systems are extremely complex, having many underlying metabolic and anabolic pathways, themselves composed of numerous fundamental reactions (not all known). Whats more, they are non-constant, with the major pathways both being modified by environmental and nutritional factors and perhaps becoming activated or deactivated only when specific coditions are met (i.e. discontinuities). But this not such a problem, as a fundamental model is not required, and would likely be too complex for practical engineering purposes. What is really needed is an approximation of the phenomena. Despite not knowing the true reaction kinetics for the underlying biological systems several recurring patterns of growth throughout the history of research have given rise to recurring empirical formulas. These formula are common enough that some semblance of understanding in the mechanics of the system can be placed in their derived parameters (as opposed to them being purely numerical).

Despite this reliance on emperical kinetics, the foundation of bioreactor modeling is almost always placed in fundamental mass balances on conserved quantities within the reactor. These quantities can either be fundamental, such as molar carbon and nitrogen, or aggregate quantities in the system, such as biomass chemical oxygen demand. A basic example of such a system model is provided in Eq. (2.1).

$$\frac{d(V_R(t)\mathbf{X}(t))}{dt} = F_{in}(t)\mathbf{X_{in}}(t) - F_{out}(t)\mathbf{X}(t) + V_R(t)\mathbf{r}(\mathbf{X},\mathbf{p},t) - V_R(t)\mathbf{q}(\mathbf{X},\mathbf{p},t) \tag{2.1}$$

where V_R is the current reactor volume, $\mathbf{X}$ is the state vector of modelled quantities, F_{in} is the flowrate into the reactor, F_{out} is the flowrate out of the reactor, $\mathbf{X_{in}}$ is the state inlet vector of modelled quantities, $\mathbf{r}()$ is the reaction rate vector explaining the kinetics of the system, $\mathbf{q}()$ is a gaseous loss term vector, $\mathbf{p}$ is the parameter vector, and t is time.

Already Eq. (2.1) makes a few simplifying assumptions over the real system. Most notably it assumes a perfectly mixed reactor and a single inlet and outlet stream. For most conventional anaerobic digester systems this is an acceptable assumption. One obvious exception to this rule would be a plug flow reactor, although this form of reactor does not appear common in the literature (and time could be conveniently switched for reactor length as the independent variable). In addition, extra inlet, outlet, and/or recycle streams would not be difficult to add, although they would complicate solution and analysis of the system. In addition to the two assumptions stated previously it is also common to assume the reactor is operated at constant volume. This simplifies Eq. (2.1) even further.

$$\frac{d\mathbf{X}(t)}{dt} = D(\mathbf{X_{in}} - \mathbf{X}) + \mathbf{r}(\mathbf{X},\mathbf{p},t) - \mathbf{q}(\mathbf{X},\mathbf{p},t) \tag{2.2}$$

with D denoting the reactor dilution rate, $D = F/V_R$.

For bioreactor modelling the most critical term in Eq. (2.2) is $\mathbf{r}()$, the growth/substrate kinetics, while $\mathbf{q}()$ can be easily modelled using fundamental transport phenomena laws.

[38; 47] provide a great review of common growth and substrate kinetics. This itself is an important distinction, as substrate consumption and organism growth need not be connected (although in most cases it is assumed these quantities are proportional). Four of the most common kinetic relations in the literature are given below:

- Monod Kinetics [42; 3]

$$r = \bar{\mu}_S \frac{S}{K_S + S} X \tag{2.3}$$

- Haldane Kinetics [2; 1; 12]

$$r = \bar{\mu}_S \frac{S}{K_S + S + \frac{S^2}{K_I}} X \tag{2.4}$$

- Droop Kinetics [23; 24; 25]

$$r = \bar{\mu}_D \left(1 + \frac{K_Q S_{cell}}{X}\right) X \tag{2.5}$$

- Contois Kinetics [19; 46]

$$r = \bar{\mu}_S \frac{S}{K_X X + S} X \tag{2.6}$$

where S is the limiting substrate, X is the biomass concentration, $\bar{\mu}_S$ is the maximum specific growth rate (i.e. saturated growth), K_S is the half saturation coefficient, K_I is the haldane inhibition coefficient, K_X is the contois half saturation coefficient, $\bar{\mu}_D$ is the droop maximum specific growth rate, K_Q is the droop limiting cell quota, and S_{cell} is the internal concentration of the limiting substrate within the biomass.

Monod kinetics (or saturation kinetics, Eq. (2.3)) are by far the most prolific in the literature and serve as a starting point for almost all bioprocess model development. However,

the literature shows that Monod kinetics are also the most simplistic as they assume no inhibitive terms. Therefore it is not uncommon to see inhibition terms added to account for unusual system conditions (such as build of NH_3 and/or fluctuations in pH, which are known to impact anaerobic performance for example). These inhibition terms can take many forms but the must common are simply multiplicative terms of the form:

$$I = \frac{K_I}{K_I + S_I} \tag{2.7}$$

Where I is the resulting inhibition factor (taking a value between 0 and 1), K_I is the inhibition constant, and S_I in the inhibitive compound concentration.

In fact, Haldane kinetics (Eq. (2.4)) are simply a specialized form of Monod kinetics subject to non-competitive substrate inhibition. Essentially this means organisms that are inhibited by excessively high substrate concentrations. Methanogenic bacteria becoming inhibited when exposed to excessively high levels acetate are a good example of this.

Droop kinetics (Eq. (2.5)) are an interesting case of substrate consumption and organism growth being explicitly decoupled. This form of rate law allows for what is known as "luxury uptake" (i.e. excessive consumption of a limiting substrate beyond its immediate need when concentrations are high). This allows for the modelling of biological organisms building cellular reserves delineated from cell growth. This type of model has been found to model the growth of microalgae very well [23; 24; 25].

Contois kinetics (Eq. (2.6)) attempt to marry the empirical growth laws of bioreactors with fundamental mass transport through the inclusion of biomass X as part of the half saturation coefficient. What this essentially does is creates inhibition within the reactor in the case of

excessive biological growth, which would indicate a decreased substrate to biomass ratio and therefore a shift from reaction driven kinetics to diffusion driven kinetics.

In order to approximate the growth or substrate utilization within bioreactors it is common to assume that there is a single limiting substrate driving the overall kinetics, with all other nutrients being assumed in excess. This has obvious parallels to limiting reactions within other industrial processes. Of course, biological systems are not static entities and so a single limiting substrate model would only remain useful in so far as the system remains under limiting conditions. Therefore the more robust models in recent literature attempt to account for multiple parallel and succesive reactions so as to account for changes in limiting substrates and system conditions as a whole (the most notable of these being the ADM1 model [3] developed by the IWA research group). These additional pathways can be modelled using any of the kinetic laws (or modified versions) presented earlier. The addition of parallel and successive pathways would naturally also result in additional components and biomasses being modelled and therefore increased complexity in the grey box model (Eq. (2.2)).

In the specific case of anaerobic digestion it is now known that the overall process consists of several broad stages (depicted in Fig. 2.1). This was also touched upon in §1.2. Therefore to ensure a robust enough model one would need to determine which steps and conditions are likely to be encountered/ rate limiting at any given moment in the reactor considered and add the according state variables and kinetics to the model. Obviously the most extensive model would have the highest rate of success when it comes to predicting all possible reactor scenarios, but this would be detrimental to control implementation and system optimization [52]. A balance of simplicity and accuracy would be the best overall strategy.

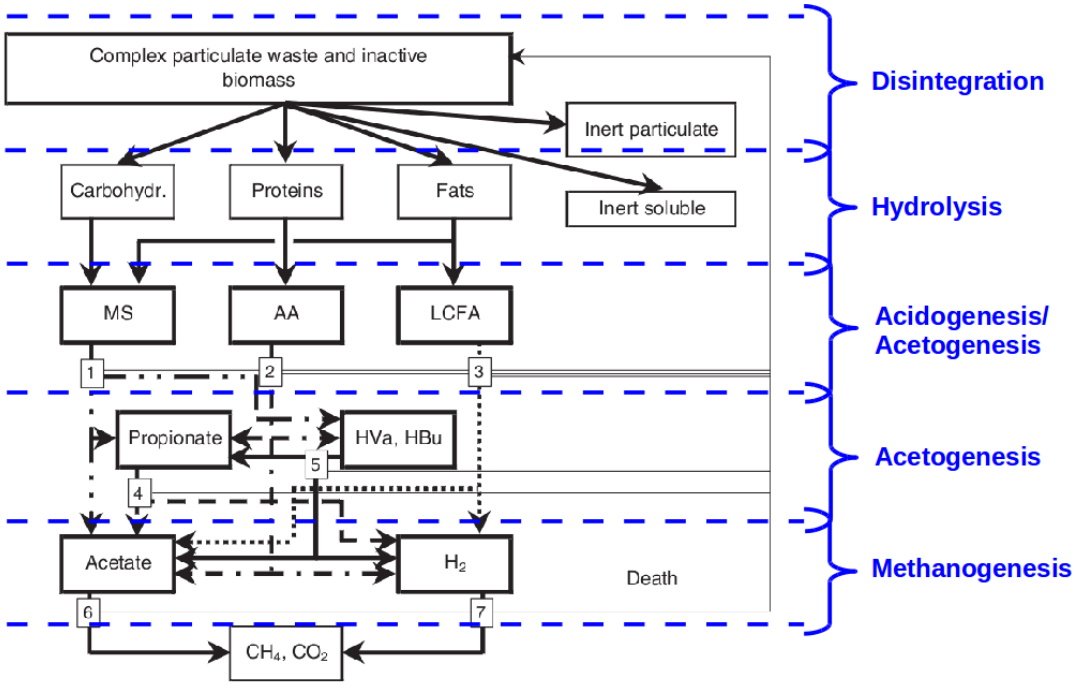

Figure 2.1: Schematic of Major Anaerobic Digester Products [4]

A quick mention should also be made regarding the role that hydrogen gas specifically plays in anaerobic digestion. Works such as that of [43] purport that hydrogen concentration is one of the key variables dictating anaerobic digester kinetics. [43] make a very compelling argument towards H_2 impacting the internal NADH/NAD balance and therefore the fundamental kinetics of the cells. However, since H_2 partial pressure was not measured during the experiment it was thought that including it in the models developed would lead to too much ambiguity in the estimated parameter sets and therefore poor results.

2.2 State-of-the-Art Modeling of Anaerobic Digestion

Two of the most popular models in the literature to date are the acidogenic-methanogenic 2 reaction model (AM2) and the 7 species anaerobic digester model (ADM1). AM2 [12] attempts to take a more simplified approach, accounting for only the necessary dynamics so as to generate a smaller model suitable for control. ADM1 [4; 3], on the other hand, attempts to comprehensively model as many major pathways in the literature as possible (and gives information on how to include more obscure pathways), regardless of how applicable they are to a given reactor. The goal in this case being to provide a comprehensive starting model that can be modified and simplified to accomodate any given reactor (i.e. to attempt to provide a future universal starting point for all AD design). As mentioned in §1.2 the basic process of anaerobic digestion is the hydrolysis of particulate matter to soluble monomers; the digestion of said monomers to H_2, CO_2, and short chain fatty acids; and the eventual digestion of these fatty acids to H_2, CO_2, and CH_4 (Fig. 2.1 also provides a graphic overview of the process).

ADM1 is by far the most comprehensive model to date. It accounts for particulate disintegration, substrate hydrolysis, acidogenesis, acetogenesis, and finally methanogenesis. It also condenses a considerable amount of literature into a set of acceptable kinetic and inhibition relationships. At its core ADM1 models the passage of the elements carbon and nitrogen through the digestion process. A real constraint of the model though is the entering feed must first be characterized and divided into carbohydrates, lipids, proteins, and inert streams. These streams must further be assigned average composition values (particularly carbon and nitrogen concentrations) so that the C,N, and COD balances may be closed. Already it is clear that ADM1 makes the simplification of assuming all carbohydrates, lipids,

and proteins have similar digestability within their substrate category. Perhaps in the future an all encompassing model will be developed that accounts for all substrate forms and all the individual biomasses that digest them, but for now it would appear that this assumption is more than acceptable (given the model's ability to match experimental data).

2.2.1 ADM1 Model

ADM1 starts by modelling the disintegration of composite particulate materials and the hydrolysis of the resulting particulate complex organics using first order kinetics [3].

$$\frac{dX_i}{dt} = k_i X_i \tag{2.8}$$

where i is the substrate in question (composite, carbohydrate, lipid, protein), k_i is rate constant, and X_i is substrate concentration in the digestor.

The disintegration of composite particulate biomass results in the complex organics (particulate or soluble) that must be hydrolized. Therefore the influent not only must be characterized in terms of its carbohydrate, lipid, protein, and inert content, but the fraction of these components that are tied up in composite particulates (for example biomass). [34] provides a method of calculating these necessary fractions from standard measurements of Total Organic Carbon (TOC), Chemical Oxygen Demand (COD), Organic Nitrogen (N_{org}, really Kjeldahl nitrogen minus ammonia), and Alkalinity (Alk). Once hydrolized, the substrates carbohydrate, protein, and lipid convert to soluble substrates sugar, long chain fatty acid (LCFA), and amino acid. ADM1 then models the uptake of these substrates using three separate acidogenic biomasses modelled with Monod kinetics and associated inhibi-

tion factors.

Acidogenesis of Sugar (S_{su}):

$$S_{su} + \beta_{su,1}\text{IN} \xrightarrow{\mu_{su} I_{\text{pH}} I_{\text{IN}}} \beta_{su,2} X_{su} + \beta_{su,3} S_{bu} + \beta_{su,4} S_{pro} + \beta_{su,5} S_{ac} + \beta_{su,6}\text{CO}_2 + \beta_{su,7}\text{H}_2 \tag{2.9}$$

Acidogenesis of LCFAs (S_{fa}):

$$S_{fa} + \beta_{fa,1}\text{IN} \xrightarrow{\mu_{fa} I_{\text{pH}} I_{\text{IN}} I_{\text{H}_2}} \beta_{fa,2} X_{fa} + \beta_{fa,3} S_{ac} + \beta_{fa,4}\text{H}_2 \tag{2.10}$$

Acidogenesis of Amino Acids (S_{aa}):

$$S_{aa} \xrightarrow{\mu_{aa} I_{\text{pH}} I_{\text{IN}}} \beta_{aa,1}\text{IN} + \beta_{aa,2} X_{aa} + \beta_{aa,3} S_{va} + \beta_{aa,4} S_{bu} + \beta_{aa,5} S_{pro} + \beta_{aa,6} S_{ac} + \beta_{aa,7}\text{CO}_2 + \beta_{aa,8}\text{H}_2 \tag{2.11}$$

where β_i are the stoichiometric coefficients; X_j are the acidogenic biomass populations of substrate j; and S_{su}, S_{fa}, S_{aa}, S_{va}, S_{bu}, S_{pro}, and S_{ac} are the concentrations of sugar, LCFA, amino acid, valerate, butyrate, propionate, and acetate. These last four components are the four intermediate VFAs accounted for by ADM1.

As mentioned before, the kinetic relation dictating the acidogenic rates is given by simple monod kinetics plus associated inhibition parameters.

$$\mu_j = \bar{\mu}_j \frac{S_j}{S_j + K_j} X_j I_{\text{pH}} I_{\text{IN}} \tag{2.12}$$

$$I_{\mathrm{pH}} = \frac{1 + 2\mathrm{x}10^{0.5(\mathrm{pH}_{LL} - \mathrm{pH}_{UL})}}{1 + 10^{(\mathrm{pH} - \mathrm{pH}_{UL})} + 10^{(\mathrm{pH}_{LL} - \mathrm{pH})}} \tag{2.13}$$

$$I_{\mathrm{IN}} = \frac{\mathrm{IN}}{\varepsilon + \mathrm{IN}} \tag{2.14}$$

$$I_{\mathrm{H_2}} = \frac{K_{\mathrm{H_2},I}}{K_{\mathrm{H_2},I} + \mathrm{H_2}} \tag{2.15}$$

where $\bar{\mu}_j$ is maximum specific growth rate of population j, K_j is the half saturation coefficient, $K_{\mathrm{H_2},I}$ is the hydrogen inhibition coefficient, ε is limiting value meant to ensure IN never reaches 0 (theoretically this value approaches 0 but in practice any reasonably small value is acceptable), and pH_{LL} and pH_{UL} are the lower and upper pH inhibition bounds.

The next layer of populations modelled by ADM1 are the acetogenic biomass. These are the populations that digest the intermediate short volatile fatty acids and produce acetate, CO_2, and H_2. The dynamics here get slightly more interesting and will be discussed after presenting the acetogenic chemical equations.

Acetogenesis of Valerate (S_{va}):

$$S_{va} + \beta_{va,1}\mathrm{IN} \overset{\mu_{va} I_{\mathrm{pH}} I_{\mathrm{IN}} I_{\mathrm{H_2}}}{\longrightarrow} \beta_{va,2} X_{va/bu} + \beta_{su,3} S_{pro} + \beta_{su,4} S_{ac} + \beta_{su,5}\mathrm{H_2} \tag{2.16}$$

Acetogenesis of Butyrate (S_{bu}):

$$S_{bu} + \beta_{bu,1}\mathrm{IN} \overset{\mu_{bu} I_{\mathrm{pH}} I_{\mathrm{IN}} I_{\mathrm{H_2}}}{\longrightarrow} \beta_{bu,2} X_{va/bu} + \beta_{bu,3} S_{ac} + \beta_{bu,4}\mathrm{H_2} \tag{2.17}$$

Acetogenesis of Propionate (S_{pro}):

$$S_{pro} + \beta_{pro,1}\text{IN} \overset{\mu_{pro} I_{\text{pH}} I_{\text{IN}} I_{\text{H}_2}}{\longrightarrow} \beta_{pro,2} X_{pro} + \beta_{pro,3} S_{ac} + \beta_{pro,4}\text{CO}_2 + \beta_{pro,5}\text{H}_2 \tag{2.18}$$

ADM1 posits that the uptake of valerate and butyrate are competitavily inhibitive, i.e. the metabolic pathways of the given population $X_{va/bu}$ must adjust to the most prominant substrate. This is reflected in an additional competative inhibition term being added to the standard monod kinetics. Propionate, on the other hand, is modelled similar to the uptake of fatty acids.

$$\mu_{va} = \bar{\mu}_{va} \frac{S_{va}}{K_{va} + S_{va}} X_{va} \frac{S_{va}}{S_{va} + S_{bu}} I_{\text{pH}} I_{\text{IN}} I_{\text{H}_2} \tag{2.19}$$

$$\mu_{bu} = \bar{\mu}_{bu} \frac{S_{bu}}{K_{bu} + S_{bu}} X_{bu} \frac{S_{bu}}{S_{bu} + S_{va}} I_{\text{pH}} I_{\text{IN}} I_{\text{H}_2} \tag{2.20}$$

$$\mu_{pro} = \bar{\mu}_{pro} \frac{S_{pro}}{K_{pro} + S_{pro}} X_{pro} I_{\text{pH}} I_{\text{IN}} I_{\text{H}_2} \tag{2.21}$$

The final step modelled in ADM1 is the methanogenic conversion of acetate and hydrogen to CH_4 and CO_2.

Methanogenises of Acetate (S_{ac})

$$S_{ac} + \beta_{ac,1}\text{IN} \overset{\mu_{ac} I_{\text{pH}} I_{\text{IN}} I_{\text{NH}_3}}{\longrightarrow} \beta_{ac,2} X_{ac} + \beta_{ac,3}\text{CH}_4 + \beta_{ac,4}\text{CO}_2 \tag{2.22}$$

Methanogenesis of Hydrogen (H_2)

$$H_2 + \beta_{H_2,1}IN + \beta_{H_2,2}CO_2 \xrightarrow{\mu_{H_2} I_{pH} I_{IN}} \beta_{H_2,3}X_{H_2} + \beta_{H_2,4}CH_4 \tag{2.23}$$

ADM1 models both methanogenic reactions using simple Monod kinetics, with the addition of an ammonia inhibition term for acetate methanogenesis (a well documented phenomena) [3; 35; 53].

$$\mu_{ac} = \bar{\mu}_{ac} \frac{S_{ac}}{K_{ac} + S_{ac}} X_{ac} I_{pH} I_{IN} I_{NH_3} \tag{2.24}$$

$$\mu_{H_2} = \bar{\mu}_{H_2} \frac{H_2}{K_{H_2} + H_2} X_{H_2} I_{pH} I_{IN} \tag{2.25}$$

$$I_{NH_3} = \frac{K_{NH_3}}{K_{NH_3} + NH_3} \tag{2.26}$$

In addition to these core relations ADM1 also makes use of an alkalinity term to track all inert charges, with this term being encorporated into a charge balance with standard equilibrium relations for all appropriate quantities. This is required to calculate pH and NH_3 derived inhibition terms. Finally, ADM1 accounts for gaseous losses (primarily CO_2) through the inclusion of liquid transfer dominated interface transfer equations. These will be addressed in greater detail in §4.2.2.

2.2.2 AM2 Model

The other model that will be relied on heavily for this thesis is the AM2 [12]. In this model all acidogenic/acetogenic and methanogenic bacteria are lumped into two bulk communities (i.e. two substrates and two biomasses). The obvious assumption here is that lipids, carbohydrates, and proteins have similar hydrolysis and consumption rates. This can be found to be approximately true as long as sufficient nutrients and substrate are provided. The model also condenses the hydrolysis and subsequent uptake of the substrate into a single step. This is acceptable as long as the kinetic constants are adjusted to account for both processes. The acidogenesis of influent substrate is modelled using monod kinetics.

Acidogenesis of Influent Substrate (S_1):

$$S_1 \xrightarrow{\mu_{S1}} \beta_{S1,1}X_1 + \beta_{S1,2}S_2 + \beta_{S1,3}\mathrm{CO_2} \tag{2.27}$$

$$\mu_1 = \bar{\mu}_1 \frac{S_1}{K_1 + S_1} \tag{2.28}$$

where all terms in the above equations have identical meanings to the terms introduced in the ADM1 discussion.

What is interesting about this work is that no additional inhibition terms were incorporated into the kinetics. This does not mean inhibition was not present. It simply means that it was not observable in the experimental data used in the study or for that particular bacterial population inhibition was less pronounced. Also of interest is the fact that H_2 production was not considered. Indeed this can be a good assumption depending on the populations

and feeds being considered. Of most importance to this particular thesis is the fact that *Chlorella sp./Scenedesmus sp.* are found to yield almost no H_2 indicating that these pathways are negligible [30]. The most interesting part of AM2 however is how it models the methanogenesis of volatile fatty acids. AM2 considers the likely inhibitory effects of accumulated VFAs (which would result in reduced pH) and accounts for this inhibition using haldane kinetics.

Methanogenesis of VFAs (S_2):

$$S_2 \xrightarrow{\mu_2} \beta_{S2,1}X_2 + \beta_{S2,2}\mathrm{CH_4} + \beta_{S2,3}\mathrm{CO_2} \tag{2.29}$$

$$\mu_2 = \bar{\mu}_2 \frac{S_2}{K_2 + S_2 + \frac{S_2^2}{K_{2,I}}} \tag{2.30}$$

Where $\bar{\mu}_2$, K_2, and $K_{2,I}$ are the maximum specific growth rate, half saturation coefficient, and haldane inhibition coefficient of S_2 respectively.

In addition to these relations, AM2 also tracks alkalinity for use in a charge balance and accounts for phase transfer of components using liquid dominant transport phenomena.

2.3 Conclusions

This chapter has outlined in detail the relevant literature that will be used to construct the anaerobic digestor models used in the remainder of this thesis. Of central importance to this model will be the construction of a grey box state space structure based on fundamental material balances. From here the empirical rate laws selected will be based on the state of the art ADM1 and AM2 models in attempt to marry simplicity with and adequate level of complexity to predict the kinetics of the observed system reasonable well.

Chapter 3

Bioprocess Model Development and Identification

Most bioprocess modelling scenarios follow the general process of experimental design, data analysis, model development, and model fitting. Note that these steps are not independent and may influence each other (for example experimental design may be based on identifying parameters within a specific model [54] or distinguish between prospective models [7]). In this case all experiments were performed by LBE-INRA before the start of this thesis and so only the last three steps were considered (experimental design will be discussed in §6.2). Data analysis (although not always performed in a quantitative way) involves the assessment (and possible filtering) of the collected experimental data to determine the information content (i.e. how many reactions are present/can be distinguished). From here (assuming a model has not yet been developed) a reaction network is designed, based on the literature, to describe the experimental data set. Finally, this model is fit using the data set (i.e. relevant parameter sets are identified). These final three steps are discussed

in this chapter.

3.1 Determination of Reaction Complexity

One of the key issues in model identification, when dealing with an experimental data set, is determining the amount of information contained within the data. This section will outline a theoretical method for determining such a quantity using the work of [11; 8; 9; 14; 15]. As detailed in §2.1, the most common approach to modelling anaerobic digesters is to use a grey box component balance system centered around a set of phenomenological rate laws. As such, this work considers a general system model of the form presented in Eq. (3.1).

$$\frac{d\xi}{dt} = K\mathbf{r}(\xi) + D\left(\xi^{in} - \xi\right) - \mathbf{q}(\xi) \tag{3.1}$$

where K is an $\mathbb{R}^{n\,x\,nr}$ stoichiometric coefficient matrix, ξ is an $\mathbb{R}^{n\,x\,1}$ liquid state variable vector (in our case using units of gCOD/L or mol/L where appropriate), D is the dilution rate, $\mathbf{r}(\xi)$ is the $\mathbb{R}^{nr\,x\,1}$ reaction rate vector, $\mathbf{q}(\xi)$ is the $\mathbb{R}^{n\,x\,1}$ gas transfer rate vector, n is the total number of components and nr is the number of reactions (to be determined).

In order to facilitate determination of the requisite reaction network complexity, a slightly modified version of Eq. (3.1) is used.

$$\frac{d\xi_m}{dt} = K_m\mathbf{r}(\xi_m, \xi_{nm}) + D\left(\xi_m^{in} - \xi_m\right) - \mathbf{q}_m(\xi_m, \xi_{nm}) \tag{3.2}$$

In Eq. (3.2) the subscripts m and nm simply refer to the "measured" and "unmeasured"

subsets of ξ respectively (i.e. $n = m + nm$).

Let us now suppose that we have conducted an experiment with $N+1$ observations of ξ_m, ξ_m^{in}, and $\mathbf{q}_m(\xi_m, \xi_{nm})$. We may therefore construct the following matrices U, V, and W based on integrating terms in the left and right sides of Eq. (3.2).

$$U = (u(t_1,t_2), \ldots, u(t_N,t_{N+1})) \tag{3.3}$$

$$V = (v(t_1,t_2), \ldots, v(t_N,t_{N+1})) \tag{3.4}$$

$$W = (w(t_1,t_2), \ldots, w(t_N,t_{N+1})) \tag{3.5}$$

where

$$u(t_1,t_2) = \xi_m(t_2) - \xi_m(t_1) - \int_{t_1}^{t_2} \left[D(t) \left(\xi_m^{in}(t) - \xi_m(t) \right) \right] dt \tag{3.6}$$

$$v(t_1,t_2) = \int_{t_1}^{t_2} \left[r(\xi_m(t), \xi_{nm}(t)) \right] dt \tag{3.7}$$

$$w(t_1,t_2) = \int_{t_1}^{t_2} \left[q_m(\xi_m(t), \xi_{nm}(t)) \right] dt \tag{3.8}$$

It is now critical to remind the reader that biological systems are notoriously complex and

the current state of the art has very few measures that are a direct measurement of individual components. Quite often available experimental measurements are a combination of state variables (e.g. total COD values, which are a combination of all substrate and biomass in the liquid phase) and/or a combination of "pseudo"system variables that can be linked directly to reaction rates (e.g. methane flowrate from an anaerobic digester can be linked to one or more reaction rates). Taking this into account it is easy to show that the evolution of combined state variables are easily modeled by multiplying (3.2) by a constant coefficient matrix $C \in \mathbb{R}^{nc\,x\,n}$ (such that $y_m = C\xi_m$), where nc is the number of "combined" state observations, that accounts for the desired experimental combinations.

$$C\frac{d\xi_m}{dt} = CK_m\mathbf{r}\left(\xi_m, \xi_{nm}\right) + CD\left(\xi_m^{in} - \xi_m\right) - C\mathbf{q}_m\left(\xi_m, \xi_{nm}\right) \tag{3.9}$$

$$\frac{dy_m}{dt} = K_m'\mathbf{r}\left(y_m\right) + D\left(y_m^{in} - y_m\right) - \mathbf{q}_m'\left(\xi_m, \xi_{nm}\right) \tag{3.10}$$

Eq. (3.10) can naturally accomodate individual component measurements as well by having the appropriate row contain a single 1 value at the appropriate column position and zeros everywhere else. This logic can be extended to the derivations of Eqs. (3.3) - (3.8) leading to quantities:

$$U' = CU \tag{3.11}$$

$$V' = CKV \tag{3.12}$$

$$W' = CW \tag{3.13}$$

Up to this point we can now write a condensed system description from (3.1) as:

$$U' = V' - W' \tag{3.14}$$

with the aforementioned "pseudo" system variables we may also define a matrix X whose contents equal linear combinations of the reaction rate vector $\mathbf{r}(\xi_m, \xi_{nm})$. These "pseudo" state variables do not relate directly to any modelled state but contain useful non-redundant information.

$$\mathbf{r}_m = C'\mathbf{r}(\xi_m, \xi_{nm}) \tag{3.15}$$

where C' is the ($\mathbb{R}^{nc\,x\,nr}$) constant coefficient matrix inscribing the appropriate reaction rate combinations, and $\mathbf{r}()$ is the ($\mathbb{R}^{nr\,x\,1}$) reaction rate vector. By integrating Eq. (3.15) in the same fashion as Eqs. (3.6) - (3.6) and subsequently appending it to Eq. (3.14), we arrive at the desired final system (Eq. 3.17).

$$\int_{t_1}^{t_2} C' \left[\mathbf{r}\left(\xi_m(t), \xi_{nm}(t)\right)\right] dt = C'v(t_1, t_2) \tag{3.16}$$

$$U'' = \begin{bmatrix} CKV \\ C'V \end{bmatrix} - \begin{bmatrix} W' \\ \mathbf{0} \end{bmatrix} \tag{3.17}$$

If we now view $\mathbf{r}_m$ as distinct variables and U" as a randomnly distributed data set then as long as we can assume the gas flowrate values of U' are zero (i.e. $W' = \mathbf{0}$), we may perform a PCA style analysis on this "dataset" to determine the number of principle components required to describe a set degree of the variability in the dataset. Under this scope the "variables" $\mathbf{r}()$ are can be seen as some combination of the original data sets projection on the principal components. Recall that in PCA the basic goal is determine a projection into a reduced dimensional space through the use of singular value decomposition.

$$X = W\Sigma V \tag{3.18}$$

where X is the original data set (in our case the $\mathbb{R}^{nc\,x\,N}$ matrix U''), W is the $\mathbb{R}^{nc\,x\,nc}$ eigenvector matrix of $U''U''^T$, Σ is the $\mathbb{R}^{nc\,x\,N}$ diagonal singular value matrix, and V is the $\mathbb{R}^{N\,x\,N}$ eigenvector matrix of U''^TU''. It therefore follows that the projection U'' onto the reduced principal component space can be facilitated by

$$Y = W^TX = \Sigma V \tag{3.19}$$

$$\underbrace{\begin{bmatrix} CK \\ C' \end{bmatrix}}_{W} \underbrace{V}_{\Sigma V} \tag{3.20}$$

Within Eq. (3.18) - (3.20) we take only the nr most dominant principle components (as dictated by the diagonal values of Σ) and so the SVD of U'' now becomes a way of estimating the number of reactions required to explain a given degree of the total variability of

the data set. How is this so? Well an equally valid version of the derivation is to use the matrix $U''U''^T = W\Sigma\Sigma W^T$ where it can be seen that the eigenvalues of this matrix simply equal the square of the singular values. It can also be shown that these eigenvalues are proportional to the squared error accounted for by each principle component. Therefore one can simply take a progressive sum of the eigenvalues (i.e. keep increasing *nr* in Eq. (3.21) by increments of 1) and divide by the total sum until one arrives at a total number of reactions that accounts for a prespecified amount of the variance *var* in the data (e.g. 95%).

$$\frac{\sum_{i=1}^{nr}\lambda_i}{\sum_{i=1}^{n\lambda}\lambda_i} > var\,? \tag{3.21}$$

where λ_i is the *i*th eigenvalue, $n\lambda$ is the total number of eigenvalues, and *var* is the predefined variability limit.

Note that as long as the number of predicted principal components (*nr*) falls below the row dimension of U'' (i.e. nc+nc') then the result is a meaningful finding on reaction set complexity. If the number of principal components equals the number of experimental observations all one can say is that the model requires at least that many reactions.

As with all PCA analysis it is important to center and normalize a data set before calculating the eigenvalues so that results are not skewed by the magnitude of the experimental values. This normalization is shown in Eq. (3.22).

$$U''_{1,i} = \frac{U''_i - \bar{U''}}{\sqrt{N}s\,(U'')} \tag{3.22}$$

Where U''_i is the ith column of U'', $\bar{U''}$ is a column vector containing the mean of each row

of U'', $s(U'')$ is a column vector containing the standard deviation of each row of U'', and all calculations of $U''_{1,i}$ are conducted on an entry by entry basis. Therefore the number of reactions required to describe the variance of the data may be estimated by calculating the eigenvalues of $U''_1 U''^T_1$ [11].

3.2 Determination of Parameter Values

3.2.1 Systematic Parameter Identification Procedure

after a candidate model structure has been identified, adequate values must be given to the parameters in the corresponding equation system. While accurate values for some of these parameters can be found in the literature (e.g. acid/base dissociation constants) other parameters may be more uncertain/unknown for a given system and need to be estimated from experimental data; this typically includes a number of stoichiometric and kinetic parameters as well as initial conditions for the state variables. This is especially true of a system such as the anaerobic digestion of microalgal biomass, which has not recieved a great deal of modelling and identification study in the literature so far.

The heart of parametric model identification is to estimate the uncertain parameters, which are denoted by p subsequently. Such estimates can be obtained by minimizing a specified objective function, typically a weighted sum of the square errors between measured outputs $\mathbf{y}^{\mathrm{m}}$ and corresponding model predictions $\mathbf{y}$ at a number of observation times t_j, $j = 0, \ldots, N_i$:

$$\min_{\mathrm{p}} \mathscr{J} := \sum_{i=1}^{N_y} \sum_{j=0}^{N_i} \omega_{i,j} \left[y_i(t_j;\mathrm{p}) - y_i^{\mathrm{m}}(t_j) \right]^2, \tag{3.23}$$

where the model outputs y correspond to some state variables ξ or, more generally, functions of the state variables (see §3.1) and $\omega_{i,j}$ denotes the weighting coefficient for the jth measurement of the ith output; for example, these weights can be chosen as the inverse of the standard deviation of the corresponding output measurement. In this work the weighting coefficients were selected both on an observational basis (as explained in the application section) and a practical one. On the practical side, all of the data sets were pre divided by their means to scale each observation. In addition, multiples of 10 were added to some of the experimental observations (explained in the application section) to offset percieved errors in the data.

The selection of such an objective function is not arbitrary. With the following assumptions it can be shown that the solution to a least squares problem results in a maximum likelihood estimate of the given parameter set:

- The data error of each observation is multivariate normally distributed;
- There is no error in model structure (This will naturally need to be determined on an after the fact basis through trial and error);
- The observation standard deviation is either known or can be reasonably estimated.

With these assumptions we may now take a multivariate normal distribution of the experimental observations.

$$f_X(x) = \frac{\exp\left(-\frac{1}{2}(x-\mu)^T \Sigma^{-1} (x-\mu)\right)}{(2\pi)^{k/2} |\Sigma|^{1/2}} \tag{3.24}$$

where x is a vector of the observed variables, k is the number of observed variables, μ is a vector of the observed variable means, and Σ is the $\mathbb{R}^{k\,x\,k}$ covariance matrix of the observed variables.

In our case we replace x with the measured variables $y^m(t)$ and μ with the model predictions $y(t,p)$ (essentially we are generating a moving mean that, if the model is perfect, will cancel out all system based correlation and leave only the experimental noise). An important pitfall of this current formulation is that an exact value of measurement standard deviation is not known and so we must come up with an appropriate approximation. Here, a base standard deviation for the measurements was estimated, assuming a perfect model, as $\mathscr{J}/v$ (v denoting the total number of measurement points included in the estimate). If we wanted to be more rigorous we would need to examine the experimental error of each observation variable but this substitution simplifies calculations greatly and was found to not drastically impact results. Taking all this into account we arrive at the modified formulation shown below.

$$f(y^m(t_j),p) = \frac{\exp\left(\sum_{i=1}^{N_y}\left(-\frac{\mathscr{J}}{2v}\frac{\omega_{i,j}\left(y_i^m(t-j)-y_i(p,t_j)\right)^2}{\bar{y}^m}\right)\right)}{(2\pi)^{N_y/2}\,|\Sigma|^{1/2}} \tag{3.25}$$

We may now formulate a maximum likelihood estimate of the parameter set p to be one that maximizes the combined probability function (3.26).

$$\max_{\mathrm{p}} \Pi_{j=1}^{N_i} f(y^m(t_j),p) \tag{3.26}$$

Looking at Eq. (3.25) it is clear that since the exponential term is always negative, assuming

all observed variables are positive (true for this case), maximizing Eq. (3.26) boils down to minimizing the squared error between the experimental data and the model (i.e. our original ojective function choice). What's more, this maximum likelihood model may be used to estimate parameter confidence (as will be explained below). It should be quickly noted that the term $\mathscr{J}/v$ was ommitted from the actual dynamic optimization stage but reincluded when assessing parameter confidence.

Mathematical models for biotechnological processes often comprise many uncertain parameters and relatively few measured outputs, which makes them notoriously hard to calibrate due to structural/practical identifiability issues [22]. Structural identifiability refers to models that have parameters that would be unable to be estimated from a given set of observed quantities even if all possible dynamic scenarios were covered (i.e. system components that have no impact on the observed quantities). Practical identifiability is a little more subtle and refers to parameters that either can't be estimated or can't be estimated to a reasonable certainty due to issues with the specific data set used (so practical identifiability is less definite than structural identifiability). Standard biological kinetic relations, such as monod kinetics, are notorious for this problem.

$$\mu = \bar{\mu}\frac{S}{S+K_S} \tag{3.27}$$

At low concentrations ($S << K_S$) the kinetics begin to mirror first order kinetics as $\mu = \frac{\bar{\mu}}{K_S}$. For this reason, attempting to fit all the parameters simultaneously almost always results in nearly zero confidence in the estimated parameters. Instead, two typically conflicting objectives must be accommodated in calibrating biotechnological process models, namely the fit quality and the estimated parameter confidence. Obtaining a close fit between the

model predictions and the experimental data is always favored by increasing the number of degrees of freedom, but additional freedom is also detrimental to the confidence in the resulting estimates due to the presence of redundancies among the parameters. Ideally, one would like to consider every possible parameter combination and run global estimation routines for each one of them, yet this is computationally intractable for more than a handful of parameters. It should also be noted that an acceptable compromise may not always be found in practice.

As a response to the issues surrounding selecting a subset of parameters to estimate, and gaining some semblance of meaning with the values, a parameter identification procedure was developed for the systematic construction of minimal parameter combinations. The idea is to start with a single parameter, and keep on adding parameters to the most promising combinations, one at a time, until some threshold on estimated parameter error is reached. To make the procedure computationally tractable, a limited number of parameter combinations are retained after each stage, for example $n_{\text{comb}}^{\max} = 3$. Naturally as $n_{\text{comb}}^{\max}$ approaches n_{param} the discussed procedure would approach the combinatorial approach, at least locally. This selection is based on two criteria:

1. Is the relative confidence of each parameter in a combination above a user-specified threshold?

2. How good is the fit in terms of the least-square error criterion?

The latter is used to rank the parameter combinations and can be directly obtained from the solution of the optimization problem Eq. (3.23)/(3.26). On the other hand, the former is used to detect and eliminate those parameter combinations which yield low confidence

estimates. The multivariate Cramer-Rao bound is used as a means of estimating parameter confidence [54]. Specifically, the confidence intervals for each parameter are estimated using Student's t-test (note that this equation assumes an unconstrained optimization problem),

$$\delta_i^{\text{rel}} = \frac{\sqrt{\mathscr{C}_{i,i}}}{p_i} \mathrm{t}_{1-\alpha,\nu}, \quad i = 1,\ldots,n_p, \tag{3.28}$$

where $\mathscr{C} = \frac{\mathscr{J}}{\nu}\left(\frac{d^2\mathscr{J}}{d\mathrm{p}^2}\right)^{-1}$ is (an estimate of) the covariance matrix of the parameter estimate errors; $\nu = N \times n_y - n_p$, the number of degrees of freedom; and $(1-\alpha)$, the desired confidence level, e.g., $1-\alpha = 95\%$. Then, the parameter confidence criterion simply reads:

$$\max\{\delta_i^{\text{rel}} : i = 1,\ldots,n_p\} \leq \delta_{\max}^{\text{rel}}, \tag{3.29}$$

with $\delta_{\max}^{\text{rel}}$ the user-specified, relative confidence threshold, e.g., $\delta_{\max}^{\text{rel}} = 50\%$.

To recap, A formal statement of the parameter identification procedure is given in Algorithm 1.

INITIALIZATION:

- Select parameter subset, $\{p_k, k = 1, \ldots, n_p\}$
- Select relative confidence threshold, $\delta_{\max}^{\text{rel}}$
- Select max. number of parameter combinations, $n_{\text{comb}}^{\max}$
- Set $\mathscr{P}_i \leftarrow \emptyset, i = 1, \ldots, n_{\text{comb}}^{\max}$

REPEAT:

- Set $\mathscr{S} \leftarrow \emptyset$
- **LOOPS:** $i = 1, \ldots, n_{\text{comb}}^{\max}$, $k = 1, \ldots, n_p$
  - **IF:** $p_k \in \mathscr{P}_i$ **OR** $\mathscr{P}_i \cup \{p_k\}$ has already been considered; **THEN:** Loop
  - Estimate the parameters in $\mathscr{P}_i \cup \{p_k\}$ by solving Eq. 3.23
  - **IF:** Confidence criterion 3.29 is satisfied; **THEN:** Insert $\mathscr{P}_i \cup \{p_k\}$ in $\mathscr{S}$
- **IF:** $\mathscr{S}$ is empty; **STOP**
- Rank parameter combination in $\mathscr{S}$ according to the least-square error criterion $\mathscr{J}$ in Eq. 3.23
- Update $\mathscr{P}_i, i = 1, \ldots, \min\{n_{\text{comb}}^{\max}, |\mathscr{S}|\}$ with the best parameter combinations in $\mathscr{S}$

Algorithm 1: Systematic parameter identification procedure.

It should be clear at this point that this is an applied method that is meant to balance efficacy with speed of identification. One of the key issues with large scale identification problems of this type is that the optimal solution is found locally. Therefore there is no guarantee a globally optimal solution will be found. This is true both for parameter combinations selected and the optimal solutions found within said combinations. One can increase the likelihood of finding global solutions by increasing the parameter $n_{\text{comb}}^{\max}$, although this will naturally increase computation time.

3.2.2 Special Case of Initial Conditions

An alternative derivation of $\mathscr{C}$ 3.28 proposed by [48] lends itself well to including constrained optima. If we assume that our original optimization problem is subject to a constraint set $g()$, where $g()$ can contain both equality and inequality constraints. Then it can be shown that the covariance matrix of the parameter and langrangian multiplier set can be given by:

$$\Sigma_{\text{p},\mu} = \frac{\mathscr{J}}{v} \begin{pmatrix} -\mathscr{P} \\ \mathscr{Q} \end{pmatrix} \left(\frac{\delta^2 \mathscr{J}}{\delta \text{p}^2}\right)^{-1} \left(\frac{\delta^2 \mathscr{J}}{\delta \text{p} \delta y}\right) \left(\frac{\delta^2 \mathscr{J}}{\delta \text{p} \delta y}\right)^{T} \left(\frac{\delta^2 \mathscr{J}}{\delta \text{p}^2}\right)^{-1} \begin{pmatrix} -\mathscr{P} \\ \mathscr{Q} \end{pmatrix}^{T} \tag{3.30}$$

where

$$\mathscr{Q} = \left[\left(\frac{\delta g_{act}}{\delta \text{p}}\right) \left(\frac{\delta^2 \mathscr{J}}{\delta \text{p}^2}\right)^{-1} \left(\frac{\delta g_{act}}{\delta \text{p}}\right)^{T}\right]^{-1} \left(\frac{\delta g_{act}}{\delta \text{p}}\right) \tag{3.31}$$

$$\mathscr{P} = I_{npxnp} - \left(\frac{\delta^2 \mathscr{J}}{\delta \mathrm{p}^2}\right)^{-1} \left(\frac{\delta g_{act}}{\delta \mathrm{p}}\right)^{T} \mathscr{Q} \tag{3.32}$$

where $\mathscr{J}$ is the objective function discussed in Eq. (3.23), g_{act} is the set of active constraints in the optimal solution, p is the set of parameters be optimized, and y is the set of experimental measurements.

The first np diagonal elements of $\Sigma_{\mathrm{p},\mu}$ correspond to the parameter variance estimates used in Eq. (3.23). The above calculations can be easily included into algorithm 1 to include additional constraints, such as the assumption of steady state that will included in part of this thesis).

3.3 Conclusions

This chapter has outlined the theory behind the techniques that will be used in the practical identification of the anaerobic digestion of microalgae. While it has already been decided that the base of the model will be formed form mass balances, the number of reactions required to describe the system dynamics is still to be determined. The PCA method outlined in section 3.1 when applied to the LBE-INRA experimental data set will allow calculation of this number and so facilitate modelling. This chapter also outlines the novel contribution of this thesis in the form of the systematic parameter identification algorithm. Once a generic model structure has been selected, this method can be used to produce identifiable subsets of parameters based on available experimental data. The next chapter will present how this algorithm performs with a real data set.

Chapter 4

Application to Anaerobic Digestion of *Chlorella Vulgaris*

Now that the necessary methods have been outlined, the next step is to apply said methods to an experimental data set to determine their effectiveness. In this case these modelling and identification tools will be applied to an experimental data set describing the anaerobic digestion of the microalgae *Chlorella Vulgaris*, provided by LBE-INRA. To this end the first section of this chapter will provide all necessary background information on the data set itslef, i.e. how it was collected, averaged properties, etc. From here the PCA technique described in section 3.1 will be applied to the data set to determine the number of rate laws required to describe the system dynamics. Once this is determined, appropriate kinetic laws are selected based on the models presented in chapter 2. Finally, the novel parameter identification developed is applied to the selected model to determine the best identifiable subset of parameters and the results of these trials are discussed.

4.1 Description of Experimental Data

The research into modelling the anaerobic digestion of algal biomass within this thesis was conducted in collaboration with *Laboratoire de Biotechnologie de l'Environnement - l'Institut National de la Recherche Agronomique (LBE-INRA)* in Narbonne, France and *Institut National de Recherche en Informatique et en Automatique - Contrôle et Modélisation de Ressources Renouvelables (INRIA-COMORE)* in Sophia Antipolis, France. Both organizations are actively researching various aspects of algal bioreactors and anaerobic digesters for the same aforementioned goal of developing combined bioreactor processes. More pertinent to this work, LBE-INRA completed a half-year study of the anaerobic digestion of *Chlorella vulgaris* in 2009 and was gracious enough to share this data with our group. What follows is a description of the trials conducted over this period and the initial work up of the data.

4.1.1 Experimental Setup

The experimental study of the anaerobic digestion of *Chlorella vulgaris* was performed over a 150 day period. This study involved the operation of a 1 L continuous-stirred-tank anaerobic digester, with 0.1 L headspace, maintained at 35 °C, and with no pH control. Feed was added to the reactor in slugs using a syringe apparatus and equal volume quantities of reactor medium were removed during feeding to maintain a constant reactor volume. Over the long run this was done to mimic a continuously fed reactor although on the micro time scale the reactor was operated more as a semi-batch process. The feed was comprised of concentrated *Chlorella vulgaris* cultured in a 20 L artificially lit photobioreactor (for additional details see [50]). The average feed to the anaerobic digester was limited to a

little under 1 gCOD/L by the culturing rate of the photobioreactor (actual average feed rate shown in Fig. 4.1). The lump average value denotes a progressively updated average value starting at time 0 and the locally calculated value denotes a value calculated separately for each addition.

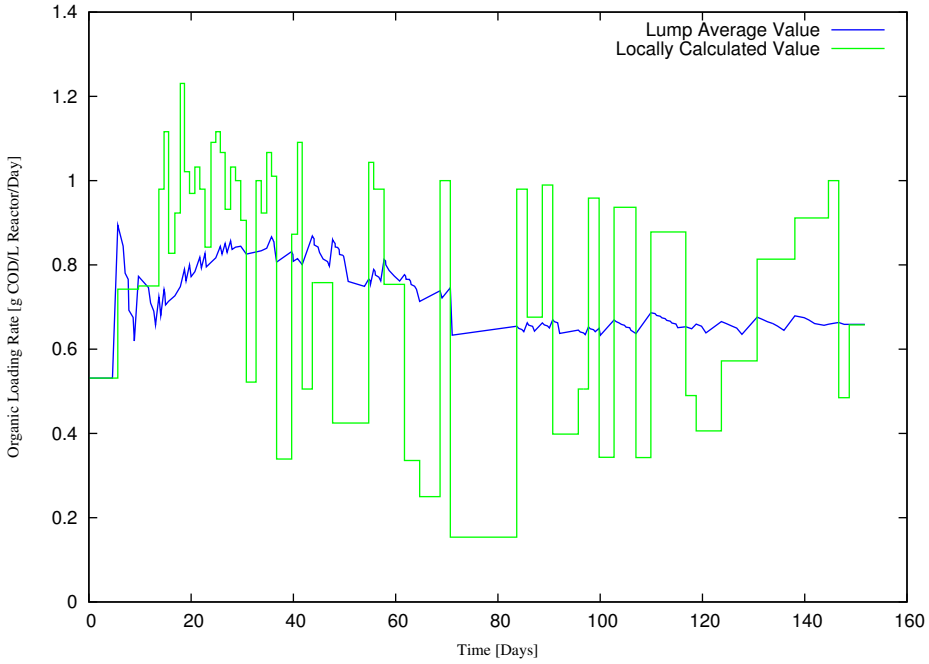

Figure 4.1: Algal Loading Rate of the Anaerobic Digester

Chlorella vulgaris was selected as the substrate for the experiment for both historical and practical reasons. As [50] points out, early interest into the anaerobic digestion of microalgae was centered around *Chlorella* and *Scenedesmus* species of microalgae because these species were observed growing in anaerobic digester settling ponds. Naturally the question was raised as to whether any value could be derived from this biomass. While these initial efforts were unrelated to biodiesel, recent efforts have also shown that *Chlorella vulgaris* is one of many microalgae species whose lipid fraction can be manipulated through adjustment of specific nutrient and reactor conditions [36]. Indeed the long-term goal of

these works is to derive a combined biodiesel/biomethane system but a short term goal was also to study the general coupling of these two systems. To this end the *Chlorella vulgaris* was cultured under non-growth limiting conditions and so the final lipid content was not ideal for biodiesel production. The focus was more on producing a generic test case for a combined microalgal/anaerobic digester system and to generate data to develop an initial model. It remains to be seen whether this model will be appropriate for the influent conditions surrounding high lipid microalgal growth (in case it is decided to simply digest the microalgae in full rather than extracting lipids for biodiesel).

4.1.2 Measurement Techniques

Readings of the following quantities were taken on an approximately daily basis: total COD (by colorimetric method); ion concentrations (by ion chromatography); biogas volume (by water displacement); biogas composition (by gas chromatography); and pH (by colorimetric method). Random samples were also selected on a less frequent basis for volatile fatty acid (VFA) determination. See [50] for more details.

4.1.3 Feed Stream Characterization

A detailed characterization of the feed stream and profile can be found in [39; 50]. A summary of the important details will be provided here. Feed was introduced as slugs, and equal volumes of reactor medium were removed to maintain a constant liquid volume. A daily and cumulative average of the dilution rate along with the substrate additions are shown in Fig. 4.2 and 4.3. During the experiment it was attempted to study the system at hydraulic retention times of $\approx$ 28 days (days 10 - 45) and $\approx$ 16 days (days 90 - 150). In

addition to these general HRT studies, a final set of "batch" studies were conducted in the final 35 days of the trial. During this time feed slugs were progressively increased to values of 1 gCOD, 2 gCOD, 4 gCOD, and 6 gCOD (this is clearly visible in Fig. 4.3). The system was allowed to return to a steady state (determined via biogas production [39; 50]) before each subsequent addition.

As for the feed stream composition, the average concentrated *Chlorella vulgaris* feedstock had a COD value of 25 - 30 gCOD/L [50]. For this work a default value of 30 gCOD/L was assumed. This value was in turn adjusted through the addition of deionized water to maintain HRT and organic loading rates, as the case required. As detailed by [39] the average composition of non-growth limited *Chlorella vulgaris* is approximately 60 wt% proteins ($C_{4.43}H_7O_{1.44}N_{1.16}S_{0.019}$), 20 wt% lipids ($C_{40}H_{74}O_5$), 20 wt% sugars ($C_6H_{12}O_6$). The average substituent compositions being estimated from [26; 28; 39]. Coupling this with an experimentally determined inert/reluctant gCOD fraction of 30%, and assuming a proportional contribution for each major component, leads to an overall gCOD composition of 40 % proteins, 15 % lipds, and 15 % sugars [39]. It was also determined experimentally that the *Chlorella vulgaris* feed contained 1.33 - 1.43 gCOD/gVSS (this will be used for literature comparisons). A value of 1.38 gCOD/gVSS was assumed for this work. The average concentrations of other relevant inlet components are provided in Tab. 4.1.

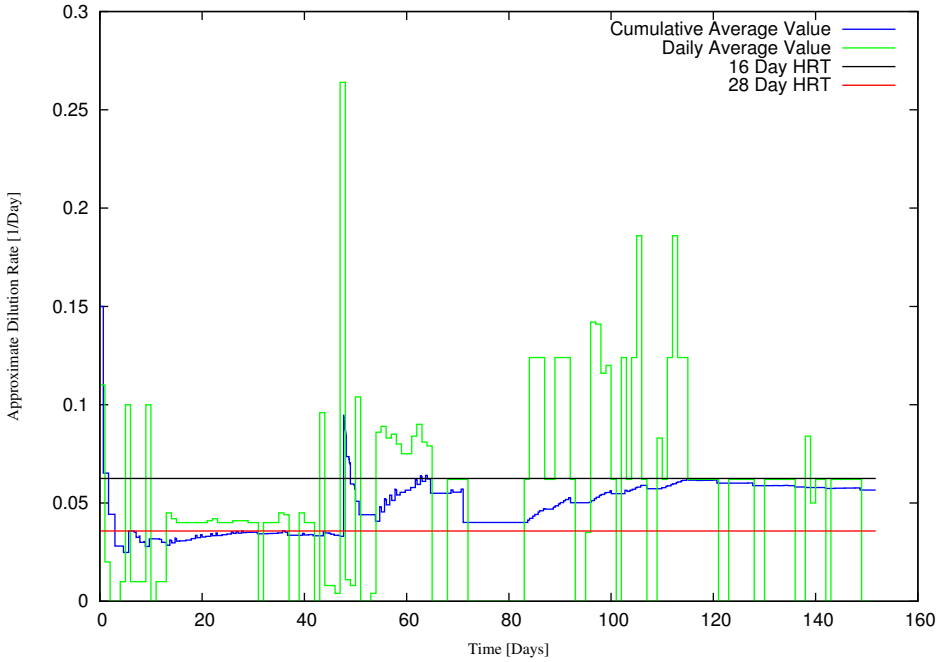

Figure 4.2: Average Dilution Rate Into the Anaerobic Digester

4.2 Selection of Model Structure

4.2.1 Minimum Number of Reactions

From §4.1.2 the available experimental measurements for the LBE-INRA trial are total chemical oxygen demand (TCOD), inorganic nitrogen (IN), volatile fatty acids (VFA), assorted inert ions (used to calculate Z), pH, biogas accumulation (q_{accum}), and methane concentration (% CH_4). Of these measurements, pH and Z measurements were ill-suited for applying the methods of §3.1 (the derivation is dependent on the ODE form of Eq. (3.1)) and so were left to act as "confirmation" data sets for the final fitted models. In order to fit the remaining measurements into the theory of §3.1 we first take the biogas accumulation and methane concentration values and multiply them to calculate methane

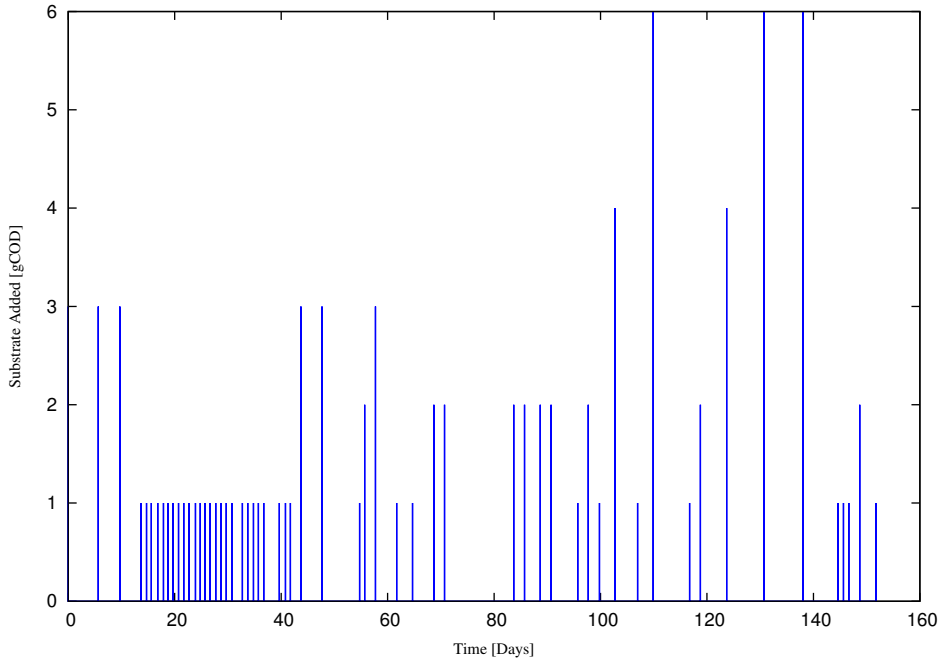

Figure 4.3: Substrate Slug Values Added to the Anaerobic Digester

accumulation values. From here we use an averaging function to approximate the profiles of methane accumulation, TCOD, IN, and VFA. This is done to facilitate the integration of experimental states dictated in Eq. (3.6) - (3.8), (3.16). In addition to this the derivative of the methane accumulation function was taken to specifically accomodate integration of Eq. (3.16). In this work the averaging function used was MATLAB's `csaps(x,y,p)` cubic smoothing spline function (part of the Curve Fitting Toolbox) and derivatives were taken using MATLAB's `fnder(f,1)`. `csaps(x,y,p)` uses the following function to smooth out experimental data [40].

$$p\left(\sum_{j=1}^{n} w(j)\left(y(:,j)-f(x(j))\right)^2\right)+(1-p)\left(\int \lambda(t)\left(\frac{\delta^2 f(t)}{dt^2}\right)^2 dt\right) \tag{4.1}$$

One of the pitfalls of this method for determination of *nr* is that the experimental observa-

Table 4.1: Feed Stream Composition

Total COD	30.0 gCOD/L
Protein Fraction	0.40 gCOD/gCOD
Lipid Fraction	0.15 gCOD/gCOD
Sugar Fraction	0.15 gCOD/gCOD
Inert Fraction	0.30 gCOD/gCOD
Volatile Fatty Acids	0.0 gCOD/L
Inorganic Nitrogen	0.011 mol/L
Inorganic Carbon	0.015 mol/L
Inert Cations - Anions	0.017 mol/L
Chlorine	0.00082 mol/L
Phosphorus	0.0051 mol/L
Sulfur	0.00050 mol/L
Sodium	0.013 mol/L
Potassium	0.0083 mol/L
Magnesium	0.00086 mol/L
Calcium	0.0020 mol/L
pH	9.4

tions must occur at identical time instants and so the calculations are limited by the smallest experimental data set. In the case of the LBE-INRA experiment approximately 218 measurement points exist total but volatile fatty acids were measured for only 75 of these points (owing to a more complicated measurement procedure) and so this dictated the measurement pairs that could be used for the subsequent calculations. Having said this, the process was applied to the experimental data set (original data provided in Appendix E) resulting in the principal component results depicted in Fig. 4.4.

Fig. 4.4 indicates that 2 or 3 reactions are required to explain 95% to 99% of the variability in the data. This work will investigate the validity of both cases.

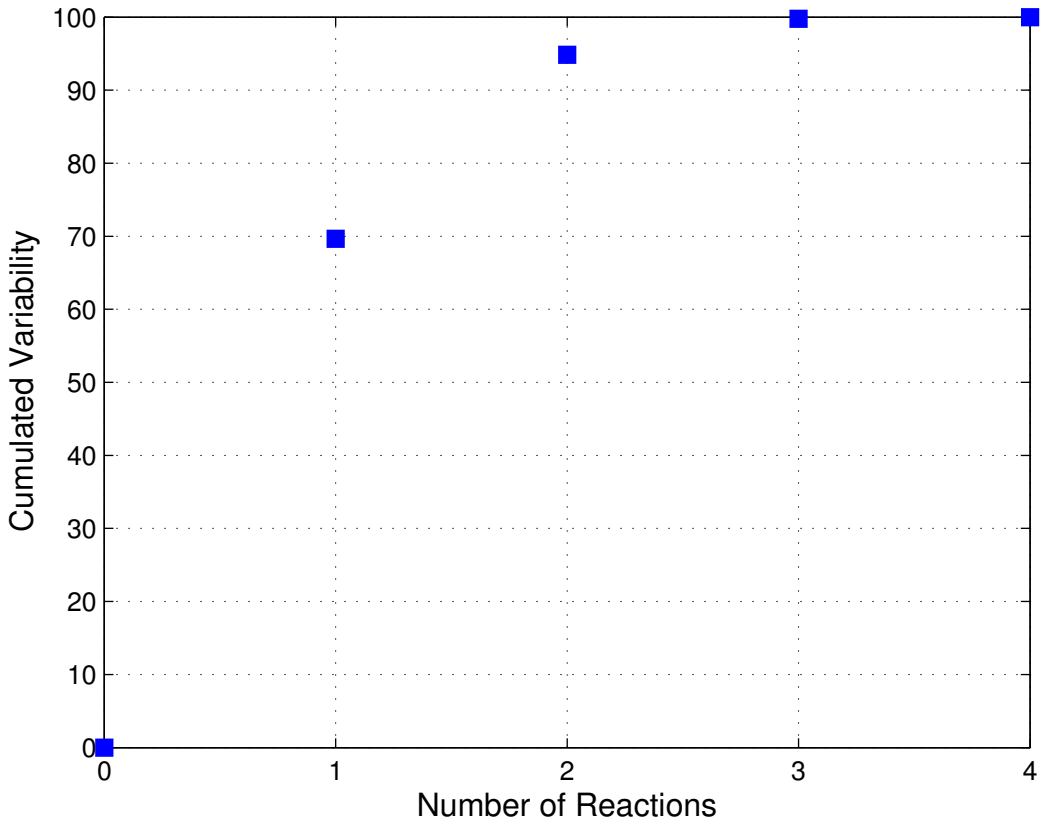

Figure 4.4: PCA results

4.2.2 Selection of Reaction Kinetics

Having settled on the number of reactions required to describe the available data, the next step is to determine what set of substrates and reaction kinetics will adequately perform this function. As was discussed in §2.1 a grey box model will be used to describe the system. As with all grey box models, much individual expertise comes into play and the choice of kinetics and overall model structure can be somewhat trial-and-error. While the procedure in §4.2.1 can help guide one towards appropriate reaction network complexity it provides no insight into what these reactions should be. Based on the current literature it was decided to meld the works of [3; 12; 39]. Of particular importance was the modelling of VFA (known to be a problem for methanogenic populations) and NH_3 (microalgae has a very high nitrogen/carbon ratio) inhibition.

We start the modelling process by selecting the individual components that will be modelled. As discussed in §2.2 the most up to date model for anaerobic digestion is the ADM1 model [3]. ADM1 considers 7 distinct bacterial populations as well as the additional biological kinetics of hydrolysis of the solid substrate (carried out by all populations). While very robust, this model is far too complex for our purposes and it is likely that the majority of the parameters in the model would be unable to be estimated due to insufficient information in the available measurements.

As shown in §4.2.1 2 or 3 reactions are needed to describe the experimental data. Having VFA and Methane production as two of the experimental measurements it is clear that methanogens are one of the key populations that should be included in the model. In addition to this, the initial hydrolysis and subsequent uptake of COD is likely to be critical to overall system dynamics (due to the inherent difficulty in breaking down microalgal

biomass). Therefore we need to include at least one set of kinetics that accounts for hydrolysis and acidogenisis/acetogenesis of the inlet organics. In the case of the two reaction model this closes the model selection process. Note that hydrolysis was compounded with the acidogenesis/acetogenesis to reduce model complexity (similar to the work of [12]).

Two Reaction Pathway

- Hydrolysis/Acidogenesis/Acetogenesis of Carbohydrates, LCFAs, and Proteins

$$\beta_1 S_1 + \beta_2 \mathrm{IN} \overset{\mu_1(S_1,\mathrm{IN})X_1}{\Longrightarrow} X_1 + \beta_3 S_2 + \beta_4 \mathrm{IC} \tag{4.2}$$

- Methanogenesis of Volatile Fatty Acids

$$\beta_5 S_2 + \beta_6 \mathrm{IN} \overset{\mu_2(\mathrm{NH_3},\mathrm{IN},S_2)X_2}{\Longrightarrow} X_2 + \beta_7 \mathrm{CH_4} + \beta_8 \mathrm{IC} \tag{4.3}$$

Where S_1 refers to the organic COD concentration (carbohydrates/ LCFAs/ proteins), IN refers to the inorganic nitrogen concentration (note that NH_4^+ is the consumed component of inorganic nitrogen but at pH near or below 7.0, IN $\approx$ NH_4^+ and so IN was modelled as the consumed quantity), X_1 refers to the acidogenic/acetogenic biomass group concentration, S_2 refers to the volatile fatty acids concentration, IC refers to the inorganic carbon conentration, X_1 refers to the methanogenic biomass group concentration, CH_4 refers to the methane gas released, and β_i refers to the ith stochiometric coefficient.

As [39] rightly points out the production of inorganic nitrogen (in the form of ammonium) of the experimental data set does not appear to correlate with the observed methane production rates. Figure set 4.5 displays the overlays of the experimentally observed Methane Flowrate with IN, VFA, and TCOD. During the first 40 days of the trial (i.e. the 28 day HRT

period) it is evident that the IN and TCOD profiles do not appear to match the methane flow trends. However, the IN and TCOD profiles appear to have roughly the same shape. This is likely because at the higher retention time a higher concentration of biomass is present and so with the longer HRT the TCOD profile follows the trend of the slowest reaction (evidently the predominant process associated with IN), as it is able to approach completion. However, once the HRT is switched to 18 days at roughly $t > 50$ days (which would wash out more bacteria) the slower IN dynamics become less of a dictating factor for the overall system COD dynamics. This is no more evident than during the last 40 days of the trial where excessive slugs were fed into the reactor to investigate batch behaviour. During this period it is obvious that the TCOD, VFA, and Methane profiles match up quite well (indicating a quick succession of COD $\rightarrow$ VFA $\rightarrow$ CH_4) where as the nitrogen does not appear to respond in a similar fashion.

Overlaying the experimental data with the feed slug regime in Figs. 4.6 and 4.7 seems to further support these original conclusions. It is clear that the initial slug pattern in quick succession would appear to coincide well with the gradual increase of TCOD and IN associated with a relatively constant feed at high HRT. However, once the HRT is decreased it becomes progressively obvious that the TCOD, VFA, and methane flow respond with the slugging pattern where as the IN profile reacts more evenly and sluggishly (indicating a disconnect with the rest of the COD consumption).

Therefore it was decided that a disconnect must be included between the core COD $\rightarrow$ VFA $\rightarrow$ CH_4 production and the COD consumption associated with the nitrogen dynamics. To this end protein was separated from carbohydrates/LCFAs and these two quantities were treated as separate substrates. Thus the final two reactions selected were the hydrolysis/acidogensis of carbohydrates/LCFAs and the hydrolysis/acidogenesis of protein.

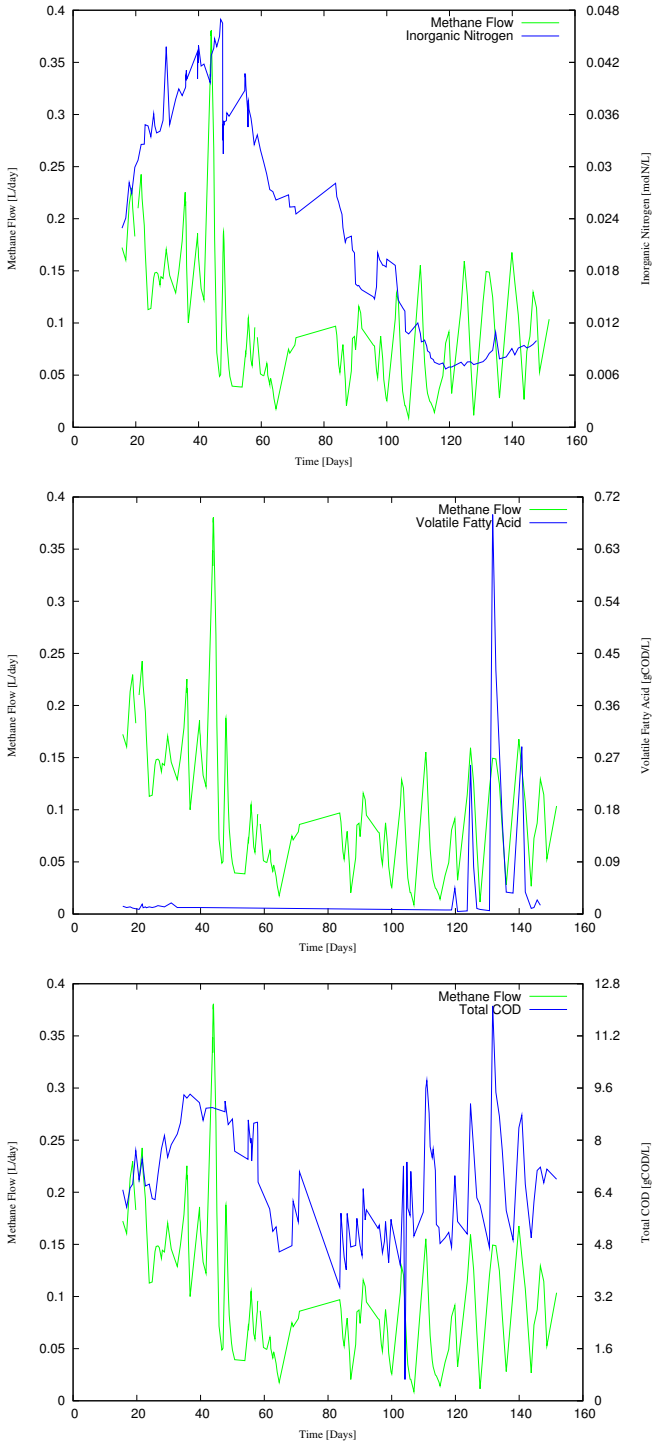

Figure 4.5: Methane Flow Rates Overlayed on all Other Experimental Measurements

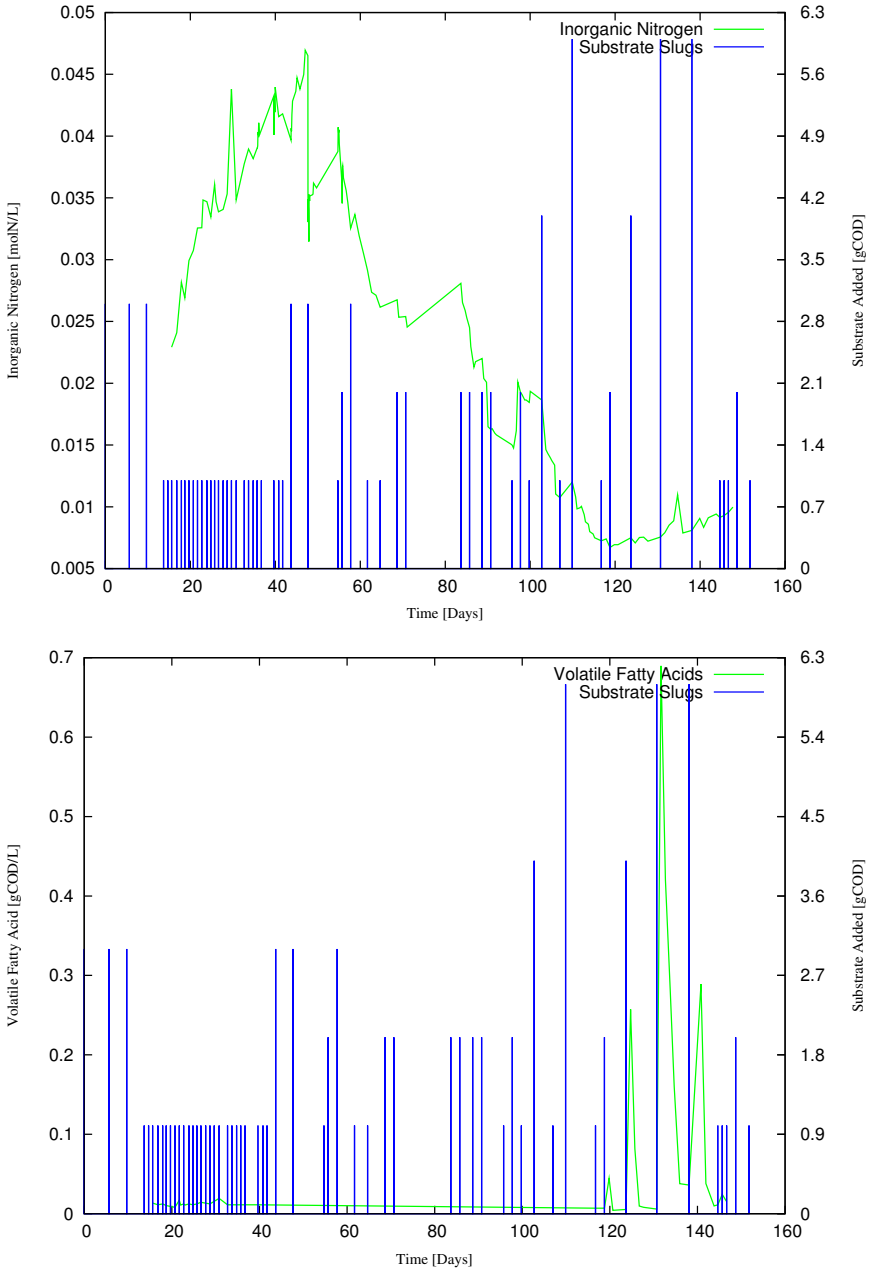

Figure 4.6: Substrate Slugs Overlayed on IN and VFA Experimental Data

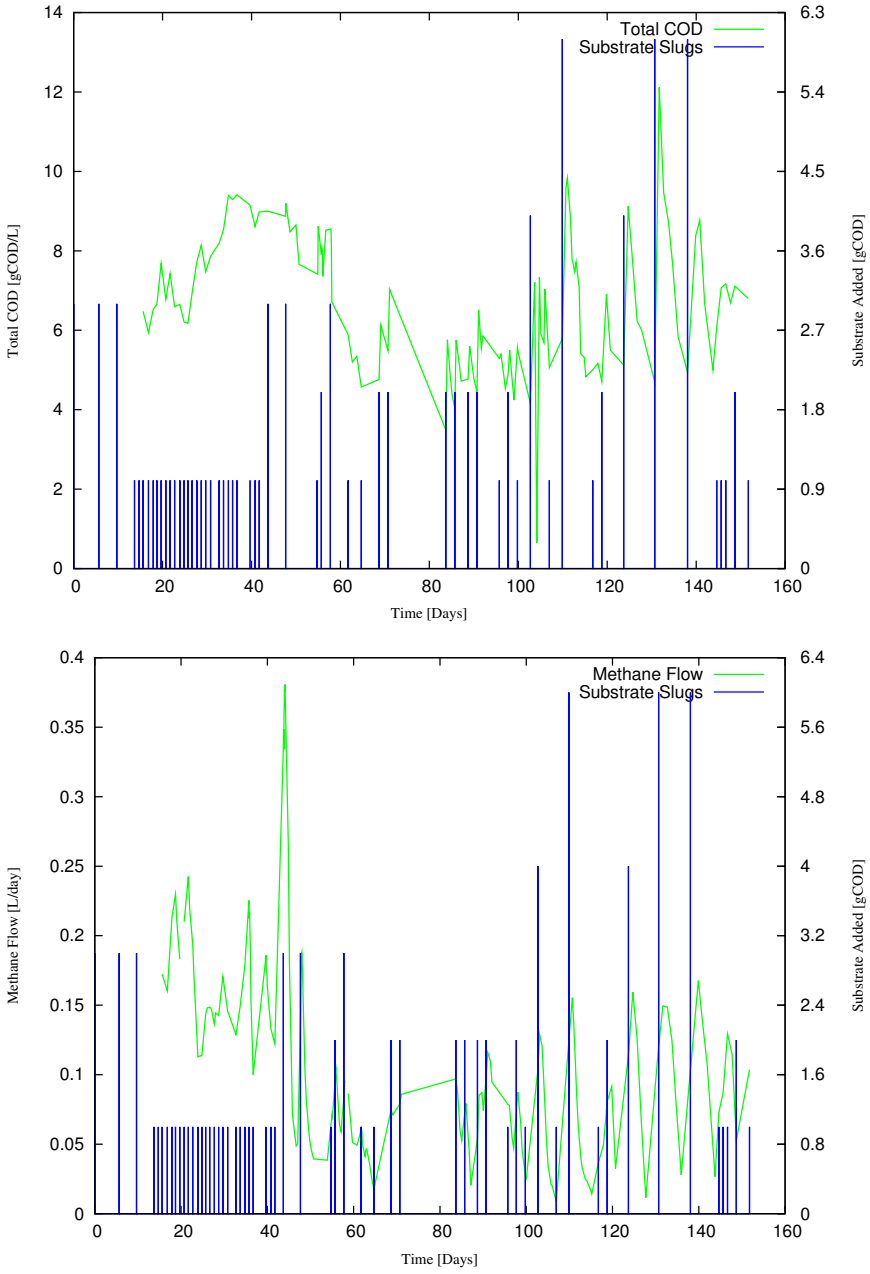

Figure 4.7: Substrate Slugs Overlayed on TCOD and Meth. Flow Experimental Data

Three Reaction Pathway

- Hydrolysis/Acidogenesis/Acetogenesis of Carbohydrates and LCFAs:

$$\beta_1 S_1 + \beta_2 \text{IN} \overset{\mu_1(S_1,\text{IN})X_1}{\Longrightarrow} X_1 + \beta_3 S_3 + \beta_4 \text{IC} \tag{4.4}$$

- Hydrolysis/Acidogenesis of Proteins:

$$\beta_5 S_2 \overset{\mu_2(S_2)X_2}{\Longrightarrow} X_2 + \beta_6 S_3 + \beta_7 \text{IN} + \beta_8 \text{IC} \tag{4.5}$$

- Methanogenesis of VFAs:

$$\beta_9 S_3 + \beta_{10} \text{IN} \overset{\mu_3(\text{NH}_3,\text{IN},S_3)X_3}{\Longrightarrow} X_3 + \beta_{11} \text{CH}_4 + \beta_{12} \text{IC} \tag{4.6}$$

Where S_1 refers to the carbohydrates/ LCFAs COD concentration, S_2 refers to the proetein COD concentration, IN refers to the inorganic nitrogen concentration, X_1 refers to the carbohydrates/ LCFAs metabolizing acidogenic biomass group concentration, X_2 refers to the protein metabolizing acidogenic biomass group concentration, S_3 refers to the volatile fatty acids concentration, IC refers to the inorganic carbon conentration, X_3 refers to the methanogenic biomass group concentration, CH_4 refers to the methane gas released, and β_i refers to the ith stochiometric coefficient.

In addition to these core substrate and bacterial populations the following quantities are included in the model:

- Inorganic Nitrogen (the other key macronutrient), IN
- Inorganic Carbon (the other major gas released during methanogenesis), IC

- Inert COD, S_4
- Hydronium, H^+
- Potassium (inert cation), K^+
- Sodium (inert cation), Na^+
- Calcium (inert cation), Ca^{2+}
- Magnesium (inert cation), Mg^{2+}
- Chlorine (inert anion), Cl^-
- Sulfur (inert anion), H_2SO_4, HSO_4^-, SO_4^{2-}
- Phosphorus (inert anion), H_3PO_4, $H_2PO_4^-$, HPO_4^{2-}, PO_4^{3-}

The ion species above were determined to be the most prominent during the experiment and will be used in alkalinity calculation (to be used as part of the pH balance).

Having selected the core components of each model the next step is to select appropriate kinetic relations. Both [3] and [12] consider anaerobic growth based on carbohydrates, LCFAs, and proteins to follow Monod kinetics. Therefore Monod kinetics will be used as starting point for both acidogenic populations:

$$\mu_1(S_1) = \bar{\mu}_1 \frac{S_1}{S_1 + K_1} \tag{4.7}$$

$$\mu_2(S_2) = \bar{\mu}_2 \frac{S_2}{S_2 + K_2} \tag{4.8}$$

As for the methanogenic population, [3] again considers monod kinetics where as the work of [12] considers the use of Haldane kinetics to incorporate possible substrate inhibition

into the kinetics. [12] observed good fit with their modified model and so it was decided to use this form for the current model.

$$\mu_3(S_3) = \bar{\mu}_3 \frac{S_3}{S_3 + K_3 + \frac{S_3^2}{K_{3,I}}} \tag{4.9}$$

In addition to these base kinetics it is also known that anaerobic digestors can react unfavourably to highly acidic or basic conditions. [3] accounts for this by multiplying kinetic rate laws by a pH inhibition factor. [3] actually gives 2 possible pH inhibition forms, one that accounts for only a lower pH threshold and one that accounts for both upper and lower bounds. The dual bound pH inhibition form was used for this work:

$$I_{\mathrm{pH}} = \frac{1 + 2\mathrm{x}10^{0.5(\mathrm{pH}_{LL} - \mathrm{pH}_{UL})}}{1 + 10^{(\mathrm{pH} - \mathrm{pH}_{UL})} + 10^{(\mathrm{pH}_{LL} - \mathrm{pH})}} \tag{4.10}$$

Where pH_{LL} and pH_{UL} are empirical lower and upper pH inhibition parameters respectively.

In addition to pH inhibition it is known that methanogens can suffer from ammonia inhibition. Since algae contain large amounts of nitrogen it was desired to include such an inhibition factor. [3] accounts for methanogen ammonia inhibition through a multiplicative inhibition factor (Eq. 4.11), which will be used for this work.

$$I_{\mathrm{NH_3}} = \frac{\mathrm{NH_3}}{\mathrm{NH_3} + K_{\mathrm{NH_3}}} \tag{4.11}$$

Finally, the COD balance that will serve as the basis for our model does not explicitly

account for a nitrogen balance. Therefore it is possible that a numerical simulator could drive inorganic nitrogen values to below zero if a lower bound is not explicitly included. This is accomplished for our system using a simply ε based lower bound function:

$$I_{\mathrm{IN}} = \frac{\mathrm{IN}}{\mathrm{IN}+\varepsilon}, \qquad \varepsilon << 1 \tag{4.12}$$

Incorporating these inhibition factors into our original base kinetic laws (Eq. (4.7) - (4.9)) leads to the following inhibited kinetic laws.

$$\mu_1'(S_1,\mathrm{IN},\mathrm{pH}) = \frac{\bar{\mu}_1 S_1}{S_1+K_1}\frac{1+2\mathrm{x}10^{0.5\left(\mathrm{pH}_{LL,A}-\mathrm{pH}_{UL,A}\right)}}{1+10^{\left(\mathrm{pH}-\mathrm{pH}_{UL,A}\right)}+10^{\left(\mathrm{pH}_{LL,A}-\mathrm{pH}\right)}}\frac{\mathrm{IN}}{\mathrm{IN}+\varepsilon} \tag{4.13}$$

$$\mu_2'(S_2,\mathrm{IN},\mathrm{pH}) = \frac{\bar{\mu}_2 S_2}{S_2+K_2}\frac{1+2\mathrm{x}10^{0.5\left(\mathrm{pH}_{LL,A}-\mathrm{pH}_{UL,A}\right)}}{1+10^{\left(\mathrm{pH}-\mathrm{pH}_{UL,A}\right)}+10^{\left(\mathrm{pH}_{LL,A}-\mathrm{pH}\right)}}\frac{\mathrm{IN}}{\mathrm{IN}+\varepsilon} \tag{4.14}$$

$$\mu_3'(S_3,\mathrm{IN},\mathrm{pH}) = \frac{\bar{\mu}_3 S_3}{S_3+K_3+\frac{S_3^2}{K_{3,I}}}\frac{\mathrm{NH_3}}{\mathrm{NH_3}+K_{\mathrm{NH_3}}}\frac{1+2\mathrm{x}10^{0.5\left(\mathrm{pH}_{LL,A}-\mathrm{pH}_{UL,A}\right)}}{1+10^{\left(\mathrm{pH}-\mathrm{pH}_{UL,A}\right)}+10^{\left(\mathrm{pH}_{LL,A}-\mathrm{pH}\right)}}\frac{\mathrm{IN}}{\mathrm{IN}+\varepsilon} \tag{4.15}$$

Naturally, to calculate both the pH and NH_3 inhibition terms in Eq. (4.13) - (4.15) we require a pH balance. The requisite charge balance presented in Eq. (4.16) is based on the assumptions that all acid/base pairs are in equilibrium and that the only major inerts contributing alkalinity are calcium, chlorine, magnesium, phosphorus, potassium, sodium, and sulfur.

$$Z + \left[H^+\right] + \left[NH_4^+\right] - \left[HCO_3^-\right] - \left[CO_3^{2-}\right] - \left[vfa_{ion}^-\right] - \left[OH^-\right] = 0 \tag{4.16}$$

$$\begin{aligned} Z = &\left[K^+\right] + \left[Na^+\right] + 2\left[Ca^{2+}\right] + 2\left[Mg^{2+}\right] - \left[Cl^-\right] - \left[H_2PO_4^-\right] - 2\left[HPO_4^{2-}\right] \\ &- 3\left[PO_4^{3-}\right] - \left[HSO_4^-\right] - \left[SO_4^{2-}\right] \end{aligned} \tag{4.17}$$

where

$$\left[NH_4^+\right] = \frac{IN\left[H^+\right]}{\left[H^+\right] + K_{NH_4^+}} \tag{4.18}$$

$$\left[NH_3\right] = IN - \left[NH_4^+\right] \tag{4.19}$$

$$\left[HCO_3^-\right] = \frac{IC K_{CO_2}}{\left[H^+\right] + K_{CO_2} + \frac{K_{CO_2} K_{HCO_3^-}}{\left[H^+\right]}} \tag{4.20}$$

$$\left[CO_3^{-2}\right] = \frac{\left[HCO_3^-\right] K_{HCO_3^+}}{\left[H^+\right]} \tag{4.21}$$

$$\left[CO_2\right] = IC - \left[HCO_3^-\right] - \left[CO_3^{-2}\right] \tag{4.22}$$

$$[H_3PO_4] = \frac{P\left[H^+\right]}{\left[H^+\right] + K_{H_3PO_4} + \frac{K_{H_3PO_4}K_{H_2PO_4^-}}{\left[H^+\right]} + \frac{K_{H_3PO_4}K_{H_2PO_4^-}K_{HPO_4^{-2}}}{\left[H^+\right]^2}} \tag{4.23}$$

$$\left[H_2PO_4^-\right] = \frac{[H_3PO_4]K_{H_3PO_4}}{\left[H^+\right]} \tag{4.24}$$

$$\left[HPO_4^{-2}\right] = \frac{\left[H_2PO_4^-\right]K_{H_2PO_4^-}}{\left[H^+\right]} \tag{4.25}$$

$$\left[OH^-\right] = \frac{K_{H_2O}}{\left[H^+\right]} \tag{4.26}$$

$$\left[HSO_4^-\right] = \frac{S\left[H^+\right]}{\left[H^+\right] + K_{HSO_4^-}} \tag{4.27}$$

$$\left[SO_4^{-2}\right] = S - \left[HSO_4^{-1}\right] \tag{4.28}$$

$$\left[vfa_{ion}^{-1}\right] = \frac{S_3}{MW_{ace}}\frac{K_{ace}}{K_{ace} + \left[H^+\right]} \tag{4.29}$$

With K_{CO_2}, $K_{HCO_3^-}$, $K_{HPO_4^-}$, $K_{H_2PO_4}$, $K_{H_3PO_4}$, K_{H_2O}, $K_{HSO_4^-}$, $K_{NH_4^+}$, and K_{ace} being respective equilibrium constants.

The final phenomena that must be accounted for is gas/liquid transfer. Without going into

complex non-equilibrium/non-ideal thermodynamics this can be modelled in two general ways. The first is through equilibrium relations and the second is through fluid dynamics. Without knowing the system overpressure and pipe friction characteristics it was decided to use the assumed equilibrium approach. This approach is generically applicable but can simplified greatly for the given system by making a few assumptions [12]. If we assume that CH_4 and CO_2 are the only significant gases produced, methane has no significant solubility, and both gases behave in a roughly ideal manner (this is consistent with [3; 12] and general engineering heuristics for low pressure gaseous systems) then we may use Henry's law and the ideal gas equation to derive equations for the gas flowrates. The fact that this is a binary gaseous system makes these derivations much simpler, but the general principle would apply to more complex systems. Since we have assumed that CH_4 has negligible solubility we may attribute its production rate directly to a reaction rate:

$$q_{\mathrm{CH_4}} = \left(\frac{\beta_{12}}{MW_{ace}}\right)\mu_3'(S_3, \mathrm{IN}, \mathrm{pH})X_3V_r \tag{4.30}$$

where $q_{\mathrm{CH_4}}$ is the methane production rate $(\mathrm{mol/day})$, β_{12} is the methanogenesis methane stoichiometric coefficient $(\mathrm{g\ COD/g\ COD})$, μ_3' is the methangoenesis rate $(\mathrm{g\ COD/day})$, X_3 is the methanogenic biomass concentration $(\mathrm{g\ COD/L})$, and V_r is the reactor volume (L).

If we assume that CO_2 is in equilibrium with the boundary layer (i.e. liquid diffusion controlled transfer) then we may approximate the release of CO_2 using standard diffusion laws and Henry's law:

$$q_{\mathrm{CO_2}} = k_L a\left([\mathrm{CO_2}] - P_{\mathrm{CO_2}}H_{\mathrm{CO_2}}\right) \tag{4.31}$$

Where q_{CO_2} is the carbon dioxide release rate (mol/day), k_La is the liquid area mass transfer coefficient $(1/\text{day})$, CO_2 is the carbon dioxide liquid concentration (mol/L), P_{CO_2} is the carbon dioxide partial pressure in the reactor headspace (atm), and H_{CO_2} is Henry's law constant for CO_2 $(\text{mol}/\text{L}*\text{atm})$.

In Eq. (4.31) the only piece of information we are missing is the carbon dioxide partial pressure P_{CO_2}. If we assume ideality then an equivalency can be formulated between partial pressures and gas flowrates.

$$\frac{P_{tot} - P_{CO_2}}{q_{CH_4}} = \frac{P_{CO_2}}{q_{CO_2}} \tag{4.32}$$

The reactor was operated with effluent gas eventually vented to atmosphere. Therefore a slight overpressure exists in the headspace (to facilitate gas motion). However, this was taken to be negligible and so P_{tot} is taken as equal to P_{atm}.

Subbing Eq. (4.31) into Eq. (4.32) and rearranging yields the quadratic Eq. 4.33.

$$H_{CO_2} P_{CO_2}^2 - \phi P_{CO_2} + P_{tot}\,[CO_2] = 0 \tag{4.33}$$

where

$$\phi = [CO_2] + P_{tot} H_{CO_2} + \left(\frac{\left(\frac{\beta_9 - 1}{MW_{ace}} \mu_3'(S_3, \text{IN}, \text{pH}) \right)}{k_{CO_2}} \right) \tag{4.34}$$

Only one of the two solutions to Eq. (4.33) yields a physical result.

$$P_{\mathrm{CO_2}} = \frac{\phi - \sqrt{\phi^2 - 4P_{tot}H_{\mathrm{CO_2}}[\mathrm{CO_2}]}}{2H_{\mathrm{CO_2}}} \tag{4.35}$$

Under perfect mixing conditions, the component-balances for the 2 reaction system are given in equation system (4.36).

$$\begin{aligned}
\dot{S}_1 &= -\beta_1\mu_1'(S_1,\mathrm{IN},\mathrm{pH})X_1 + D(Y_1 COD^{in} - S_1) \\
\dot{S}_2 &= \beta_3\mu_1'(S_1,\mathrm{IN},\mathrm{pH})X_1 - \beta_5\mu_2'(S_2,\mathrm{IN},\mathrm{pH})X_2 + D(Y_2 COD^{in} - S_2) \\
\dot{\mathrm{IN}} &= \beta_2\mu_1'(S_1,\mathrm{IN},\mathrm{pH})X_1 - \beta_6\mu_2'(S_2,\mathrm{IN},\mathrm{pH})X_2 + D(\mathrm{IN}^{in} - \mathrm{IN}) \\
\dot{S}_4 &= D(Y_4 COD^{in} - S_4) \\
\dot{X}_1 &= \mu_1'(S_1,\mathrm{IN},\mathrm{pH})X_1 + D(0 - f_b X_1) \\
\dot{X}_2 &= \mu_2'(S_2,\mathrm{IN},\mathrm{pH})X_2 + D(0 - f_b X_2) \\
\dot{\mathrm{IC}} &= \beta_4\mu_1'(S_1,\mathrm{IN},\mathrm{pH})X_1 + \beta_8\mu_2'(S_2,\mathrm{IN},\mathrm{pH})X_2 + D(\mathrm{IC}^{in} - \mathrm{IC}) + q_{\mathrm{CO_2}} \\
\dot{[\mathrm{Na}^+]} &= D([\mathrm{Na}^+]^{in} - [\mathrm{Na}^+]) \\
\dot{[\mathrm{K}^+]} &= D([\mathrm{K}^+]^{in} - [\mathrm{K}^+]) \\
\dot{[\mathrm{Ca}^{+2}]} &= D([\mathrm{Ca}^{+2}]^{in} - [\mathrm{Ca}^{+2}]) \\
\dot{[\mathrm{Mg}^{+2}]} &= D([\mathrm{Mg}^{+2}]^{in} - [\mathrm{Mg}^{+2}]) \\
\dot{[\mathrm{Cl}^-]} &= D([\mathrm{Cl}^-]^{in} - [\mathrm{Cl}^-]) \\
\dot{\mathrm{S}} &= D(\mathrm{S}^{in} - \mathrm{S}) \\
\dot{\mathrm{P}} &= D(\mathrm{P}^{in} - \mathrm{P}) \\
0 &= \mathrm{Z} + [\mathrm{H}^+] + [\mathrm{NH}_4^+] - [\mathrm{HCO}_3^-] - [\mathrm{CO}_3^{-2}] - [vfa_{ion}^-] - [\mathrm{OH}^-]
\end{aligned} \tag{4.36}$$

And the 3 reaction system are given in equation system (4.37).

$$
\begin{aligned}
\dot{S}_1 &= -\beta_1\mu_1'(S_1,\mathrm{IN},\mathrm{pH})X_1 + D(Y_1 COD^{in} - S_1) \\
\dot{S}_2 &= -\beta_5\mu_2'(S_2,\mathrm{IN},\mathrm{pH})X_2 + D(Y_2 COD^{in} - S_2) \\
\dot{S}_3 &= \beta_3\mu_1'(S_1,\mathrm{IN},\mathrm{pH})X_1 + \beta_7\mu_2'(S_2,\mathrm{IN},\mathrm{pH})X_2 \\
&\quad -\beta_9\mu_3'(S_3,\mathrm{IN},\mathrm{pH})X_3 + D(Y_3 COD^{in} - S_3) \\
\dot{\mathrm{IN}} &= -\beta_2\mu_1'(S_1,\mathrm{IN},\mathrm{pH})X_1 + \beta_6\mu_2'(S_2,\mathrm{IN},\mathrm{pH})X_2 \\
&\quad -\beta_{10}\mu_3'(S_3,\mathrm{IN},\mathrm{pH})X_3 + D(\mathrm{IN}^{in} - \mathrm{IN}) \\
\dot{S}_4 &= D(Y_4 COD^{in} - S_4) \\
\dot{X}_1 &= \mu_1'(S_1,\mathrm{IN},\mathrm{pH})X_1 + D(0 - f_b X_1) \\
\dot{X}_2 &= \mu_2'(S_2,\mathrm{IN},\mathrm{pH})X_2 + D(0 - f_b X_2) \\
\dot{X}_3 &= \mu_3'(S_3,\mathrm{IN},\mathrm{pH})X_3 + D(0 - f_b X_3) \\
\dot{\mathrm{IC}} &= \beta_4\mu_1'(S_1,\mathrm{IN},\mathrm{pH})X_1 + \beta_6\mu_2'(S_2,\mathrm{IN},\mathrm{pH})X_2 \\
&\quad +\beta_{10}\mu_3'(S_3,\mathrm{IN},\mathrm{pH})X_3 + D(\mathrm{IC}^{in} - \mathrm{IC}) + q_{\mathrm{CO}_2} \\
\dot{[\mathrm{Na}^+]} &= D([\mathrm{Na}^+]^{in} - [\mathrm{Na}^+]) \\
\dot{[\mathrm{K}^+]} &= D([\mathrm{K}^+]^{in} - [\mathrm{K}^+]) \\
\dot{[\mathrm{Ca}^{+2}]} &= D([\mathrm{Ca}^{+2}]^{in} - [\mathrm{Ca}^{+2}]) \\
\dot{[\mathrm{Mg}^{+2}]} &= D([\mathrm{Mg}^{+2}]^{in} - [\mathrm{Mg}^{+2}]) \\
\dot{[\mathrm{Cl}^-]} &= D([\mathrm{Cl}^-]^{in} - [\mathrm{Cl}^-]) \\
\dot{\mathrm{S}} &= D(\mathrm{S}^{in} - \mathrm{S}) \\
\dot{\mathrm{P}} &= D(\mathrm{P}^{in} - \mathrm{P}) \\
0 &= \mathrm{Z} + [\mathrm{H}^+] + [\mathrm{NH}_4^+] - [\mathrm{HCO}_3^-] - [\mathrm{CO}_3^{-2}] - [vfa_{ion}^-] - [\mathrm{OH}^-]
\end{aligned}
\tag{4.37}
$$

Note that both of these models make the following assumptions (as alluded to in its derivation).

- The reactor is perfectly mixed
- The reactor is operated at constant volume
- The VFAs are composed entirely of acetic acid
- VFA, Sulfur, Oxygen, and all other trace gas sources are negligible
- Phosphorus and all other micronutrient needs are negligible and non-limiting
- Cl, S, P, Na, K, Ca, and Mg are the major contributing inert charges
- All acid/base pairs are in equilibrium
- Ammonia/ammonium is the only major inorganic nitrogen form
- Methane is insoluble

4.3 Systematic Parameter Identification

A large part of the research was spent testing and refining the applied identification algorithm. As mentioned in §4.2.1, both a 2 reaction and 3 reaction scheme were selected for our data set. Before going into actual fitting results it is important to first discuss an anomaly observed in the experimental data. It was observed during the 6 month experiment that a difference in influent and effluent COD values arose (effluent COD included both liquid effluent and methane). This difference was observed to accumulate gradually over the entire experimental run (shown in Fig. 4.8) but did not appear to progress linearly and so was likely a result of multiple influences, the three most obvious being:

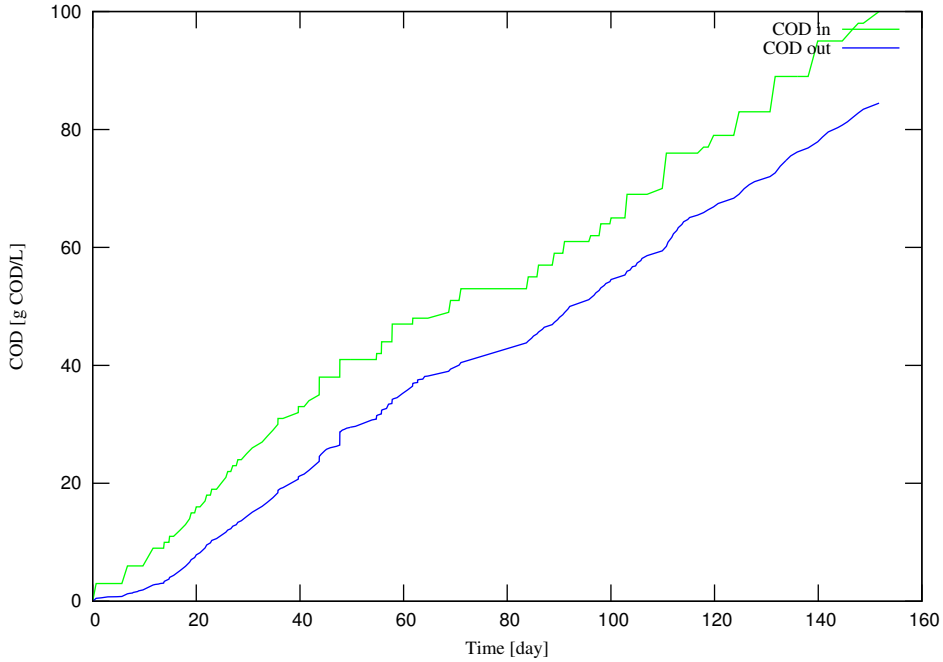

Figure 4.8: Observed Imbalance Between Inlet and Outlet COD

- Several times during the experiment a leak was located in the biogas outlet resulting in misread biogas accumulation values
- Near the end of the experiment it was observed that biofilms had formed on the walls and the pH probe resulting in diluted TCOD readings throughout the experiment
- The algae feed could potentially contain oxygen (produced during growth) that could promote heterotrophic growth in the anarobic digester

The clear consequence of this was that less confidence could be placed in the TCOD and Biogas Accumulation/Flow measurement. To this end a weighting factor of 10 was applied to the inorganic nitrogen, VFA, and % methane measurements during fitting.

4.3.1 Two Reaction System

First the two reaction system presented on page 72 will be examined. As mentioned in §4.2.2 there are numerous types of parameters contained within a model but not all need to be examined. For this system it was determined, primarily through discussion with LBE-INRA staff, that stoichiometric and acid/base constants are likely to be fairly constant and so could be reasonably estimated from literature. This left the kinetic and initial concentration parameters. As implied during the derivation of the identification algorithm, not all parameters will be estimated. Therefore suitable defaults must be selected. These are provided in Tab. 4.2.

Table 4.2: Default Parameter Values for Two Reaction System (Eq. 4.36)

Var.	Val.	Unit	Ref.	Var.	Val.	Unit	Ref.	Var.	Val.	Unit	Ref.
Y_1	0.7	$\left[\frac{\text{g COD}}{\text{g COD}}\right]$	[39]	f_b	1.0	$[-]$	[50]	K_{CO_2}	4.937 x 10^{-7}	$\left[\frac{\text{mol}}{\text{L}}\right]$	[3]
Y_I	0.3	$\left[\frac{\text{g COD}}{\text{g COD}}\right]$	[39]	K_1	0.3	$\left[\frac{\text{g COD}}{\text{L}}\right]$	[3]	$K_{HCO_3^-}$	5.670 x 10^{-11}	$\left[\frac{\text{mol}}{\text{L}}\right]$	[3]
β_1	12.5	$\left[\frac{\text{g COD}}{\text{g COD}}\right]$	[3]	K_{NH_3}	0.0018	$\left[\frac{\text{mol N}}{\text{L}}\right]$	[3]	$K_{HPO_4^{-2}}$	1.777 x 10^{-13}	$\left[\frac{\text{mol}}{\text{L}}\right]$	[3]
β_2	0.04	$\left[\frac{\text{mol N}}{\text{g COD}}\right]$	[3]	K_2	0.15	$\left[\frac{\text{g COD}}{\text{L}}\right]$	[3]	$K_{h_2PO_4}$	6.464 x 10^{-8}	$\left[\frac{\text{mol}}{\text{L}}\right]$	[3]
β_3	11.5	$\left[\frac{\text{g COD}}{\text{g COD}}\right]$	[3]	$K_{2,I}$	16.384	$\left[\frac{\text{g COD}^2}{\text{L}^2}\right]$	[12]	$K_{H_3PO_4}$	6.855 x 10^{-3}	$\left[\frac{\text{mol}}{\text{L}}\right]$	[3]
β_4	0.04	$\left[\frac{\text{mol C}}{\text{g COD}}\right]$	[3]	ε	10^{-15}	$\left[\frac{\text{"unit"}}{\text{L}}\right]$		K_{H_2O}	2.079 x 10^{-14}	$\left[\frac{\text{mol}}{\text{L}}\right]$	[3]
β_5	13.1	$\left[\frac{\text{g COD}}{\text{g COD}}\right]$	[3]	$\bar{\mu}_1$	0.2	$\left[\frac{1}{\text{day}}\right]$	[3]	$K_{HSO_4^-}$	8.943 x 10^{-3}	$\left[\frac{\text{mol}}{\text{L}}\right]$	[3]
β_6	0.006	$\left[\frac{\text{mol N}}{\text{g COD}}\right]$	[3]	$\bar{\mu}_2$	0.2	$\left[\frac{1}{\text{day}}\right]$	[3]	$K_{NH_4^+}$	1.110 x 10^{-9}	$\left[\frac{\text{mol}}{\text{L}}\right]$	[3]
β_7	12.1	$\left[\frac{\text{g COD}}{\text{g COD}}\right]$	[3]	k_{CO_2}	5.0	$\left[\frac{1}{\text{day}}\right]$	[39]	K_{ace}	1.729 x 10^{-7}	$\left[\frac{\text{mol}}{\text{L}}\right]$	[3]
β_8	0.12	$\left[\frac{\text{mol C}}{\text{g COD}}\right]$	[3]	$S_1(0)$	1.0	$\left[\frac{\text{g COD}}{\text{L}}\right]$		H_{CO_2}	0.027	$\left[\frac{\text{mol}}{\text{L*atm}}\right]$	[3]
				$X_1(0)$	1.0	$\left[\frac{\text{g COD}}{\text{L}}\right]$		$\text{pH}_{UL,AA}$	5.5 (13.5)	$[-]$	[3]
				$X_2(0)$	1.0	$\left[\frac{\text{g COD}}{\text{L}}\right]$		$\text{pH}_{LL,AA}$	4.0 (0.5)	$[-]$	[3]
								$pH_{UL,M}$	7.0 (13.5)	$[-]$	[3]
								$pH_{LL,M}$	6.0 (0.5)	$[-]$	[3]

Of the trials conducted for the 2 reaction system, the two most revealing runs will be dis-

cussed here. The pertinent details of Trial #1 are provided in the list below (Trial #2 was conducted using the same details but the n_{keep} threshold was changed to 50 %). Recall that n_{keep} refers to the number of "top" combinations kept between each identification stage, $Thresh$ is the base confidence required by all estimates, LS weights are any additional weighting factors applied to each observation, and Parameter Set is the set of all parameters being considered during the identification run (as explained in §3.2.1).

- $n_{keep} = 3$
- $Thresh = 25\ \%$
- LS Weights: IN (10), VFA (10), TCOD (1), Biogas Flow (10), % CH_4 (1)
- Parameter Set: $\bar{\mu}_1$, K_1, $\bar{\mu}_2$, K_2, $K_{2,I}$, K_{NH_3}, k_{CO_2}, $S_1(0)$, $X_1/X_2(0)$

A summary of each stage of the identification run for trial #1 and #2 are provided in Tab. B.1 and B.2 in Appendix B The final "best three" combinations (for $n_{keep} = 3$) are provided in Tab. 4.3. From Tab. B.1 and B.2 it appears clear that the algorithm quickly zeros in on the kinetic parameters of K_1, K_2, K_{NH_3}, at least one appearing in almost all of the combinations. The only clear difference for the 50% case was the addition of the substrate inhibition parameter $K_{2,I}$ to the best combinations. Looking at the progression of solved for tolerances in Tab. B.1 and B.2 it is clear that K_2 just missed the 25% threshold and would appear to suffer from the same correlation issues as K_{NH_3}. In response to these correlations (as will be discussed in §6.2.1) the next logical step would be to design experiments to reduce the correlations amongst the parameters.

It is also of interest that a kinetic parameter from each of the two rate laws was selected, indicating that there is a significant enough amount of information contained within the data sets to distinguish the two reactions (as predicted by §4.2.1). Of interest in this vain is the

value of K_1, whose value appears to be insensitive to changes in other parameters. This was found to be true (within tolerances) in both the 25% and 50% threshold trials. This is not as true for the values of $K_{vfa_{b1}}$ and $K_{nh_{3b}}$, which appear to have some dependence on each others value. This is not entirely unexpected as they are associated with the same rate law and so to a certain extent depend on the same system dynamics for identification (resulting in a higher potential for correlation). Despite the presence of kinetic terms from both laws being present, the fact that one or more parameters are ommitted from each rate law indicates that there is likely a high degree of correlation between certain parameter pairs (such as the $\bar{\mu}$ and K as is quite common in biological rate laws). A study of contour plots of $\bar{\mu}_1$ vs. K_1 and $\bar{\mu}_2$ vs. K_2 showed fairly evident contour elongation nearing the local optimum, indicating a high degree of correlation. This will have ramifications on later steady state analysis.

Table 4.3: Final Optimal Parameter Combinations for Two Reaction Set Trial #1 and #2

Trial #1					
$\mathscr{J}$	**934.645**	$\mathscr{J}$	**941.896**	$\mathscr{J}$	**980.384**
$\mathbf{K_1}$	$\mathbf{1.54x10^{0} \pm 2.1x10^{-1}}$	$\mathbf{K_1}$	$\mathbf{1.61x10^{0} \pm 1.7x10^{-1}}$	$\mathbf{K_1}$	$\mathbf{1.41x10^{0} \pm 1.9x10^{-1}}$
$\mathbf{K_2}$	$\mathbf{8.48x10^{-2} \pm 1.72x10^{-2}}$	$\mathbf{K_2}$	$\mathbf{8.55x10^{-2} \pm 1.71x10^{-2}}$	$\mathbf{K_2}$	$\mathbf{1.37x10^{-1} \pm 1.4x10^{-2}}$
$\mathbf{K_{NH_3}}$	$\mathbf{5.37x10^{-4} \pm 1.27x10^{-4}}$	$\mathbf{K_{NH_3}}$	$\mathbf{5.14x10^{-4} \pm 1.11x10^{-4}}$	$\mathbf{S_1(0)}$	$\mathbf{8.41x10^{-1} \pm 9.2x10^{-2}}$
$\mathbf{S_1(0)}$	$\mathbf{9.40x10^{-1} \pm 1.0x10^{-1}}$				
Trial #2					
$\mathscr{J}$	**935.069**	$\mathscr{J}$	**940.355**	$\mathscr{J}$	**941.896**
$\mathbf{K_1}$	$\mathbf{1.71x10^{0} \pm 2.4x10^{-1}}$	$\mathbf{K_1}$	$\mathbf{1.54x10^{0} \pm 2.0x10^{-1}}$	$\mathbf{K_1}$	$\mathbf{1.61x10^{0} \pm 1.7x10^{-1}}$
$\mathbf{K_2}$	$\mathbf{1.09x10^{-1} \pm 1.3x10^{-2}}$	$\mathbf{K_2}$	$\mathbf{8.48x10^{-2} \pm 1.71x10^{-2}}$	$\mathbf{K_2}$	$\mathbf{8.55x10^{-2} \pm 1.71x10^{-2}}$
$\mathbf{K_{2,I}}$	$\mathbf{1.31x10^{0} \pm 4.04x10^{-1}}$	$\mathbf{K_{NH_3}}$	$\mathbf{5.37x10^{-4} \pm 1.27x10^{-4}}$	$\mathbf{K_{nH_3}}$	$\mathbf{5.14x10^{-4} \pm 1.11x10^{-4}}$
$\mathbf{S_1(0)}$	$\mathbf{8.43x10^{-1} \pm 9.0x10^{-2}}$	$\mathbf{S_1(0)}$	$\mathbf{9.40x10^{-1} \pm 1.0x10^{-1}}$		

Profiles for the top three combinations (as determined by least squares fit) are provided in Fig. 4.9 - 4.11 and Fig. 4.12 - 4.14. From these plots it is clear that fit over the first 80 days

or so is quite good, but things appear to break down after that. This is most evident in the inorganic nitrogen fits, which clearly indicate that nitrogen is being overproduced for the given quantities of biomass and substrate in the system. This very much falls in line with the initial observations made in §4.2.2. It would appear that a clear distinction between net nitrogen producing and nitrogen consuming biomass is important to overall fit. As will be seen when examining the three reaction system, the acidogenesis of proteins turned out to be the slowest of the three kinetic relations, which would naturally cause its kinetics to become more evident in the system dynamics as biomass concentrations decrease (as would occur when the HRT is decreased but overall load is maintained, like in this experiment). Thus it would appear that a more appropriate two reaction system might be to model the direct conversion of sugars/lipids to methane and proteins to methane (perhaps incorporating some of the substrate inhibition of the vfa model into these two systems). There was insufficient time to study such a system but it would be very interesting to examine if it sures up the nitrogen fit issues. For now it is enough to conclude that this particular two reaction system does not appear to model the experimental data well. This agrees positively with the independent identification attempts conducted by [39] on the same data set.

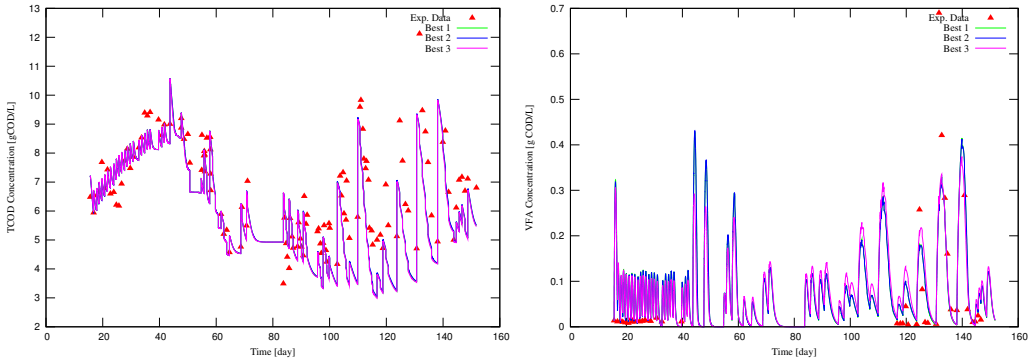

(a) Total COD (b) VFA

Figure 4.9: Top 3 TCOD and VFA Prediction Results for Two Reaction Set Trial # 1

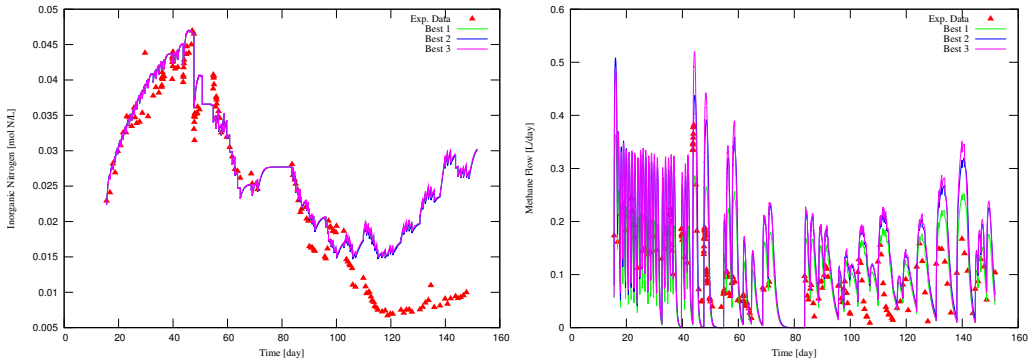

(a) Inorganic Nitrogen (b) Methane Flow

Figure 4.10: Top 3 IN and Meth. Flow Prediction Results for Two Reaction Set Trial # 1

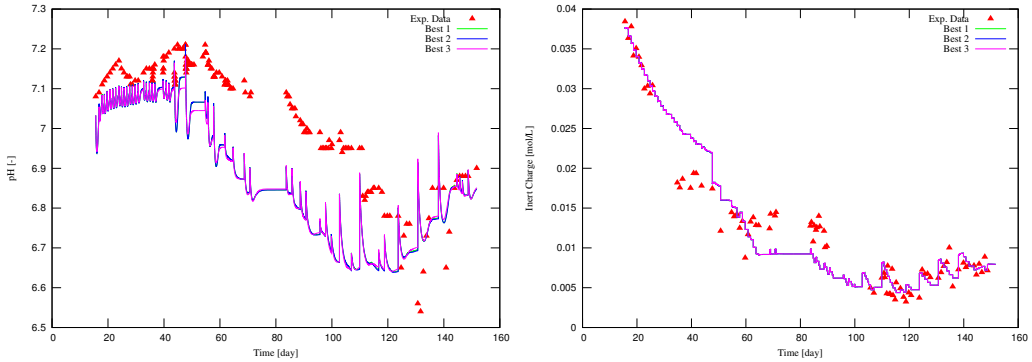

(a) pH (b) Inert Charge

Figure 4.11: Top 3 pH and Inert Charge Prediction Results for Two Reaction Set Trial # 1

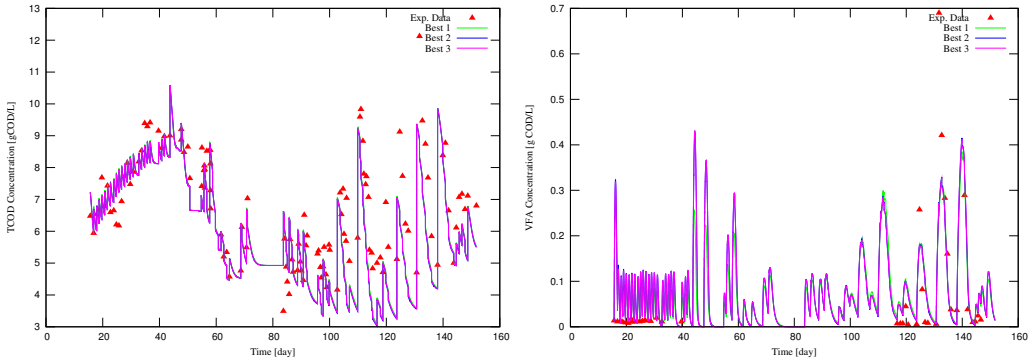

(a) Total COD (b) VFA

Figure 4.12: Top 3 TCOD and VFA Prediction Results for Two Reaction Set Trial # 2

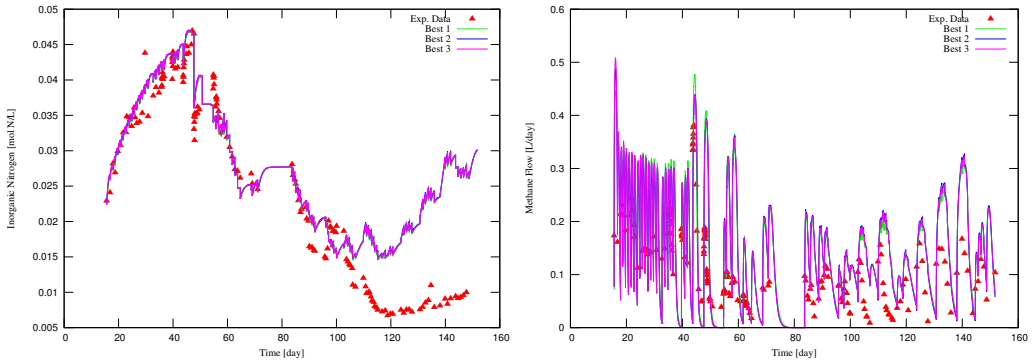

(a) Inorganic Nitrogen (b) Methane Flow

Figure 4.13: Top 3 IN and Meth. Flow Prediction Results for Two Reaction Set Trial # 2

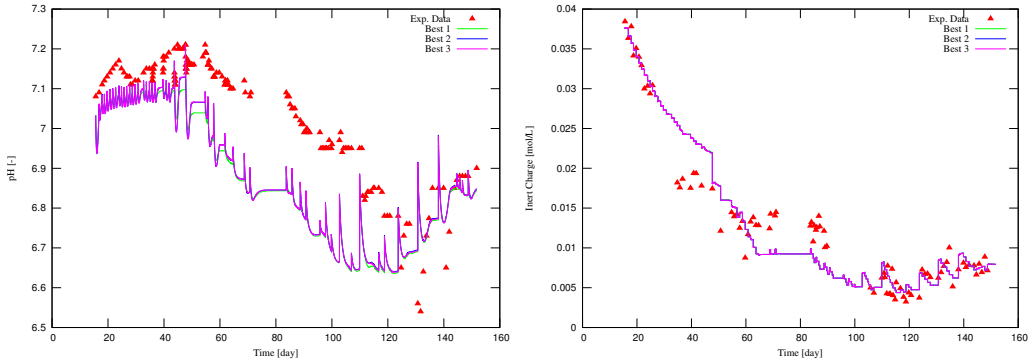

(a) pH (b) Inert Charge

Figure 4.14: Top 3 pH and Inert Charge Prediction Results for Two Reaction Set Trial # 2

All this being said, the proposed parameter identification algorithm appears to operate consistently and results in reasonable fits (model mismatches aside). This will become especially apparent when the three reaction system is examined.

4.3.2 Three Reaction System

Having discounted the current two reaction scheme the next step was to examine the selected three reaction scheme (as presented in Eq. (4.37)). As with the two reaction scheme a set of default parameters was selected from the literature. These are presented in Tab. 4.4.

Table 4.4: Default Parameter Values for Three Reaction System (Eq. 4.37)

Var.	Val.	Unit	Ref.	Var.	Val.	Unit	Ref.	Var.	Val.	Unit	Ref.
Y_1	0.3	$\left[\frac{\text{g COD}}{\text{g COD}}\right]$	[39]	f_b	1.0	$[-]$	[50]	K_{CO_2}	4.937 x 10^{-7}	$\left[\frac{\text{mol}}{\text{L}}\right]$	[3]
Y_2	0.4	$\left[\frac{\text{g COD}}{\text{g COD}}\right]$	[39]	K_2	0.3	$\left[\frac{\text{g COD}}{\text{L}}\right]$	[3]	K_{HCO_3}	5.670 x 10^{-11}	$\left[\frac{\text{mol}}{\text{L}}\right]$	[3]
Y_I	0.3	$\left[\frac{\text{g COD}}{\text{g COD}}\right]$	[39]	K_1	0.45	$\left[\frac{\text{g COD}}{\text{L}}\right]$	[3]	$K_{HPO_4^{-2}}$	1.777 x 10^{-13}	$\left[\frac{\text{mol}}{\text{L}}\right]$	[3]
β_1	12.5	$\left[\frac{\text{g COD}}{\text{g COD}}\right]$	[3]	K_{NH_3}	0.0018	$\left[\frac{\text{mol N}}{\text{L}}\right]$	[3]	$K_{H_2PO_4^-}$	6.464 x 10^{-8}	$\left[\frac{\text{mol}}{\text{L}}\right]$	[3]
β_2	0.00625	$\left[\frac{\text{mol N}}{\text{g COD}}\right]$	[3]	K_3	0.15	$\left[\frac{\text{g COD}}{\text{L}}\right]$	[3]	$K_{H_3PO_4}$	6.855 x 10^{-3}	$\left[\frac{\text{mol}}{\text{L}}\right]$	[3]
β_3	11.5	$\left[\frac{\text{g COD}}{\text{g COD}}\right]$	[3]	$K_{3,I}$	16.384	$\left[\frac{\text{g COD}^2}{\text{L}^2}\right]$	[12]	K_{H_2O}	2.079 x 10^{-14}	$\left[\frac{\text{mol}}{\text{L}}\right]$	[3]
β_4	0.045	$\left[\frac{\text{mol C}}{\text{g COD}}\right]$	[3]	ε	10^{-15}	$\left[\frac{\text{"unit"}}{\text{L}}\right]$		$K_{HSO_4^-}$	8.943 x 10^{-3}	$\left[\frac{\text{mol}}{\text{L}}\right]$	[3]
β_5	12.5	$\left[\frac{\text{g COD}}{\text{g COD}}\right]$	[3]	$\bar{\mu}_1$	0.175	$\left[\frac{1}{\text{day}}\right]$	[3]	$K_{NH_4^+}$	1.110 x 10^{-9}	$\left[\frac{\text{mol}}{\text{L}}\right]$	[3]
β_6	0.08125	$\left[\frac{\text{mol N}}{\text{g COD}}\right]$	[3]	$\bar{\mu}_2$	0.2	$\left[\frac{1}{\text{day}}\right]$	[3]	K_{ace}	1.729 x 10^{-7}	$\left[\frac{\text{mol}}{\text{L}}\right]$	[3]
β_7	11.5	$\left[\frac{\text{g COD}}{\text{g COD}}\right]$	[3]	$\bar{\mu}_3$	0.2	$\left[\frac{1}{\text{day}}\right]$	[3]	H_{CO_2}	0.027	$\left[\frac{\text{mol}}{\text{L*atm}}\right]$	[3]
β_8	0.045	$\left[\frac{\text{mol C}}{\text{g COD}}\right]$	[3]	k_{co_2}	5.0	$\left[\frac{1}{\text{day}}\right]$	[39]	$\text{pH}_{UL,AA}$	5.5 (13.5)	$[-]$	[3]
β_9	13.1	$\left[\frac{\text{g COD}}{\text{g COD}}\right]$	[3]	$S_1(0)$	1.0	$\left[\frac{\text{g COD}}{\text{L}}\right]$		$\text{pH}_{LL,AA}$	4.0 (0.5)	$[-]$	[3]
β_{10}	0.00625	$\left[\frac{\text{mol N}}{\text{g COD}}\right]$	[3]	$S_2(0)$	1.0	$\left[\frac{\text{g COD}}{\text{L}}\right]$		$\text{pH}_{UL,M}$	7.0 (13.5)	$[-]$	[3]
β_{11}	0.19	$\left[\frac{\text{mol CH}_4}{\text{g COD}}\right]$	[3]	$S_3(0)$	1.0	$\left[\frac{\text{g COD}}{\text{L}}\right]$		$\text{pH}_{LL,M}$	6.0 (0.5)	$[-]$	[3]
β_{12}	0.12	$\left[\frac{\text{mol C}}{\text{g COD}}\right]$	[3]	$X_1(0)$	1.0	$\left[\frac{\text{g COD}}{\text{L}}\right]$					
				$X_2(0)$	1.0	$\left[\frac{\text{g COD}}{\text{L}}\right]$					
				$X_3(0)$	1.0	$\left[\frac{\text{g COD}}{\text{L}}\right]$					

Of the trials conducted, six key experimental runs will be discussed here. The basic trial conditions (identical to those of trial #1 for the two reaction system) are presented below.

- $n_{keep} = 3$
- $Thresh = 25\ \%$
- LS Weights: IN (10), VFA (10), TCOD (1), Biogas Flow (1), % CH_4 (10)
- Parameter Set: $\bar{\mu}_1$, K_1, $\bar{\mu}_2$, K_2, $\bar{\mu}_3$, K_3, $K_{3,I}$, K_{NH_3}, k_{CO_2}, $S_{\#}(0)$, $X_{\#}(0)$

The basic thought pattern of the six presented trials is as follows. Trial #1 and #2 follow the same logic as the two reaction tests (§4.3.1) and examine the impact of changing the algorithm threshold ($Thresh = 25\ \% \rightarrow 50\ \%$) on the weighted system results (recall that the weighting was selected to offset perceived errors in the Gas Flow and TCOD measurements). Trial #3 assesses the impact of splitting the data set in half to provide both an identification set and a verification set (standard process identification practice). One of the key issues noticed through out the model development phase was the selection of consistent/optimal initial conditions (there was simply too little information in the experimental data). Trial #4 attempts to address this issue by assuming the experimental trial began at steady state (this involves applying the theory covered in §3.2.2). Finally, trials #5 and #6 examine the impact of the original weighting scheme assumptions made at the beginning of this chapter (i.e. setting all least squares weight factors to 1). The analysis of these last two trials has been moved to Appendix C.

Appendix B contains the complete runs of each of these trials. The more pertinent sets of top 3 combinations determined in each trial are presented in Tab. 4.5. These will be discussed in further detail throughout this section.

Table 4.5: Final Optimal Parameter Combinations for Three Reaction Set Trials

Trial #1					
$\mathscr{J}$	**649.701**	$\mathscr{J}$	**681.441**	$\mathscr{J}$	**686.002**
$\bar{\mu}_1$	$3.69\text{x}10^{-1} \pm 1.8\text{x}10^{-2}$	$\bar{\mu}_1$	$3.58\text{x}10^{-1} \pm 1.7\text{x}10^{-2}$	$\bar{\mu}_1$	$3.54\text{x}10^{-1} \pm 1.7\text{x}10^{-2}$
$\bar{\mu}_2$	$3.64\text{x}10^{-2} \pm 2.7\text{x}10^{-3}$	$\bar{\mu}_2$	$3.77\text{x}10^{-2} \pm 3.2\text{x}10^{-3}$	$\bar{\mu}_2$	$3.46\text{x}10^{-2} \pm 2.1\text{x}10^{-3}$
K_3	$7.12\text{x}10^{-2} \pm 1.45\text{x}10^{-2}$	K_3	$1.16\text{x}10^{-1} \pm 1.0\text{x}10^{-2}$	K_3	$1.16\text{x}10^{-1} \pm 1.0\text{x}10^{-3}$
$K_{3,I}$	$1.98\text{x}10^{0} \pm 4.9\text{x}10^{-1}$	$S_{\#}(0)$	$8.38\text{x}10^{-1} \pm 1.19\text{x}10^{-1}$		
Trial #2					
$\mathscr{J}$	**593.444**	$\mathscr{J}$	**613.985**	$\mathscr{J}$	**616.651**
$\bar{\mu}_1$	$3.95\text{x}10^{-1} \pm 2.3\text{x}10^{-2}$	$\bar{\mu}_1$	$3.79\text{x}10^{-1} \pm 1.9\text{x}10^{-2}$	$\bar{\mu}_1$	$3.69\text{x}10^{-1} \pm 1.7\text{x}10^{-2}$
K_2	$4.83\text{x}10^{0} \pm 7.6\text{x}10^{-1}$	K_2	$6.43\text{x}10^{0} \pm 9.3\text{x}10^{-1}$	K_2	$6.38\text{x}10^{0} \pm 9.5\text{x}10^{-1}$
K_3	$4.10\text{x}10^{-2} \pm 1.27\text{x}10^{-2}$	K_3	$5.45\text{x}10^{-2} \pm 1.35\text{x}10^{-2}$	$\bar{\mu}_3$	$1.54\text{x}10^{-1} \pm 6.0\text{x}10^{-3}$
$K_{3,I}$	$1.33\text{x}10^{0} \pm 1.7\text{x}10^{-1}$	$K_{3,I}$	$1.55\text{x}10^{0} \pm 2.5\text{x}10^{-1}$	K_3	$2.68\text{x}10^{-2} \pm 1.28\text{x}10^{-2}$
$S_{\#}(0)$	$4.08\text{x}10^{-1} \pm 1.06\text{x}10^{-1}$	$S_{\#}(0)$	$7.22\text{x}10^{-1} \pm 5.0\text{x}10^{-2}$	$S_{\#}(0)$	$7.44\text{x}10^{-1} \pm 4.9\text{x}10^{-2}$
$X_{\#}(0)$	$4.47\text{x}10^{-1} \pm 2.04\text{x}10^{-1}$				
Trial #3					
$\mathscr{J}$	**132.874**	$\mathscr{J}$	**143.597**	$\mathscr{J}$	**151.543**
$\bar{\mu}_1$	$5.40\text{x}10^{-1} \pm 1.1\text{x}10^{-2}$	$\bar{\mu}_1$	$5.43\text{x}10^{-1} \pm 1.2\text{x}10^{-2}$	$\bar{\mu}_1$	$5.21\text{x}10^{-1} \pm 1.0\text{x}10^{-2}$
$\bar{\mu}_2$	$2.71\text{x}10^{-2} \pm 3.0\text{x}10^{-3}$	$\bar{\mu}_2$	$3.45\text{x}10^{-2} \pm 1.4\text{x}10^{-3}$	$\bar{\mu}_2$	$3.97\text{x}10^{-2} \pm 1.8\text{x}10^{-3}$
$\bar{\mu}_3$	$3.53\text{x}10^{-1} \pm 3.2\text{x}10^{-2}$	$\bar{\mu}_3$	$3.47\text{x}10^{-1} \pm 3.8\text{x}10^{-2}$	K_3	$8.30\text{x}10^{-2} \pm 1.05\text{x}10^{-2}$
K_{NH_3}	$2.60\text{x}10^{-4} \pm 6.0\text{x}10^{-5}$	K_{NH_3}	$4.14\text{x}10^{-4} \pm 6.6\text{x}10^{-5}$	$K_{3,I}$	$2.12\text{x}10^{0} \pm 2.3\text{x}10^{-1}$
$K_{3,I}$	$5.43\text{x}10^{-1} \pm 1.28\text{x}10^{-1}$	$K_{3,I}$	$5.28\text{x}10^{-1} \pm 1.28\text{x}10^{-1}$	$S_{\#}(0)$	$7.80\text{x}10^{-1} \pm 4.1\text{x}10^{-2}$
$S_{\#}(0)$	$1.49\text{x}10^{0} \pm 2.4\text{x}10^{-1}$				
Trial #4					
$\mathscr{J}$	**95.601**	$\mathscr{J}$	**109.458**	$\mathscr{J}$	**116.004**
$\bar{\mu}_1$	$5.27\text{x}10^{-1} \pm 6.0\text{x}10^{-3}$	$\bar{\mu}_1$	$5.27\text{x}10^{-1} \pm 7.0\text{x}10^{-3}$	$\bar{\mu}_1$	$5.09\text{x}10^{-1} \pm 6.0\text{x}10^{-3}$
K_2	$7.13\text{x}10^{0} \pm 5.0\text{x}10^{-1}$	K_2	$6.95\text{x}10^{0} \pm 4.8\text{x}10^{-1}$	K_2	$6.52\text{x}10^{0} \pm 5.2\text{x}10^{-1}$
K_3	$5.40\text{x}10^{-2} \pm 8.3\text{x}10^{-3}$	$\bar{\mu}_3$	$2.83\text{x}10^{-1} \pm 1.4\text{x}10^{-2}$	$\bar{\mu}_3$	$1.59\text{x}10^{-1} \pm 2.0\text{x}10^{-3}$
K_{NH_3}	$2.54\text{x}10^{-4} \pm 3.1\text{x}10^{-5}$	K_{NH_3}	$3.13\text{x}10^{-4} \pm 4.4\text{x}10^{-5}$	K_3	$6.39\text{x}10^{-2} \pm 6.5\text{x}10^{-3}$
$K_{3,I}$	$2.23\text{x}10^{0} \pm 1.3\text{x}10^{-1}$	$K_{3,I}$	$9.18\text{x}10^{-1} \pm 1.22\text{x}10^{-1}$	k_{CO_2}	$3.75\text{x}10^{-1} \pm 8.6\text{x}10^{-2}$
k_{CO_2}	$4.01\text{x}10^{-1} \pm 7.9\text{x}10^{-2}$	k_{CO_2}	$3.27\text{x}10^{-1} \pm 7.2\text{x}10^{-2}$		
Trial #5					
$\mathscr{J}$	**156.086**	$\mathscr{J}$	**156.171**	$\mathscr{J}$	**156.21**
$\bar{\mu}_1$	$2.52\text{x}10^{-1} \pm 2.0\text{x}10^{-2}$	$\bar{\mu}_1$	$2.54\text{x}10^{-1} \pm 2.0\text{x}10^{-2}$	$\bar{\mu}_1$	$2.55\text{x}10^{-1} \pm 1.9\text{x}10^{-2}$
$\bar{\mu}_2$	$3.40\text{x}10^{-2} \pm 2.5\text{x}10^{-3}$	$\bar{\mu}_2$	$3.40\text{x}10^{-2} \pm 2.48\text{x}10^{-2}$	$\bar{\mu}_2$	$3.40\text{x}10^{-2} \pm 2.5\text{x}10^{-3}$
$\bar{\mu}_3$	$1.97\text{x}10^{-1} \pm 8.0\text{x}10^{-3}$	K_3	$1.53\text{x}10^{-1} \pm 1.6\text{x}10^{-2}$	$S_{\#}(0)$	$8.33\text{x}10^{-1} \pm 7.0\text{x}10^{-2}$
$S_{\#}(0)$	$8.48\text{x}10^{-1} \pm 8.2\text{x}10^{-2}$	$S_{\#}(0)$	$8.41\text{x}10^{-1} \pm 8.0\text{x}10^{-2}$		
Trial #6					
$\mathscr{J}$	**141.96**	$\mathscr{J}$	**146.58**	$\mathscr{J}$	**148.346**
$\bar{\mu}_1$	$3.71\text{x}10^{-1} \pm 2.8\text{x}10^{-2}$	$\bar{\mu}_1$	$2.60\text{x}10^{-1} \pm 2.5\text{x}10^{-2}$	$\bar{\mu}_1$	$3.60\text{x}10^{-1} \pm 2.7\text{x}10^{-2}$
$\bar{\mu}_2$	$2.65\text{x}10^{-2} \pm 3.0\text{x}10^{-3}$	K_2	$6.64\text{x}10^{0} \pm 1.08\text{x}10^{0}$	$\bar{\mu}_2$	$2.52\text{x}10^{-2} \pm 4.5\text{x}10^{-3}$
K_3	$4.89\text{x}10^{-2} \pm 1.74\text{x}10^{-2}$	$\bar{\mu}_3$	$1.53\text{x}10^{-1} \pm 1.7\text{x}10^{-2}$	K_3	$7.57\text{x}10^{-2} \pm 1.73\text{x}10^{-2}$
K_{NH_3}	$1.56\text{x}10^{-4} \pm 3.6\text{x}10^{-5}$	K_3	$5.81\text{x}10^{-2} \pm 2.63\text{x}10^{-2}$	K_{NH_3}	$1.53\text{x}10^{-4} \pm 5.2\text{x}10^{-5}$
$K_{3,I}$	$2.70\text{x}10^{0} \pm 8.9\text{x}10^{-1}$	$S_{\#}(0)$	$4.33\text{x}10^{-1} \pm 8.4\text{x}10^{-2}$	$S_{\#}(0)$	$1.49\text{x}10^{0} \pm 3.7\text{x}10^{-1}$
$S_{\#}(0)$	$1.49\text{x}10^{0} \pm 2.3\text{x}10^{-1}$	$X_{\#}(0)$	$3.19\text{x}10^{-1} \pm 1.46\text{x}10^{-1}$		

The progression of trial #1 is presented in Tab. B.3. Once again we see the identification algorithm zeroing in early on. In this case the algorithm appears to zero in on the parameters $\bar{\mu}_1$, $\bar{\mu}_2$, and K_3. In a certain sense this is consistent with the two reaction scheme in that it appears the identification algorithm zeroes in on at least one parameter from each rate law, indicating that experimental data has significant enough information contained within it to distinguish the selected three reactions. This is as much a testament to the calculations of §4.2.1 (i.e. theoretical reaction number) as it is to the expertise behind the model selected. We also see again a relative consistency for the parameters $\bar{\mu}_1$ and $\bar{\mu}_2$ indicating adequate independence of the solved for values under the current weighting scheme.

Examining the top three combinations of trial #1 (Figs. 4.15 - 4.17) we immediately see an improvement in overall fit as compared to the two reaction scheme. This is especially apparent in the inorganic nitrogen, VFA, and methane flow plots. The two reaction fits tended to break down after the 80 day point in these profiles. There does appear to be some model mismatch in the later stages of the inorganic nitrogen plots but this is actually believed to be a result of poor default biomass and substrate concentration values. As can be seen from the fitted kinetic constants, the hydrolysis/acidogenesis of protein appears to be the slowest of the three reactions. This appears to be a piculiarity of microalgae (hydrolysis tends to be the limiting step for complex waste while methanogenesis tends to be the limiting step in most anaerobic digester situations taking in solubilized feed due to its susceptability to inhibition). This is the subtlety in the dynamics that the two reaction scheme was missing, but this also means that improper selection of substrate and biomass concentrations will become more apparent as these values begin to decrease (consistent with an increased HRT), where slight differences have a larger impact. This particular issue will be examined

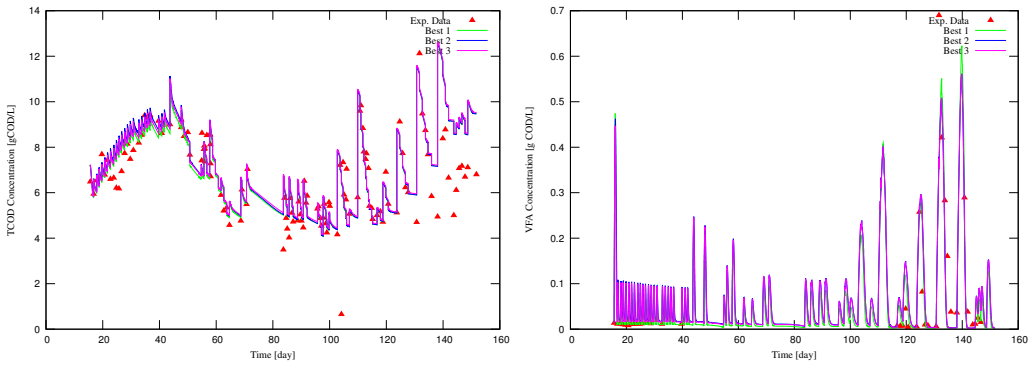

(a) Total COD (b) VFA

Figure 4.15: Top 3 TCOD and VFA Prediction Results for Three Reaction Set Trial # 1

in Trial #4 where it will be seen that proper selection of initial values can have a noticeable impact on this particular system. Examining Fig. 4.17 we also see that the model has a decent capacity to model the two "test" observations ommitted from the least squares fitting algorithm. The major issue appears to be with modelling pH. The major trends are modelled but there appears to be a minor offset. One can only speculate as to why this is. It is possible that the number of acid/base species involved is too simplistic and so we are missing some ionic species. It is also possible that additional classification measurements of the inlet stream would better quantify any fluctuations in inlet ion concentrations and therefore their impact on the pH.

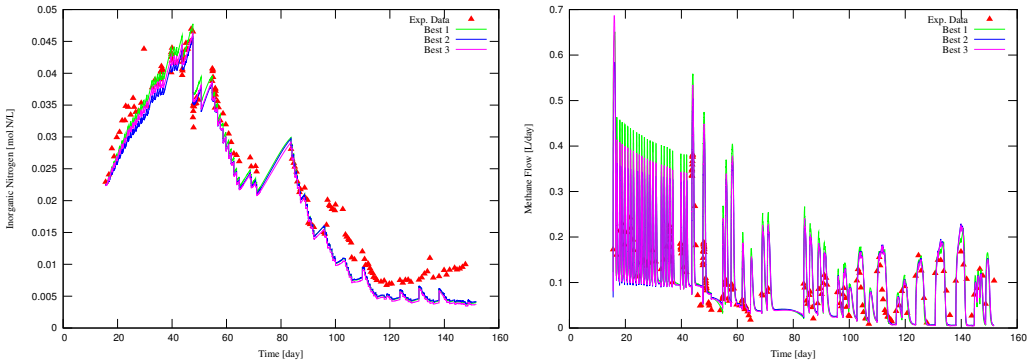

(a) Inorganic Nitrogen (b) Methane Flow

Figure 4.16: Top 3 IN and Meth. Flow Prediction Results for Three Reaction Set Trial # 1

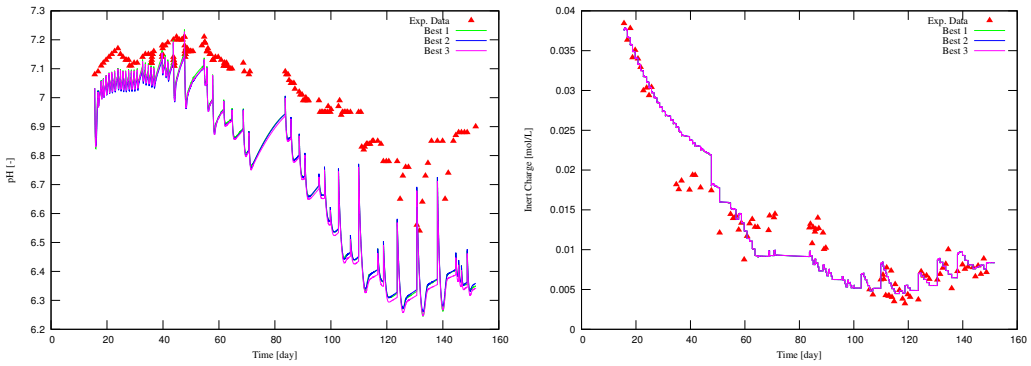

(a) pH (b) Inert Charge

Figure 4.17: Top 3 pH and Inert Charge Prediction Results for Three Reaction Set Trial # 1

For Trial #2 we again see that the algorithm quickly selects out one of the two key kinetic parameters of the two acidogenesis steps as well as two of the kinetic parameters in the methanogenesis step (Tab. B.4). This seems to indicate that more information for the methanogenesis step is contained within the data. A few interesting things also arise in comparison to the 25% threshold (trial #1) results. First, we see that at the 50 % threshold K_2 is favoured over $\bar{\mu}_2$. This is not a problem since it was expected that there is a high degree of correlation between $\bar{\mu}_2$ and K_2. Therefore it would be expected that one would end up performing marginally better in the optimization and in this case it was K_2.

Comparing the 50 % threshold trial #1 results to the 25 % threshold trial #2 results (in Tab. 4.5) we see that the estimates for $\bar{\mu}_1$ synch up well (It would appear that with this weighting scheme a value of 0.36 ± 0.03 fits the data fairly well). The estimate of K_2 appears slightly less consistent throughout the stages of the optimization indicating some degree of correlation. The value appears stable at 6.0 ± 1.0 until the starting biomass is adjusted (in the tier 6 combination of Tab. B.4) at which point a sudden drop is noted. This indicated what was already suspected, since the protein acidogens are the slowest biomass it was expected that starting biomass concentration would have a huge impact on fitting results. This also indicated a need to have a better handle on starting conditions. Finally, comparing the K_3 and $K_{3,I}$ results to the 25% progression we again see a larger dependence on the other parameters being estimated in the subset. The final estimated values are less consistent with the 25% threshold values (especially in the case of K_3) but it is believed this is because the initial biomass and substrate concentrations were also manipulated (indicating a correlation).

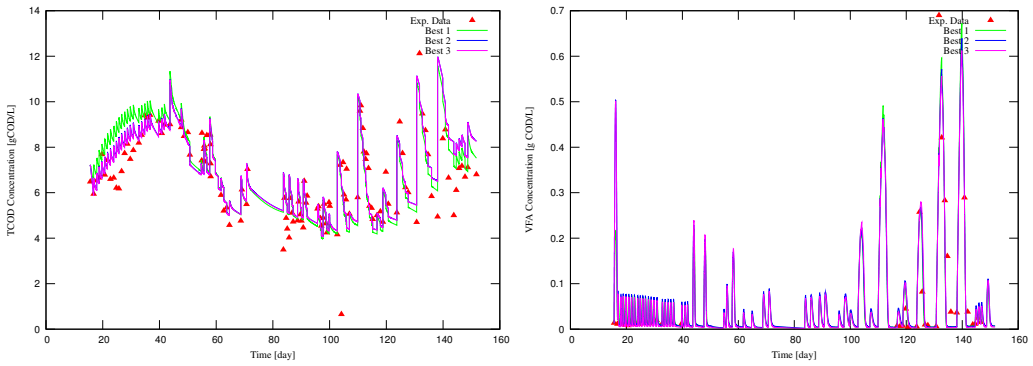

(a) Total COD (b) VFA

Figure 4.18: Top 3 TCOD and VFA Prediction Results for the Three Reaction Set Trial # 2

The top three combination results of trial #2 are presented in Fig. 4.18 - 4.20. Again we see very good fit with the experimental data. Combinations 2 and 3 actually appear to have eliminated the nitrogen offset (possibly through manipulating the starting substrate concentrations). However combination 1 appears to have gone slightly overboard in attempting to compensate for the inorganic nitrogen offset. It is believed that this problem arises from the underestimation of the protein biomass. This here underlines the inherent problem in trying to optimize all three biomasses uniformly (a problem that will be tackled in trial #4). That being said, the fits are still very good and so it would appear the identification algorithm was successful in finding an identifiable parameter subset to fit the data.

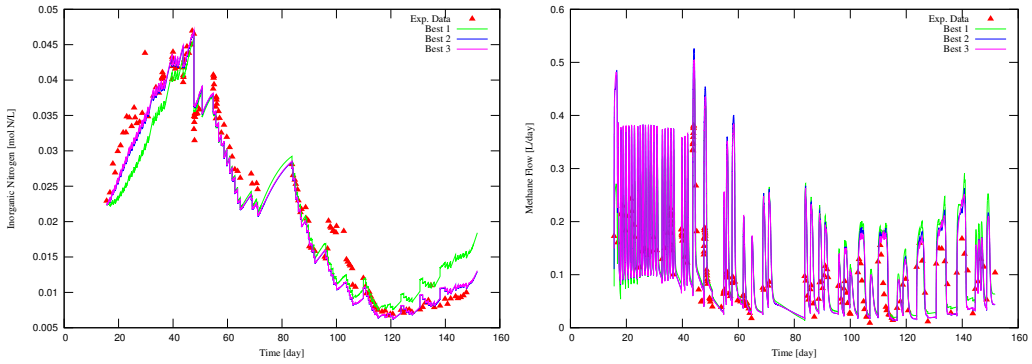

(a) Inorganic Nitrogen (b) Methane Flow

Figure 4.19: Top 3 IN and Meth. Flow Prediction Results for the Three Reaction Set Trial # 2

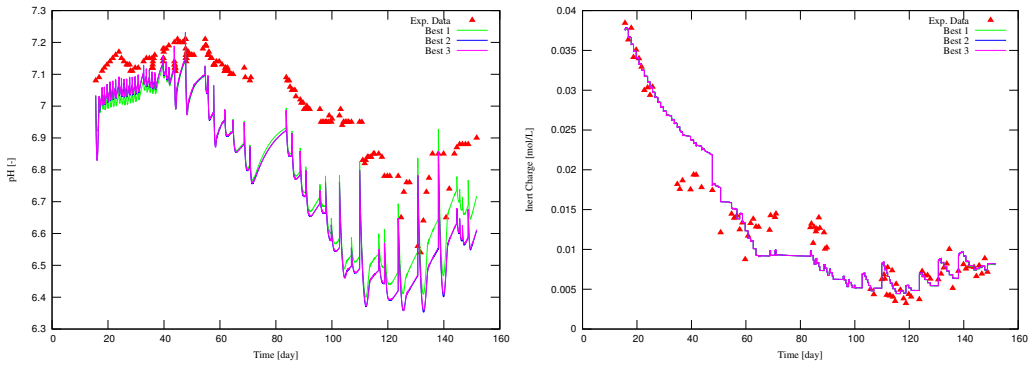

(a) pH (b) Inert Charge

Figure 4.20: Top 3 pH and Inert Charge Prediction Results for the Three Reaction Set Trial # 2

Since there was no data set available to act as a confirmation for the fitting results, the next step was naturally to randomnly partition the data set into "experimental" and "confirmation" data sets and re-run the identification algorithm on the "experimental" data set. The randomization pattern used for each observation is provided in appendix E.

The progression of the "experimental" data set identification run are presented in Tab. B.5. Again we see that the algorithm zeros in on a single parameter from each of the two acidogenesis/acetogenesis reactions and a group of parameters from the methanogenesis reaction. The first thing that pops out from this progression is the dramatic change in the value of $\bar{\mu}_1$ (it jumps from ≈ 0.36 in the first two trials to ≈ 0.5). While it is not known exactly why this happened it is observed that there appears to be quite abit of noise in the TCOD measurements (one of the key observations that would impact fitting the sugar/lipid kinetics). Therefore it is possible that the randomization may caused the fitting to shift to accomodate these new results. The protein acidogenesis results on the other hand actually match up fairly well with trail#1 (both predicted values of $\approx 0.031/d$). Once again the methanogenesis results appear highly contigent on the parameter set being estimated. A rough sense of the parameter space is able to be gained but additional experiments are clearly required.

Fig. 4.21 - 4.23 show the top three fitting results for trial #3. Although the parameter fits appeared to lack consistency with trials #1 and #2 it is still interesting to note that the algorithm identified parameter subsets that fit both the "experimental" and "confirmation" data sets fairly well.

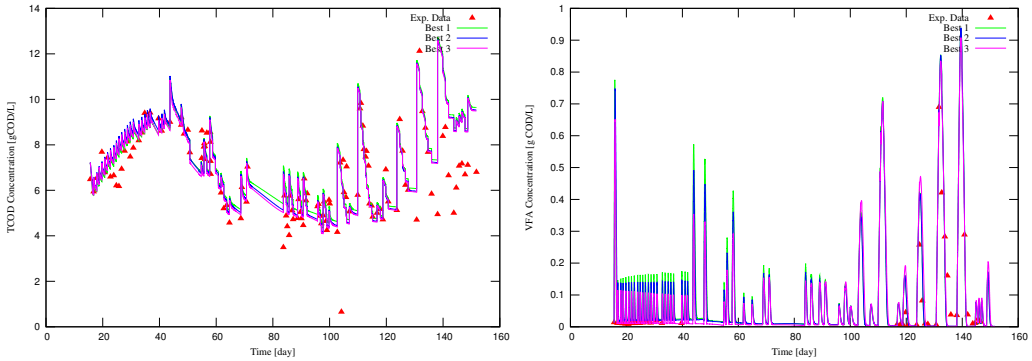

(a) Total COD (b) VFA

Figure 4.21: Top 3 TCOD and VFA Prediction Results for Three Reaction Set Trial # 3

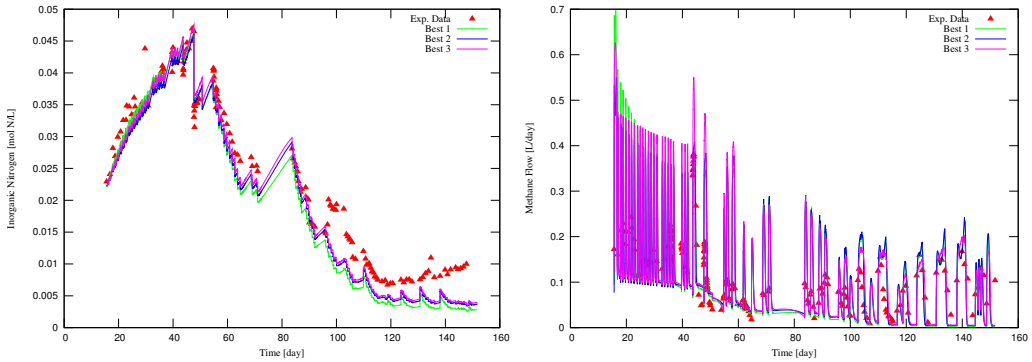

(a) Inorganic Nitrogen (b) Methane Flow

Figure 4.22: Top 3 IN and Meth. Flow Prediction Results for Three Reaction Set Trial # 3

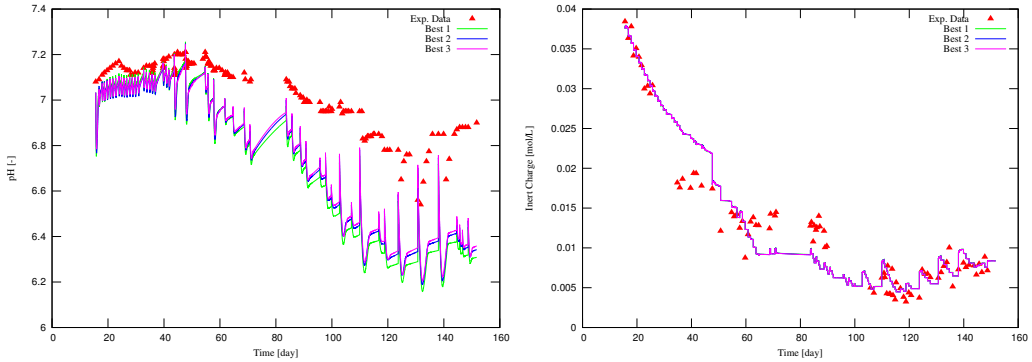

(a) pH (b) Inert Charge

Figure 4.23: Top 3 pH and Inert Charge Prediction Results for Three Reaction Set Trial # 3

One of the key concerns throughout the identification process was a lack of consistent initial conditions. It was attempted to add these initial conditions as parameters within the identification but this led to inconsistent results (since most of the parameters appeared to be correlated to the initial conditions). Upon examining the TCOD (with inerts removed) it appears that a semi-steady state is achieved in the biomass and substrate around the 15 - 40 day period (shown in Fig. 4.24). It is fairly obvious in the inorganic nitrogen, and inert ion profiles that the system is not at a true steady state. In addition, a true steady state would have an inerts value of 9 gCOD/L based on the inlet concentration (obviously much higher than the 6 - 8 gCOD/L TCOD measurements during this period). However, the relatively rapid and consistent substrate additions (e.g. in Fig. 4.3) over the 15 - 40 day period coupled with the rough flattening out of the TCOD curve led to the belief that a "pseudo-steady state" could be used in an effort to remove some of this uncertainty in the initial state estimates. So what does "pseudo-steady state" mean? Well it was already established that the inorganic nitrogen, inert ion, and inert COD concentrations are not at steady state. However, initial values for these concentrations are known or can be estimated (an initial TCOD value is known and so once all other initial concentrations are solved for the inert COD value can be back calculated). This just leaves the initial values of S_1, S_2, S_3, X_1, X_2, and X_3. Taking the steady state versions of these six variables from the core equation system 4.37 we add the following six equality constraints to the original dynamic optimization system:

$$
\begin{aligned}
0 &= -\beta_1\mu_1'(S_1(0),\mathrm{IN}(0),\mathrm{pH}(0))X_1(0) + D_{SS}(Y_1 COD^{in}(0) - S_1(0)) \\
0 &= -\beta_5\mu_2'(S_2(0),\mathrm{IN}(0),\mathrm{pH}(0))X_2(0) + D_{SS}(Y_2 COD^{in}(0) - S_2(0)) \\
0 &= \beta_3\mu_1'(S_1(0),\mathrm{IN}(0),\mathrm{pH}(0))X_1(0) + \beta_7\mu_2'(S_2(0),\mathrm{IN}(0),\mathrm{pH}(0))X_2 \\
&\quad -\beta_9\mu_3'(S_3(0),\mathrm{IN}(0),\mathrm{pH}(0))X_3(0) + D_{SS}(S_3^{in}(0) - S_3(0)) \qquad (4.38) \\
0 &= \mu_1'(S_1(0),\mathrm{IN}(0),\mathrm{pH}(0))X_1(0) + D_{SS}(0 - f_b X_1(0)) \\
0 &= \mu_2'(S_2(0),\mathrm{IN}(0),\mathrm{pH}(0))X_2(0) + D_{SS}(0 - f_b X_2(0)) \\
0 &= \mu_3'(S_3(0),\mathrm{IN}(0),\mathrm{pH}(0))X_3(0) + D_{SS}(0 - f_b X_3(0))
\end{aligned}
$$

Where $S_1(0)$, $S_2(0)$, $S_3(0)$, $X_1(0)$, $X_2(0)$, and $X_3(0)$ are initial value parameters added to each level of the identification algorithm and estimated along side the current parameter subset, and D_{SS} is the approximate steady state dilution rate of 0.0357 1/d associated with the 28 HRT period of the experiment.

With these equality constraints added the estimation of the parameter error estimates would now fall to the theory discussed in §3.2.2. It should also be mentioned that the randomization pattern used in trial #3 was also used for this trial. The rest of the pertinent details are provided in the list below. The progression of this identification run is provided in Tab. B.6. As an aside, in almost all cases (and all cases past the 3rd tier) the following steady state conditions were identified for the best parameter fits.

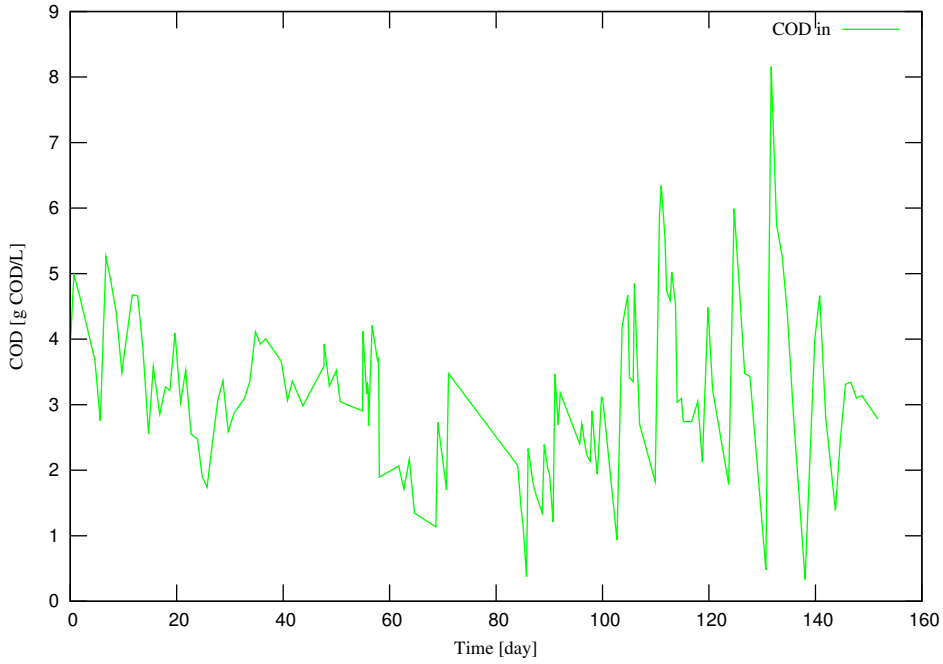

Figure 4.24: Measured Reactive TCOD Concentration

$co_b(0)$	0.033 $gCOD/L$
$cn_b(0)$	1.6 $gCOD/L$
$vfa_b(0)$	0.030 $gCOD/L$
$x_{co_b}(0)$	0.72 $gCOD/L$
$x_{cn_b}(0)$	0.84 $gCOD/L$
$x_{vfa_b}(0)$	1.4 $gCOD/L$

It is interesting to note that the optimal steady state biomasses are relatively close to the original default values of 1 gCOD/L (this possibly improved the default fitting results of Trials #1 - 3). The protein is also somewhat close. The only values that are drastically different are the sugar/lipid and VFA, but it is now known that these reactions are much faster than the protein acidogenesis and so it would be expected that they are lower.

Looking at Tab. B.6 we see that the algorithm progression was similar to Trial #1 - #3 in that 1 kinetic parameter from each of the acidogenesis/acetogenesis steps was picked out and multiple methanogenesis parameters were picked out. It is also interesting to note that a similar $\bar{\mu}_1 \approx 0.51/d$ was picked out indicating that the random points selected for the "experimental" data set appear to have some impact on the fitting results. As mentioned before, it is speculated that noise in some of the measurements (such as TCOD) likely contributed to this changing value. On the other hand the estimate of K_2 remains consistent with trial #1 and 2, and presumably #3 (since the value of $\bar{\mu}_2$ in trial #3 is consistent with those combinations in trial #1 and #2, where $\bar{\mu}_2$ appeared). This can all be seen in Tab. 4.5. The values estimated for $\bar{\mu}_3$, K_3, $K_{3,I}$, and K_{NH_3} also appear to be in the same ballpark as trials #1 - #3, indicating moderate consistency amongst the trials (although correlations are definitely evident).

Looking at the predictions of the top three combinations for Trial #4 (Fig. 4.25 - 4.27) it is quite evident that the assumption of pseudo-steady state resulted in offset free inorganic nitrogen predictions. This seems to lend more creedance to the hypothesis that proper biomass and substrate estimates would sure up the observed offset. All the other experimental variable predictions appear to fair just as well as trial #1 - #3. The only obvious anomaly is the pH trend, which has a much more prominent offset as compared to trials #1 - #3. This is likely due to the decreased estimates of k_{CO_2}, which would lead to increased concentrations of CO_2 and therefore decreases in pH. This would also be more prominent under longer HRTs (i.e. the first period of the reactor operation). It is not clear why this parameter was only selected for the steady state optimization. It is possible that the in-

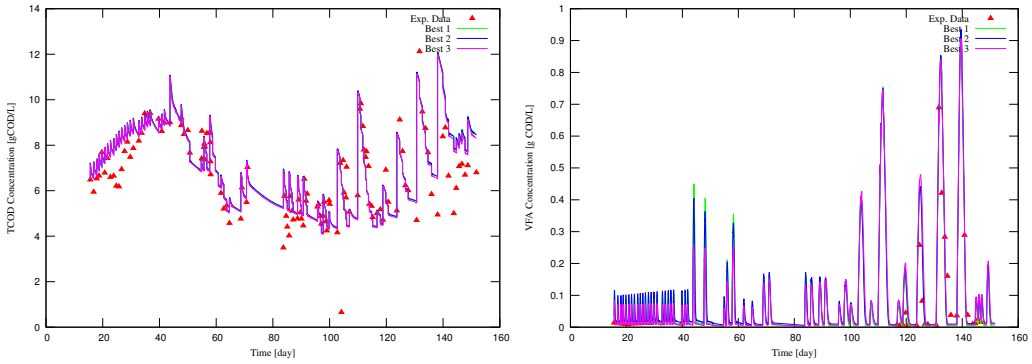

(a) Total COD (b) VFA

Figure 4.25: Top 3 TCOD and VFA Prediction Results for Three Reaction Set Trial # 4

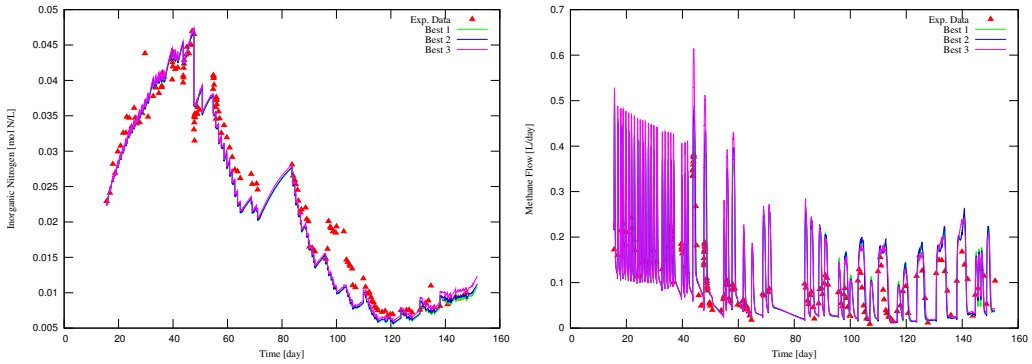

(a) Inorganic Nitrogen (b) Methane Flow

Figure 4.26: Top 3 IN and Meth. Flow Prediction Results for Three Reaction Set Trial # 4

crease in initial methanogen biomass would lead to increases in CO_2 production leading to a need to decrease CO_2 release to balance out gas flow and composition values (this is only speculation though).

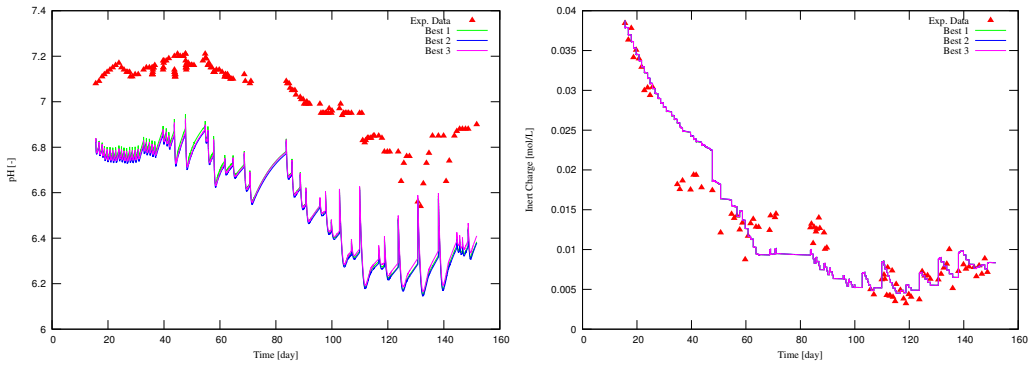

(a) pH (b) Inert Charge

Figure 4.27: Top 3 pH and Inert Charge Prediction Results for Three Reaction Set Trial # 4

4.4 Conclusions

Condensing the results of all 2 two reaction trials and all 6 three reaction trials presented we arrive at a the following conclusions:

1. Initial tests of the developed identification algorithm are promising and the results for the three reaction system consistently lead to good dynamic predictions

2. The two reaction scheme appears unsuitable for this system, although changing the core rate laws to two hydrolysis/acidogenesis/methanogenesis steps may mitigate this

3. Within each rate law there appears to be insufficient information in the data set to identify all parameters. This means that only a select subset (or in a broader sense, ratios) can be identified with any degree of confidence.

4. The maximum specific growth rate/ half saturation coefficient of the two acidogens appear to be the only parameters that are roughly consistent throughout the identification run. A general sense on the scale of methanogenesis parameters is also gained

but better experimental design is needed to further refine these estimates

$\bar{\mu}_1$ 0.3 $\pm$ 0.1 1/day

$\bar{\mu}_2$ 0.03 $\pm$ 0.01 1/day or K_2 6.0 $\pm$ 1.0 gCOD/L

5. Estimation of the methanogenesis parameters appears to be highly contingent on initial conditions and the current parameter subset being estimated. Ensuring that the reaction is at steady state (i.e. ensuring TCOD, VFA, IN, Ions, etc. measurements have consistently plateaued) before beginning the experimental trials would go a long way towards simplifying the identification problem and reducing the number of observed correlations

6. The fact that only a select few of the parameters were able to be identified indicates that while this model is able to predict the current experimental data set well, there is likely to be very little confidence in predictions outside this range (as will be seen in the steady state analysis)

7. Optimal experimental design is the logical next step to improve prediction confidence

Chapter 5

Optima Studies

Having yielded relatively consistent parameter estimates the next step is to examine the optimal predictions of the fitted models. Due to its poor performance during the parameter estimation stage the two reaction scheme is ommitted from this analysis. For the three reaction model the optimal steady state performance is examined and compared against available literature data. The sensitivity of these predictions to variations in core parameters is then tested to examine the impact of estimation error on the optimal predictions.

5.1 Steady State Optimization

As was discovered during the model development of Chapter 4 the current data set does not contain sufficient information to fit every parameter in the developed model. The model appears to be mechanistically sound in that it can represent the experimental data very well over the dynamic range encountered, but the individual parameters show varying degrees of

correlation with each other. The kinetics of the acidogenesis/acetogens of both sugar/lipids and proteins appears to be fairly consistent in terms of identifying one of the two key kinetic parameters but this still hints at a large correlation between these parameter pairs. The methanogenesis parameters, on the other hand, appear highly dependent on each other and so one can only yield a ballpark range for these values from this data set. The issue with this is that all parameters within a model need to have a high degree of confidence before any stock can be placed in the models predictions. As will be seen in this chapter, only broad conclusions about optimal operation can be gained from the fitted results of §4.3. It was still of interest to study such optima to get a feel for the degree of variability likely to be encountered in the predicted optima, dependent on the fitted parameter subset selected, as well as to compare these general values to literature to see if they are realistic.

The primary application for any calibrated grey-box model is naturally monitoring, control and optimization. In this section, the problem of optimizing the rate of biogas (methane) production, q_{CH_4}, from the digester is considered, with emphasis on steady-state operation. Of primary importance will be the examination of how changing parameter combinations impacts the optimal profile as well as how variability in parameter confidence impacts prediction confidence. Formally, the optimization problem can be stated as a standard NLP with equality constraints defined by the equation system 4.37 at steady state. Note that only the 3 reaction model will be studied as the two reaction model has already been discounted due to its inability to recreate the experimental data.

maximize: ρ_{CH_4}

subject to:

$$
\begin{aligned}
0 = \;& -\beta_1\mu_1'(S_1,\mathrm{IN},\mathrm{pH})X_1 + D(Y_1 COD^{in} - S_1) \\
0 = \;& -\beta_5\mu_2'(S_2,\mathrm{IN},\mathrm{pH})X_2 + D(Y_2 COD^{in} - S_2) \\
0 = \;& \beta_3\mu_1'(S_1,\mathrm{IN},\mathrm{pH})X_1 + \beta_7\mu_2'(S_2,\mathrm{IN},\mathrm{pH})X_2 \\
& -\beta_9\mu_3'(S_3,\mathrm{IN},\mathrm{pH})X_3 + D(Y_3 COD^{in} - S_3) \\
0 = \;& -\beta_2\mu_1'(S_1,\mathrm{IN},\mathrm{pH})X_1 + \beta_6\mu_2'(S_2,\mathrm{IN},\mathrm{pH})X_2 \\
& -\beta_{10}\mu_3'(S_3,\mathrm{IN},\mathrm{pH})X_3 + D(\mathrm{IN}^{in} - \mathrm{IN}) \\
0 = \;& D(Y_4 COD^{in} - S_4) \\
0 = \;& \mu_1'(S_1,\mathrm{IN},\mathrm{pH})X_1 + D(0 - f_b X_1) \\
0 = \;& \mu_2'(S_2,\mathrm{IN},\mathrm{pH})X_2 + D(0 - f_b X_2) \\
0 = \;& \mu_3'(S_3,\mathrm{IN},\mathrm{pH})X_3 + D(0 - f_b X_3) \\
0 = \;& \beta_4\mu_1'(S_1,\mathrm{IN},\mathrm{pH})X_1 + \beta_6\mu_2'(S_2,\mathrm{IN},\mathrm{pH})X_2 \\
& +\beta_{10}\mu_3'(S_3,\mathrm{IN},\mathrm{pH})X_3 + D(\mathrm{IC}^{in} - \mathrm{IC}) + q_{CO_2} \\
0 = \;& D(\left[\mathrm{Na}^{+}\right]^{in} - \left[\mathrm{Na}^{+}\right]) \\
0 = \;& D(\left[\mathrm{K}^{+}\right]^{in} - \left[\mathrm{K}^{+}\right]) \\
0 = \;& D(\left[\mathrm{Ca}^{+2}\right]^{in} - \left[\mathrm{Ca}^{+2}\right]) \\
0 = \;& D(\left[\mathrm{Mg}^{+2}\right]^{in} - \left[\mathrm{Mg}^{+2}\right]) \\
0 = \;& D(\left[\mathrm{Cl}^{-}\right]^{in} - \left[\mathrm{Cl}^{-}\right]) \\
0 = \;& D(\mathrm{S}^{in} - \mathrm{S}) \\
0 = \;& D(\mathrm{P}^{in} - \mathrm{P}) \\
0 = \;& \mathrm{Z} + \left[\mathrm{H}^{+}\right] + \left[\mathrm{NH}_4^{+}\right] - \left[\mathrm{HCO}_3^{-}\right] - \left[\mathrm{CO}_3^{-2}\right] - \left[vfa_{ion}^{-}\right] - \left[\mathrm{OH}^{-}\right]
\end{aligned}
\tag{5.1}
$$

This model may actually be simplified significantly with a few observations. First, all inert ions solve to a constant value independent of the other state variables (and only dependent on the input variable D). Therefore these equations may be removed and constant values of the form "$x = x_{in}/D$" used in the calculation of Z. The equation for S_4 may be similarly simplified. Second, since we assume that no active biomass enters in the feed we may rearrange the equations of S_1, X_1, S_2, X_2 to solve for exact steady state values:

$$S_1 = \frac{Df_bK_1}{\bar{\mu}_1 I_{\text{IN}} I_{\text{pH}AA} - Df_b} \tag{5.2}$$

$$X_1 = \frac{D\left(Y_1 S_1^{in} - S_1\right)}{\beta_1 \bar{\mu}_1 I_{\text{IN}} I_{\text{pH}AA} \frac{S_1}{K_1+S_1}} \tag{5.3}$$

$$S_2 = \frac{Df_bK_2}{\bar{\mu}_2 I_{\text{IN}} I_{\text{pH}AA} - Df_b} \tag{5.4}$$

$$X_2 = \frac{D\left(Y_2 S_2^{in} - S_2\right)}{\beta_5 \bar{\mu}_2 I_{\text{IN}} I_{\text{pH}AA} \frac{S_2}{K_2+S_2}} \tag{5.5}$$

The above relations come with the implied restriction that $\bar{\mu} I_{\text{IN}} I_{\text{pH}AA} > Df_b$. Otherwise wash out conditions have been reached and biomass values go to 0 while substrate values go to their inlet concentrations.

With the above simplifications system (5.1) shortens to system (5.6).

maximize: ρ_{CH_4}

subject to:

$$\begin{aligned}
0 = \;& \beta_3\mu_1'(S_1,\mathrm{IN},\mathrm{pH})X_1 + \beta_7\mu_2'(S_2,\mathrm{IN},\mathrm{pH})X_2 \\
& - \beta_9\mu_3'(S_3,\mathrm{IN},\mathrm{pH})X_3 + D(Y_3 COD^{in} - S_3) \\
0 = \;& - \beta_2\mu_1'(S_1,\mathrm{IN},\mathrm{pH})X_1 + \beta_6\mu_2'(S_2,\mathrm{IN},\mathrm{pH})X_2 \\
& - \beta_{10}\mu_3'(S_3,\mathrm{IN},\mathrm{pH})X_3 + D(\mathrm{IN}^{in} - \mathrm{IN}) \\
0 = \;& \mu_3'(S_3,\mathrm{IN},\mathrm{pH})X_3 + D(0 - f_b X_3) \\
0 = \;& \beta_4\mu_1'(S_1,\mathrm{IN},\mathrm{pH})X_1 + \beta_6\mu_2'(S_2,\mathrm{IN},\mathrm{pH})X_2 \\
& + \beta_{10}\mu_3'(S_3,\mathrm{IN},\mathrm{pH})X_3 + D(\mathrm{IC}^{in} - \mathrm{IC}) + q_{CO_2} \\
0 = \;& \mathrm{Z} + \left[\mathrm{H}^+\right] + \left[\mathrm{NH}_4^+\right] - \left[\mathrm{HCO}_3^-\right] - \left[\mathrm{CO}_3^{-2}\right] - \left[vfa_{ion}^-\right] - \left[\mathrm{OH}^-\right]
\end{aligned} \tag{5.6}$$

This NLP has been reduced to a system of 5 major variables: X_3, S_3, IN, IC, and $\left[\mathrm{H}^+\right]$.

The decision variables in this optimization can be both the dilution rate and the feed composition. For the first set of studies the feed composition was assumed equal to the experimentally determined composition (given in Tab. 4.1) and the dilution rate D was varied manually over a broad range. For the second set of studies the feed composition was adjusted to maintain a constant loading rate of 1 gCOD/L (≈ 0.719 gVSS/L). This was done to compare model predictions against the limited literature data available [30; 29; 55]. These three papers examine the anaerobic digestion of *Chlorella*/*Scenedesmus* mixtures in a continuously operated CSTR and so were the closest thing available to gauge model validity. Additional papers have looked at the anaerobic digestion of *Chlorella vulgaris* in batch

settings as well as the continuous anaerobic digestion of other micro and macroalgae types but neither contain data that can legitimately be compared to this model. As in the work of [50], all results were standardized against 1 gVSS fed to reactor for comparison purposes. The optimal predictions of the best combinations from each trial in §4.3.2 will now be compared (as these 6 combinations contain a large enough variation in the observed identifiable parameter combinations and values to provide valuable insight into the optimal space).

Tab. 5.1 resummarizes the top result of each of the 6 three reaction system identification runs discussed in §4.3.2.

Table 5.1: Final Optimal Parameter Combinations for Three Reaction Set Trials

Trial #1		Trial #2		Trial #3	
$\mathscr{J}$	**649.701**	$\mathscr{J}$	**593.444**	$\mathscr{J}$	**132.874**
$\bar{\mu}_1$	$\mathbf{3.69x10^{-1} \pm 1.8x10^{-2}}$	$\bar{\mu}_1$	$\mathbf{3.95x10^{-1} \pm 2.3x10^{-2}}$	$\bar{\mu}_1$	$\mathbf{5.41x10^{-1} \pm 1.1x10^{-2}}$
$\bar{\mu}_2$	$\mathbf{3.64x10^{-2} \pm 2.7x10^{-3}}$	$\mathbf{K_2}$	$\mathbf{4.83x10^{0} \pm 7.6x10^{-1}}$	$\bar{\mu}_2$	$\mathbf{2.71x10^{-2} \pm 3.0x10^{-3}}$
$\mathbf{K_3}$	$\mathbf{7.12x10^{-2} \pm 1.45x10^{-2}}$	$\mathbf{K_3}$	$\mathbf{4.10x10^{-2} \pm 1.27x10^{-2}}$	$\bar{\mu}_2$	$\mathbf{3.53x10^{-1} \pm 3.2x10^{-2}}$
$\mathbf{K_{3,I}}$	$\mathbf{1.98x10^{0} \pm 4.9x10^{-1}}$	$\mathbf{K_{3,I}}$	$\mathbf{1.33x10^{0} \pm 1.7x10^{-1}}$	$\mathbf{K_{NH_3}}$	$\mathbf{2.60x10^{-4} \pm 6.0x10^{-5}}$
		$\mathbf{S_{\#}(0)}$	$\mathbf{4.08x10^{-1} \pm 1.06x10^{-1}}$	$\mathbf{K_{3,I}}$	$\mathbf{5.43x10^{-1} \pm 1.28x10^{-1}}$
		$\mathbf{X_{\#}(0)}$	$\mathbf{4.47x10^{-1} \pm 2.04x10^{-1}}$	$\mathbf{S_{\#}(0)}$	$\mathbf{1.49x10^{0} \pm 2.4x10^{-1}}$
Trial #4		**Trial #5**		**Trial #6**	
$\mathscr{J}$	**95.601**	$\mathscr{J}$	**156.086**	$\mathscr{J}$	**141.96**
$\bar{\mu}_1$	$\mathbf{5.27x10^{-1} \pm 6.0x10^{-3}}$	$\bar{\mu}_1$	$\mathbf{2.52x10^{-1} \pm 2.0x10^{-2}}$	$\bar{\mu}_1$	$\mathbf{3.71x10^{-1} \pm 2.8x10^{-2}}$
$\mathbf{K_2}$	$\mathbf{7.13x10^{0} \pm 5.0x10^{-1}}$	$\bar{\mu}_2$	$\mathbf{3.40x10^{-2} \pm 2.5x10^{-3}}$	$\bar{\mu}_2$	$\mathbf{2.65x10^{-2} \pm 3.0x10^{-3}}$
$\mathbf{K_3}$	$\mathbf{5.40x10^{-2} \pm 8.3x10^{-3}}$	$\bar{\mu}_3$	$\mathbf{1.97x10^{-1} \pm 8.0x10^{-3}}$	$\mathbf{K_3}$	$\mathbf{4.89x10^{-2} \pm 1.74x10^{-2}}$
$\mathbf{K_{NH_3}}$	$\mathbf{2.54x10^{-4} \pm 3.1x10^{-5}}$	$\mathbf{S_{\#}(0)}$	$\mathbf{8.48x10^{-1} \pm 8.2x10^{-2}}$	$\mathbf{K_{NH_3}}$	$\mathbf{1.56x10^{-4} \pm 3.6x10^{-5}}$
$\mathbf{K_{3,I}}$	$\mathbf{2.23x10^{0} \pm 1.3x10^{-1}}$			$\mathbf{K_{3,I}}$	$\mathbf{2.70x10^{0} \pm 8.9x10^{-1}}$
$\mathbf{k_{CO_2}}$	$\mathbf{4.01x10^{-1} \pm 7.9x10^{-2}}$			$\mathbf{S_{\#}(0)}$	$\mathbf{1.49x10^{0} \pm 2.3x10^{-1}}$

Of particular importance is any switch between "paired" parameters (i.e. μ and K parameters), which display a high degree of correlation and significantly impact the steady state of system (5.6). Fig. 5.1 and 5.2 show the predicted steady state optima for each top trial

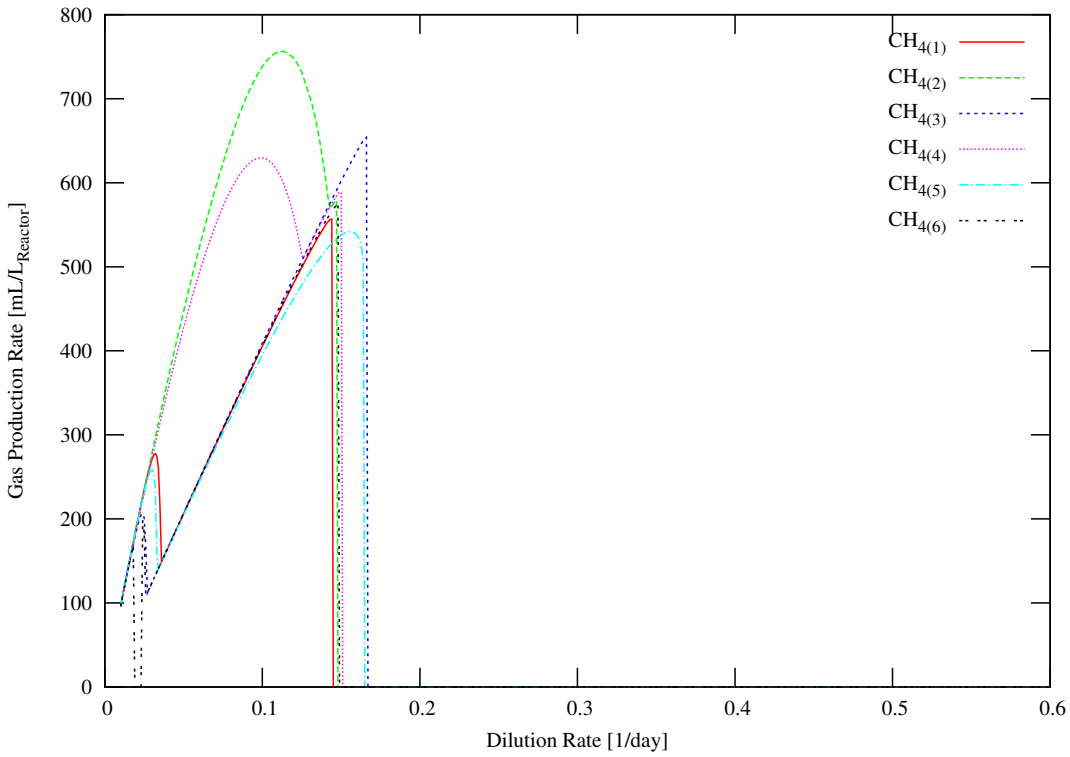

Figure 5.1: Predicted Steady State Optima as a Function of Dilution Rate Using Tab. 5.1 Parameters and $\alpha = 1.0$

result as a function of dilution rate (with feed conditions unmodified).

Within these plots it is clear that interesting things start to happen at higher dilution rates. This is also where the different combinations of estimated parameters begin to show how they impact optimal predictions. Fortunately, most conventional anaerobic digesters operate at hydraulic and solids retention times of greater than 10 days (this corresponds to dilution rates of less than 0.1). In this range it would appear that all 6 trial combinations predict relatively consistent results (these will later be compared to literature data), especially for a reactor with some form of solids recycle (which would be modelled by a value of $\alpha < 1$). The differences in the kinetic parameter combinations begin to take form at

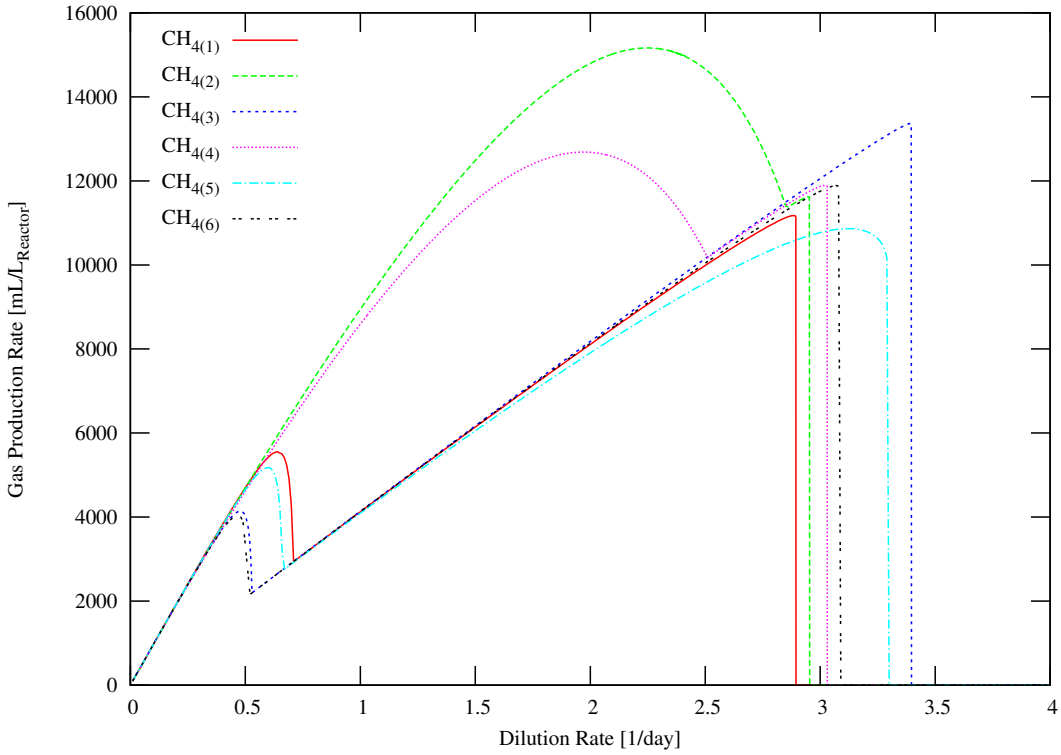

Figure 5.2: Predicted Steady State Optima as a Function of Dilution Rate Using Tab. 5.1 Parameters and $\alpha = 0.05$

higher dilution rates. This makes sense as it is at higher dilution rates (near washout) that the difference between selecting μ or K within a correlated pair, for example, would become more evident. As is clear in comparing Figs. 5.1 to 5.2 the differences in predictions may become significant for systems without recycles (i.e. $\alpha = 1.0$) as these will have a higher tendency to washout (explaining why the optima curves are "squished" to the left of the graph).

Examining each curve as a whole it is clear that two optimal methane flowrates are predicted in all cases. Knowing that the slowest reaction kinetics correspond to protein degradation (as evidenced by there calibrated reaction constants) it can be shown that the first optimal peak and decline is associated with the rise and eventual decline of protein acidogenic biomass. This is followed by the eventual washout of the methanogenic biomass (associated with the second optima). Determining when and how large these optima occur is where things get interesting. It should be immediately obvious that the first predicted optima of trial #2 and #4 are much higher than those of the other 4 trials (and in fact become global optimum). It is also no coincidence that for these 2 trials K_2 was selected instead of μ_2 within the correlated pair (refer to Tab. 5.1). Looking back to equations 5.4 and 5.5 it is clear that for a given ratio $\frac{\mu_2}{K_2}$ decreasing μ_2 to achieve a given ratio value has a pronounced effect on predicted steady state values than does increasing K_2. It is this effect being observed, which also casts some doubt on the models predictions as a whole. Indeed for any correlated pair within the model, one parameter was held constant at a default value while the other parameter was adjusted. But if the optimal prediction is so highly dependent on the parameter selected and we have no way of knowing the default value is itself correct, we can place very little confidence in the overall prediction. This would seem to indicate

additional experiments need to be conducted to distinguish these two parameters.

On the other hand, differences in the carbohydrate/lipid acidogen/acetogen and VFA methanogen kinetics appear to have less of an impact on the predicted optima. It is fairly evident that after the protein acidogens washout the second predicted optima is fairly consistent for all six trials. This is likely the case because even though there is correlation in these values as well, they do not appear to stray as far from the default paramater values as do the protein acidogens. The key kinetic methanogen parameters of μ_3 and K_3 for example have estimated values of $\approx 0.2-0.35$ 1/day and $\approx 0.05-0.07$ gCOD/L respectively (when estimated individually). The default values for these parameters are 0.2 1/day and 0.15 gCOD/L and so even though correlations within the estimates are known to exist, they appear to be less of an issue. On the other hand, the predicted parameter values for protein acidogenesis are in the $\mu_2 = 0.02-0.04$ 1/day and $K_2 = 4.0-7.0$ gCOD/L range as compared to their defaults of 0.2 1/day and 0.3 gCOD/L respectively.

Fig. 5.3 and 5.4 show the predicted steady state optima for each top trial result as a function of HRT (with feed conditions adjusted to obtain a constant throughput of 1 gCOD/L/day). It is under these conditions that we may compare model predictions against data available in the literature.

[50] asserts that the data in the literature appears to fit an inverse exponential form. Indeed this would seem to be the case and to that end the model predictions are not quite as expected (they appear to be a concatenation of two saturation profiles and therefore not

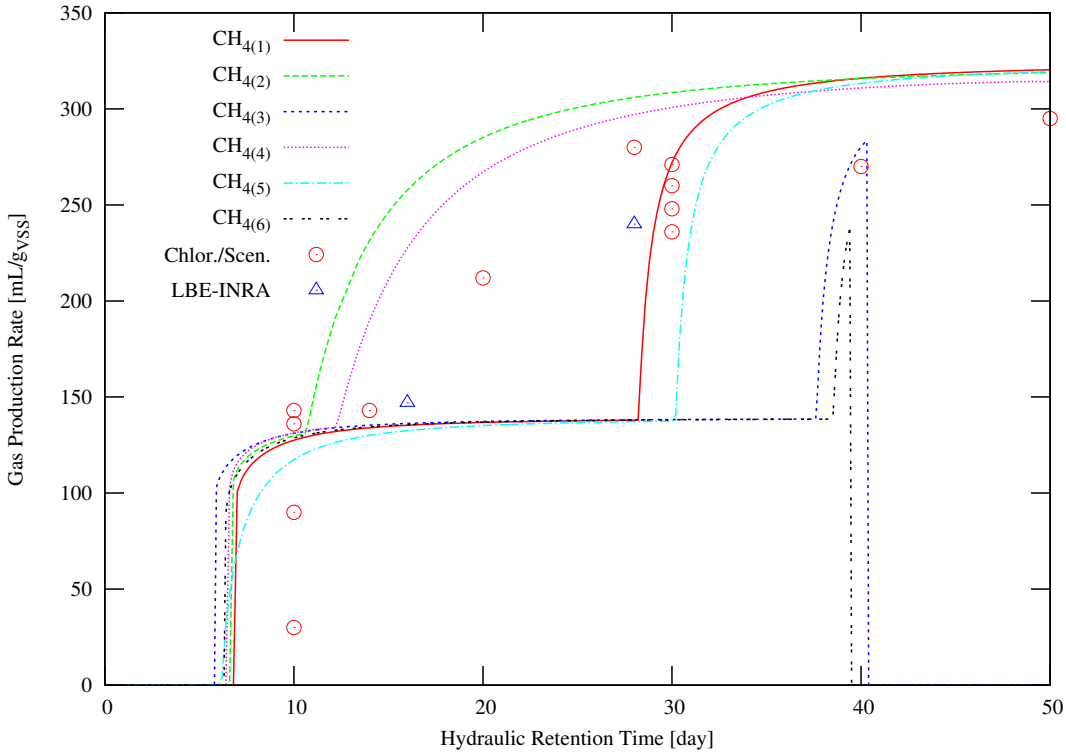

Figure 5.3: Predicted Steady State Optima as a Function of HRT Using Tab. 5.1 Parameters and $\alpha = 1.0$

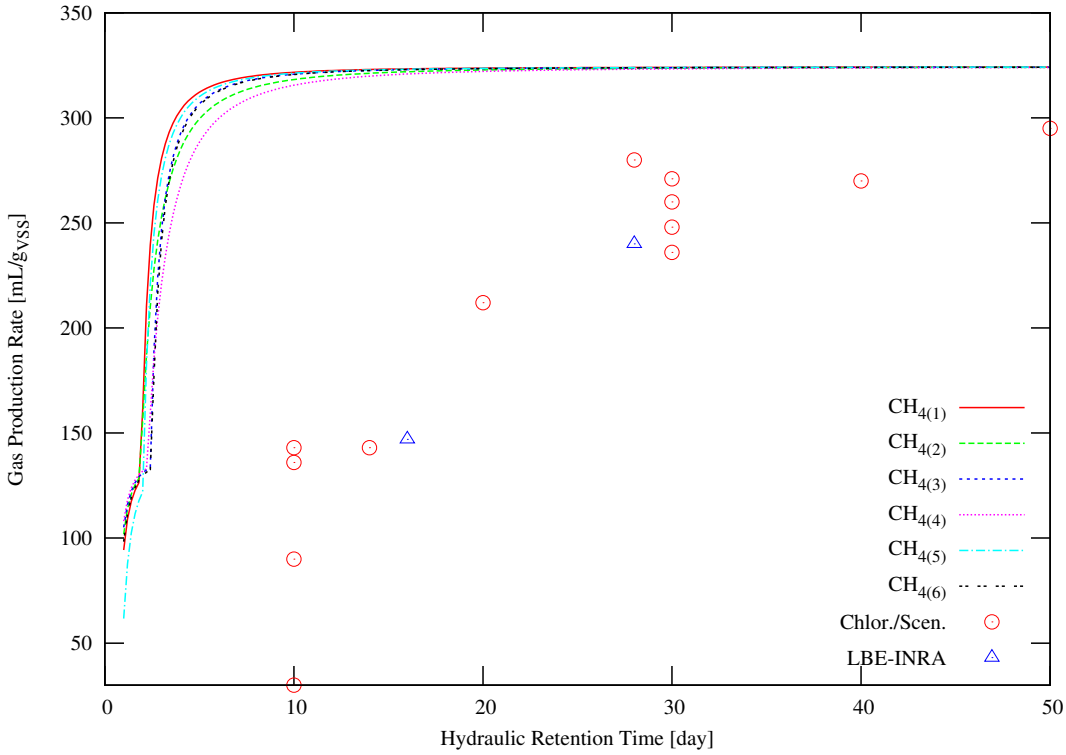

Figure 5.4: Predicted Steady State Optima as a Function of HRT Using Tab. 5.1 Parameters and $\alpha = 0.05$

exactly inverse exponential). Having said this the results of trial #2 and #4 still appear to predict the literature data very well and approximate this inverse exponential form. Even in the cases of Trial #1,3,5,6 the predictions are still in the ballpark of the literature data (i.e. same order of magnitude). The variation in the steady state model predictions as a function of identified parameter combinations shows a clear need to better identify each individual parameter. However, the fitted model still appears to be approximately valid despite individual parameter combination selections thus validating the overall dynamic model generated in §4.2.2.

5.2 Sensitivity Analysis

It was already observed that correlated pairs (most notably μ_2 and K_2) indicate a need for further experimental study. However, apart from these obvious issues it was also desired to examine how the uncertainty in the parameter estimates themseleves impacted model optimal predictions (the results of Tab. 4.5 clearly show varying degrees of uncertainty based on the variability in the experimental data). Since thresholds of 25% and 50% were used in the identification procedure variability within this range was studied. Of the potential parameter pool, variations of μ_1, K_1, K_{NH_3}, and k_{CO_2} within the 50% range were found to have negligible effect on optimal predictions. Fig. 5.5 and 5.6 give sample results for the Trial #1 parameter combination predictions but their representation of the impact of variability is representative of all 6 trials.

This was not entirely unexpected in the case of μ_1 and K_1 seeing as the hydrolysis/acidogenesis/acetogenesis of carbohydrates/long chain fatty acids is by far the fastest kinetic rate in the model and so variations between “somewhat fast” and “very fast” have little impact

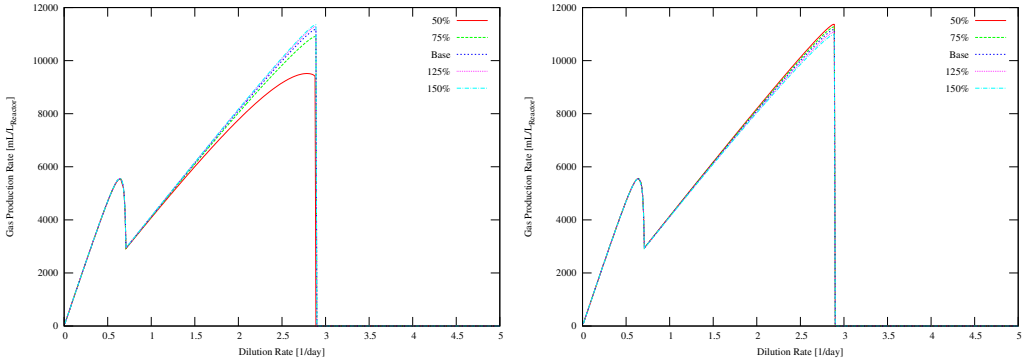

(a) μ_1 (b) K_1

Figure 5.5: Effects of μ_1 and K_1 Variation on Trial # 1 Optimal Results

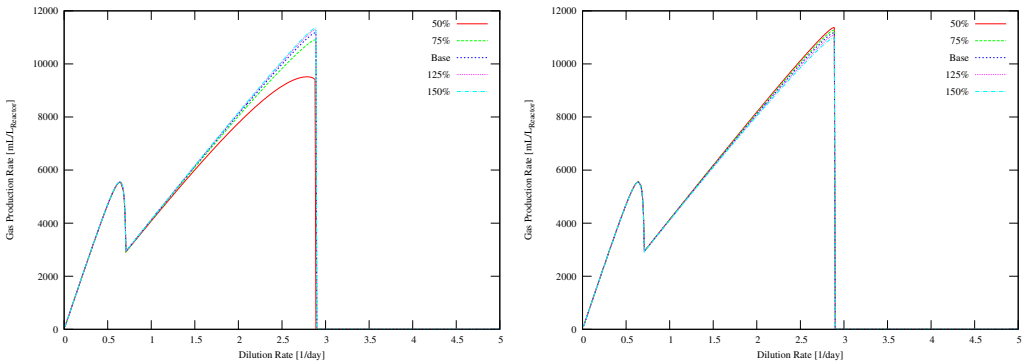

(a) K_{NH_3} (b) k_{CO_2}

Figure 5.6: Effects of K_{NH_3} and k_{CO_2} Variation on Trial # 1 Optimal Results

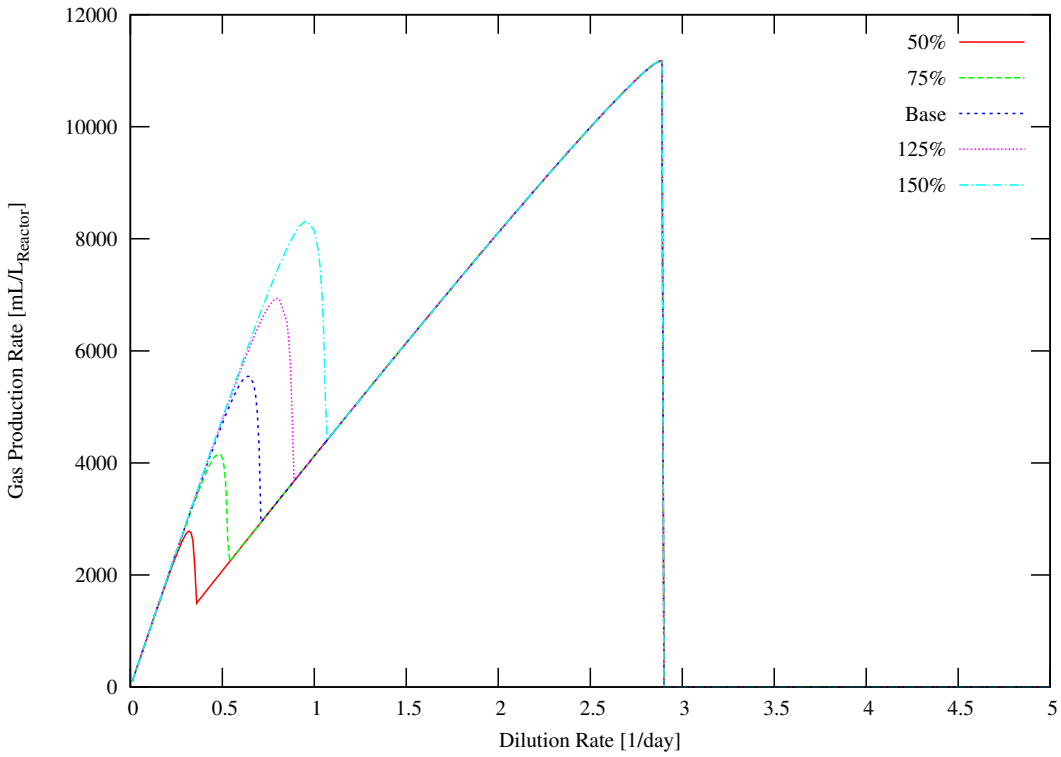

Figure 5.7: Effects of μ_2 Variation on Trial # 1 Optimal Results

on the overall optima (since the reaction goes to completion regardless).

Of particular interest is the impact of variation of μ_2, K_2, μ_3, K_3, and $K_{3,I}$. The impact of variation of these 5 parameters is fairly consistent for all 6 trial cases and so trial #1 will be used as a representative sample. Fig. 5.7 depicts the impact of variations in μ_2. As the rate limiting step in our model it would be expected to see a great degree of sensitivity towards the protein acidogenic parameters and indeed this would appear to be the case. Variations in μ_2 appear to lead to almost proportional variations in steady state methane production. Again this might not be an issue for reactors operated at high SRT (where this effect would only be observed at unrealistically high dilution rates), but for reactors operated without recycle this variability in optimal predictions could lead to real issues with model validity.

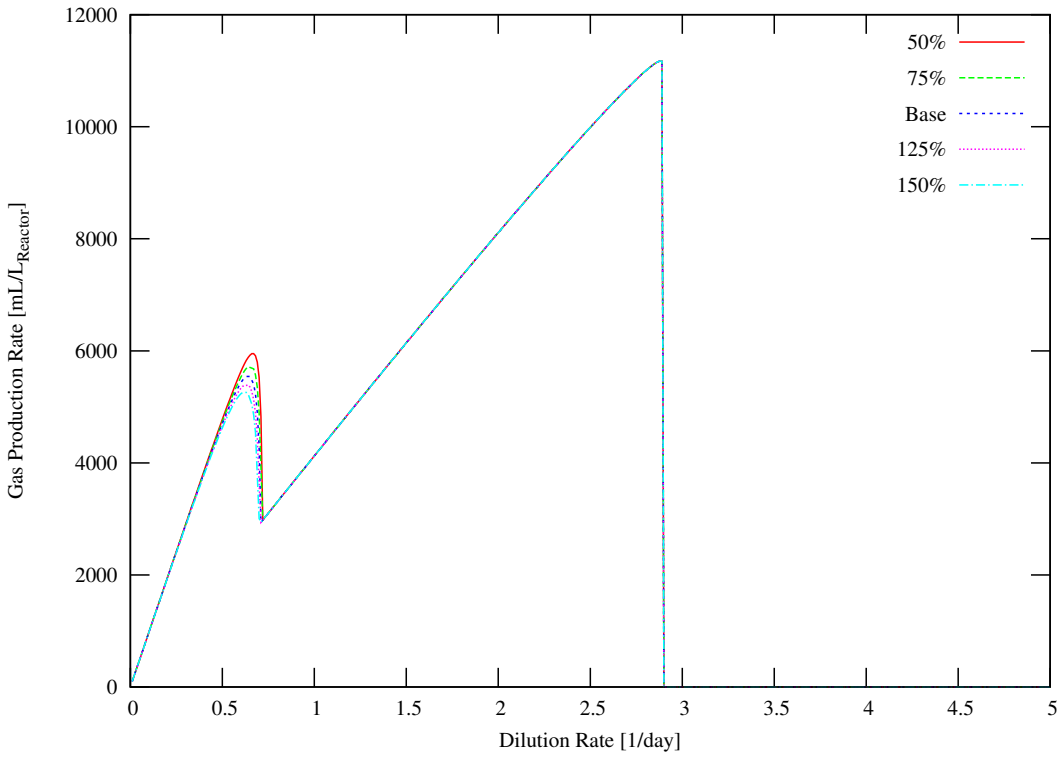

Figure 5.8: Effects of K_2 Variation on Trial # 1 Optimal Results

Fig. 5.8 displays the impact of variability in K_2. In this case the variability is still obvious, but is slightly damped in comparison to the impact of changing μ_2. This is interesting in itself but one must also remember that on top of this individual variation there is also a larger variation observed depending on which of the two parameters is estimated in the first place (as already discussed in §5.1) adding a further layer of uncertainty to these predictions.

Fig. 5.9 displays the impact of varying μ_3. Recall that once the protein acidogens are washed out, the VFA methanogens become the rate limiting step. This explains the heightened sensitivity to variations after the first optimum. One could argue the necessity for refining this parameter estimate though because its peculiarities really only show up at extremely high dilution rates (not likely to be encountered in practice). Thus the model is sensitive, but only in regions that are of little practical importance.

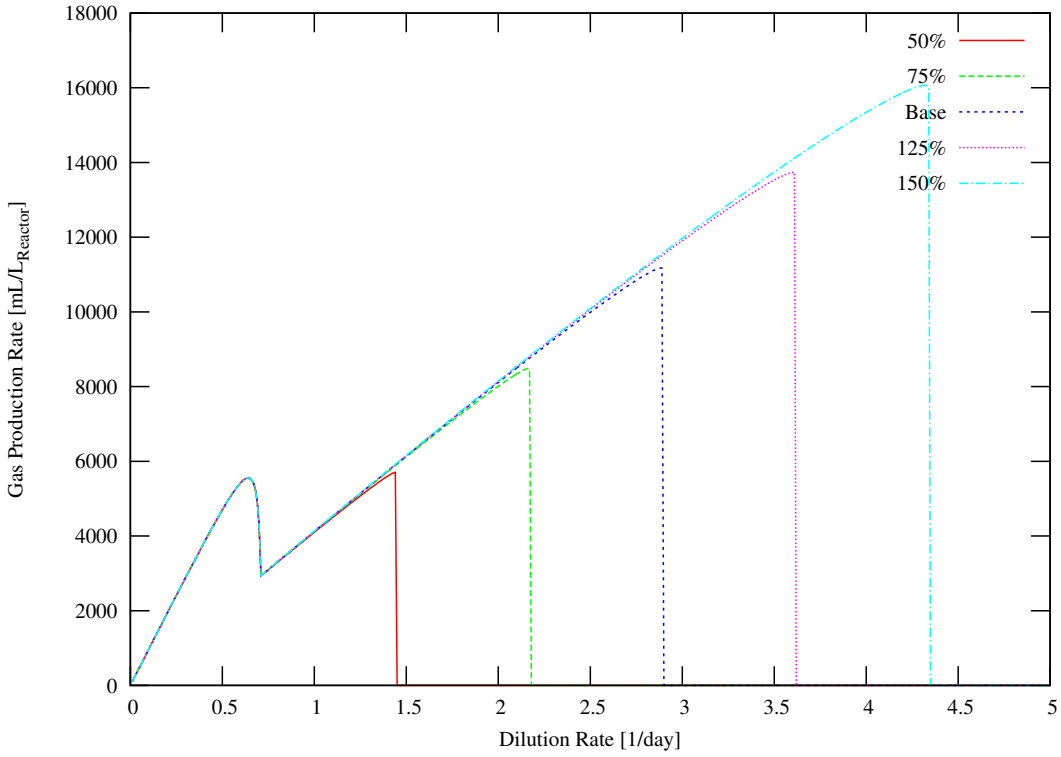

Figure 5.9: Effects of μ_3 Variation on Trial # 1 Optimal Results

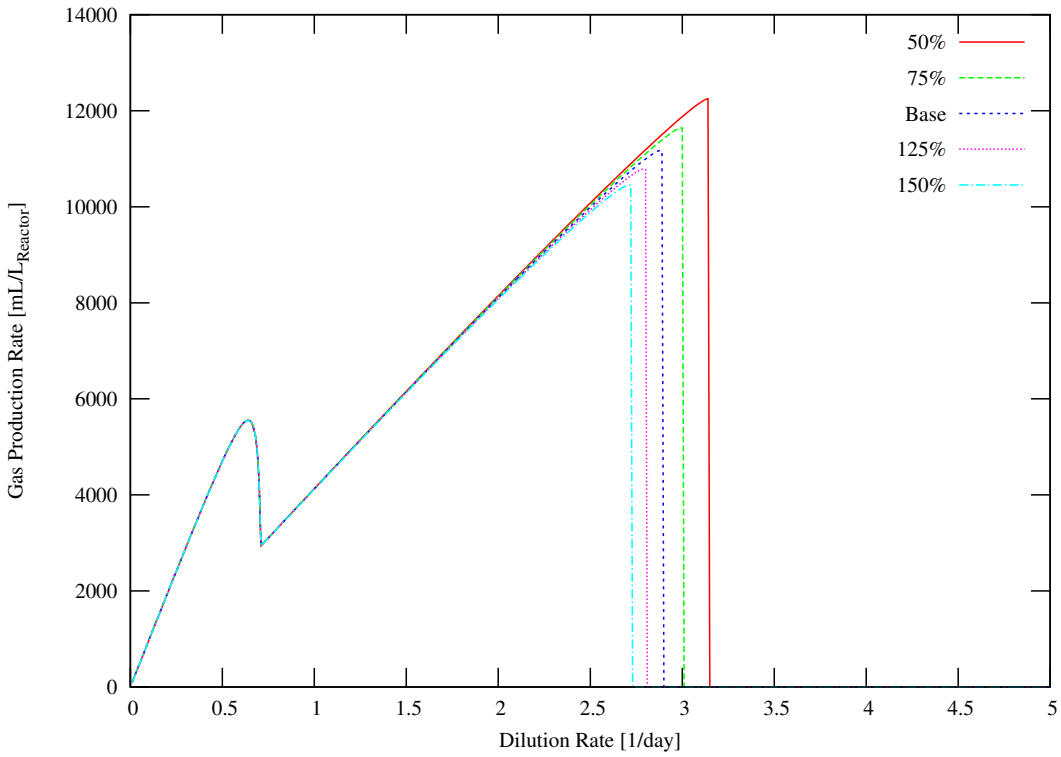

Figure 5.10: Effects of K_3 Variation on Trial # 1 Optimal Results

Fig. 5.10 and 5.11 finally show a similar damping effect to that observed for the denominator term K_2. Similar to μ_3 however, it is unlikely that this sensitivity would become important in most model cases since it occurs at very high dilution rates.

Obviously it would be ideal to be able to identify all parameters exactly but from the above results it would appear that special focus must be placed on identifying μ_2, K_2, μ_3, K_3, and $K_{3,I}$. More specifically, refining the estimates of μ_2, K_2, and perhaps μ_3 would go the furthest towards generating robust, accurate model predictions. Tab. 4.5 shows that calculated variability of these estimates for this LBE-INRA data set was in the range of 10 - 20 % (i.e. within the range of noticeable variation in optimal prediction).

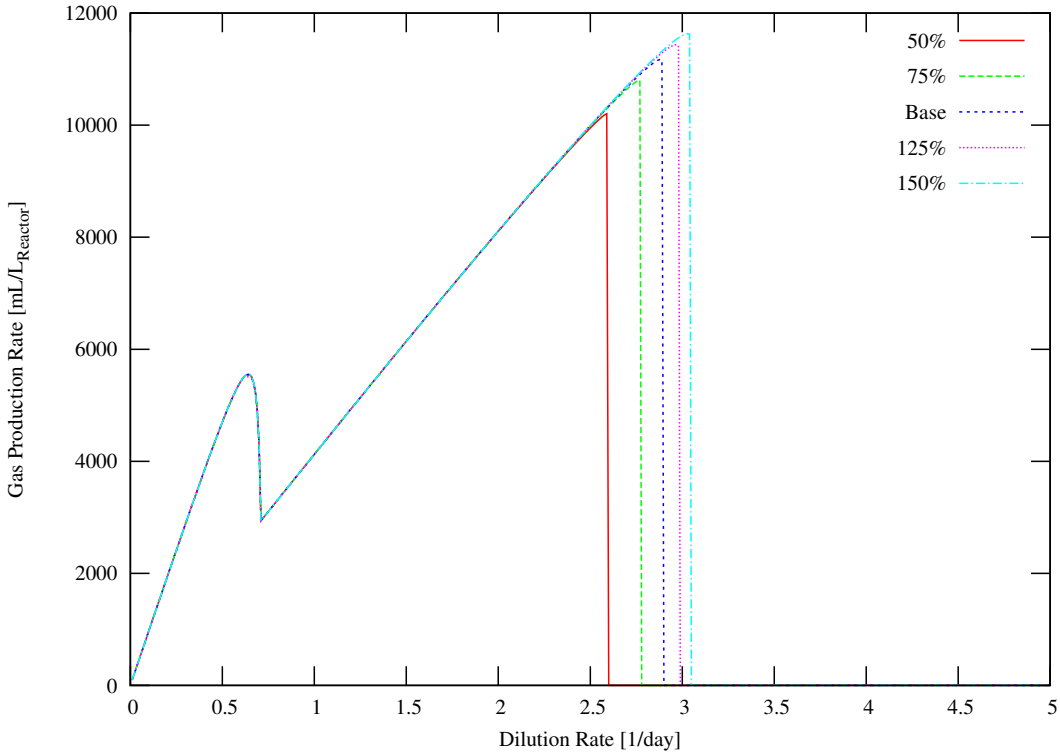

Figure 5.11: Effects of $K_{3,I}$ Variation on Trial # 1 Optimal Results

5.3 Conclusions

μ and K parameter pairs appear to be particularly problematic during steady state optimization. This is a problem inherited from the parameter identification algorithm, likely due to lack of information contained in the data. This lack of information means only the ratio appears to be identifiable and which of the two parameters is actually identified greatly impacts the placement of both local maximums. Luckily these problems only occur at dilution rates not commonly encountered in practice. Within realistic operating ranges the predicted steady state optima compare very well with available literature data. In terms of individual parameter sensitivity μ_2, μ_3, K_3, and $K_{3,I}$ appear to be particularly problematic and result in doubts about the reliability of the optimal predictions. Before reliable optimal study can be continued the parameter estimations must be improved.

Chapter 6

Conclusions and Future Work

6.1 Conclusions

The purpose of this work was to study the anaerobic digestion of algal biomass for its eventual inclusion in a combined photobioreactor/ anaerobic digestor system. In support of this, experiments were conducted by LBE-INRA on the anaerobic digestion of *Chlorella vulgaris* (a potential biofuel stock). Using this experimental data models were developed and fit using a novel identification algorithm. To this end a three reaction model including the hydrolysis/acidogenic/acetogenic degradation of carbohydrates/LCFAs, hydrolysis/acidogenic degradation of proteins, and the methanogenic breakdown of VFAs was found to fit the experimental data very well. It is believed that this model is of sufficient complexity to describe the observed dynamics and yet is simple enough to be involved in future control efforts. Several trials were run assuming different data weighting factors and starting conditions and the consistency of the results were promising. Specifically it was found that the

kinetics of the hydrolysis/acidogenic/acetogenic degradation of carbohydrates/long chain fatty acids, and hydrolysis/acidogenic degradation of proteins yielded reasonable consistent parameter estimates despite changes in the other parameters being estimatd. Despite this overall quality of fit the identification of many parameters involved in the model was mired by the presence of correlations in the data. To this end it is highly recommended that additional experiments (generated using proper experimental design procedures) be conducted to further refine these parameter estimates and therefore the validity of the model. Despite these uncertainties it was still found that the model operated reasonably well in predicting steady state performance as compared to the literature.

6.2 Future Work

6.2.1 Experimental Design to Improve Critical Parameter Precision

The presence of correlated parameter pairs and the general uncertainty of specific parameter estimates discussed in §4.3 and §5 indicate a need for rigorous experimental design to help reduce these issues. [54] provide a thorough discussion of experimental design approaches, a major group of which are based on minimizing functionals of the Fisher information matrix (a measurement of parameter confidence). Recall that the inverse of the Fisher information matrix can be used to estimate parameter estimate confidence.

$$\overset{min}{e}\ \Phi\left(M_F(\theta,e)\right) \tag{6.1}$$

$$M_F(\theta, e) = \frac{1}{N}\sum_{i=1}^{N}\frac{1}{w_i(e_i)}\frac{\delta y_i^m(\theta, e_i)}{\delta\theta}\left(\frac{\delta y_i^m(\theta, e_i)}{\delta\theta}\right)^T \tag{6.2}$$

where e_i denotes the ith experimental condition, θ is the parameter set, y_i^m is the ith set of model predictions, and $w_i(e_i)$ is the ith weighting factor.

From here different experiments can be designed around different control variable sets and functions of M_F. For example, in the case of bioprocesses, we might choose to hold the inlet concentrations constant and vary the inlet flowrate to elicit details of the dynamics. From here we might then choose to minimize the determinant inverse of M_F (the determinant being our chosen functional in this case) and generate an inlet flow profile that achieves this minimization over N experimental stages. This constitutes a classic dynamic optimization problem. The reason the inverse of the determinant would be a satisfactory optimality criterion is that the determinant represents the "size" of a matrix. If our confidence estimates are based on the inverse of the Fisher information then logically we would want the size of M_F to be as large as possible so as to minimize its inverse. One issue with this optimality criterion is it makes no account of relative parameter confidence. The matrix M_F could be "big" due to one parameter or all the parameters. A possible way to remedy this is to minimize the ratio of the largest and smallest eigenvalue of M_F. Such an optimality criterion generates a more uniform confidence region but also carries with it the issue of using derivative based solving methods. Naturally there are many more possible criteria and the choice depends on what the experimenter is looking for.

6.2.2 Modelling of Algal Photobioreactor and Coupling of System

On top of generating models for the anaerobic digestion of microalgae, the end goal of creating an optimized combined anaerobic/microalgal process will require a comprehensive model of the microalgal photobioreactor. A nitrogen limited Droop-type model is the current choice for the algal photobioreactor [10; 23; 44]. A model currently being developed by INRIA-COMORE is as below. These basic reaction steps and kinetic laws should serve as a basis for further testing and model identification in the vain of this thesis.

Microalgal Uptake of Inorganic Nitrogen:

$$\mathrm{IN} \overset{\rho(\mathrm{IN}_a,\mathrm{IN},X)X}{\Longrightarrow} \mathrm{IN}_a \tag{6.3}$$

Microalgal Autotrophic Growth:

$$\mathrm{IC} \overset{\mu_1(\mathrm{IC},I(z),\mathrm{IN}_a,X)X}{\Longrightarrow} \alpha_1 X + \alpha_2 \mathrm{O}_2 \tag{6.4}$$

Microalgal Heterotrophic Growth:

$$S_3 + \alpha_3 \mathrm{O}_2 \overset{\mu_2(\mathrm{IN}_a,S_3,X)X}{\Longrightarrow} \alpha_4 X \tag{6.5}$$

Algal autotrophic growth rate:

$$\mu_1(\mathrm{IC},I(z),\mathrm{IN}_a,X) = \frac{\bar{\mu}_1}{L}\left[\int_0^L \frac{I(z)}{I(z)+K_{I1}+\frac{I(z)^2}{K_{I2}}}dz\right]\left(\left(1-\frac{Q_0 X}{\mathrm{IN}_a}\right)\left(\frac{\mathrm{IC}}{\varepsilon+\mathrm{IC}}\right)\right) - resp \tag{6.6}$$

with the light distribution:

$$I(z) = I_0 e^{-\lambda z} \tag{6.7}$$

and the light attenuation coefficient:

$$\lambda = \lambda_0 + \lambda_1 \mathrm{IN}_a + \lambda_2 X + \lambda_3 S_1 + \lambda_4 S_2 + \lambda_5 S_4 + \lambda_6 X \tag{6.8}$$

Algal heterotrophic growth rate:

$$\mu_2(\mathrm{IC}, \mathrm{IN}_a, S_3, X) = \bar{\mu}_2 \frac{S_3}{K_3 + S_3} \left(1 - \frac{Q_0 X}{\mathrm{IN}_a}\right) \tag{6.9}$$

Algal nitrogen uptake rate:

$$\rho(\mathrm{IN}_a, \mathrm{IN}, X) = \bar{\rho} \frac{\mathrm{IN}}{K_{\mathrm{IN}} + \mathrm{IN}} \left(Q_L - \frac{\mathrm{IN}_a}{X}\right) \tag{6.10}$$

Where $\rho()$ is the algal nitrogen uptake rate, $\bar{\rho}$ is the maximum algal nitrogen uptake rate, IN is the external inorganic nitrogen concentration, K_{IN} is the algal nitrogen uptake half saturation constant, $\mu()$ is the specific algal growth rate, $\bar{\mu}_1$ is the maximum specific algal growth rate, X is the algal biomass concentration, Q_0 is the maximum cell quota, IN_a is the internal nitrogen concentration, Q_L is the maximum internal nitrogen concentration, IC is the external inorganic carbon concentration, and ε is the minimum allowable external inorganic carbon concentration. Future experiments are planned to fit parameters to the above model and to confirm that the model is of sufficient complexity to account for the majority of observed system dynamics (determined through principle component analysis

[11; 15]). Droop-type kinetics generally model algal reactors fairly well, although certain discrepancies may become an issue as research continues. The above does not provide any means of determining the weight fraction of LCFAs currently stored in the biomass. If biodiesel is to be one of the main products of the optimized reactor then determination of this quantity will also be something that needs to be examined further.

List of References

[1] John F. Andrews. Dynamic model of the anaerobic digestion process. *J. Sanit. Eng. Div. Amer. Soc. Civ. Eng.*, 95:95–116, 1969.

[2] John F. Andrews. Dynamic models and control strategies for wastewater treatment processes. *Water Research*, 8:261–289, 1974.

[3] D.J. Batstone, J. Keller, I. Angelidaki, S.V. Kalyuzhnyi, S.G. Pavlostathis, A. Rozzi, W.T.M. Sanders, H. Siegrist, and V.A. Vavilin. Anaerobic digestion model no. 1. Scientific and Technical Report 13, International Water Association, 2002.

[4] D.J. Batstone, J. Keller, I. Angelidaki, S.V. Kalyuzhnyi, S.G. Pavlostathis, A. Rozzi, W.T.M. Sanders, H. Siegrist, and V.A. Vavilin. The iwa anaerobic digestion model no 1 (adm1). *Water Science and Technology*, 45(10):65–73, 2003.

[5] E.W. Becker. *Microalgae: Biotechnology and Microbiology*. Cambridge Studies in Biotechnology. Cambridge University Press, New York, New York, 1994.

[6] E.W. Becker. Microalgae as a source of protein. *Biotechnology Advances*, 25(2):207–210, 2007.

[7] Moshe Ben-Akiva and Joffre Swait. The akaike likelihood ratio index. *Transportation Science*, 20(2):133–136, 1986.

[8] O. Bernard and G. Bastin. On the estimation of the pseudo-stoichiometric matrix for macroscopic mass balance modelling of biotechnological processes. *Mathematical Biosciences*, 193:51–77, 2005.

[9] O. Bernard, B. Chachuat, A. Hélias, and J. Rodriguez. Can we assess the model complexity for a bioprocess? Theory and example of the anaerobic digestion process. *Water Science and Technology*, 53(1):85–92, 2006.

[10] O. Bernard, A.-L. Mouly, F. Mairet, F. Grognard, and A. Dannappe. Modèles du couplage entre une lagune et un fermenteur anaérobie, 2009. Personal Communication.

[11] Olivier Bernard, Benoît Chachuat, Arnaud Helias, and Jean-Philippe Steyer. Assessing model complexity from anaerobic digestion data: When is model ADM1 required?

[12] Olivier Bernard, Zakaria Hadj-Sadok, Denis Dochain, Antoine Genovesi, and Jean-Philippe Steyer. Dynamical model development and parameter identification for an anaerobic wastewater treatment process. *Biotechnology and Bioengineering*, 75(4):424–438, 2001.

[13] J.-P. Cadoret and O. Bernard. La production de biocarburants lipidiques avec des microalgues: Promesses et défis. *Journal de la Société de Biologie*, 202(3):201–211, 2008.

[14] Benoît Chachuat and Olivier Bernard. Estimation of the yield coefficients in mass-balance based models for bioprocesses: Application to the anaerobic digestion process. Technical report, WRIA-COMORE, 2003.

[15] Benoît Chachuat, Olivier Bernard, and Jean-Philippe Steyer. A two-step procedure for estimating the parameters in mass-balance based bioprocess models.

[16] P.H. Chen and W.J. Oswald. Thermochemical treatment for algal fermentation. *Environment International*, 24(8):889–897, 1998.

[17] Yusuf Chisti. Biodiesel from microalgae. *Biotechnology Advances*, 25:294–306, 2007.

[18] Yusuf Chisti. Biodiesel from microalgae beats bioethanol. *Trends in Biotechnology*, 26(3):126–131, 2008.

[19] D.E. Contois. Kinetics of bacterial growth: Relationship between population density and specific growth rate of continuous cultures. *Journal of General Microbiology*, 21:40–50, 1959.

[20] A. Converti, R.P.S. Oliveira, B.R. Torres, A. Lodi, and M. Zilli. Biogas production and valorization by means of a two-step biological process. *Bioresource Technology*, 100(23):5771–5776, 2009.

[21] Burak Demirel and Orhan Yenigün. Two-phase anaerobic digestion processes: A review. *Journal of Chemical Technology and Biotechnology*, 77:743–755, 2002.

[22] D. Dochain and P.A. Vanrolleghem. *Dynamical Modelling and Estimation in Wastewater Treatment Processes*. IWA Publishing, London, UK, 2001.

[23] M.R. Droop. Vitamin B12 and marine ecology. iv. the kinetics of uptake, growth, and inhibition in *monochrysis lutheri*. *Journal of the Marine Biology Association of the United Kingdom*, 48:689–733, 1968.

[24] M.R. Droop. Some thoughts on nutrient limitation in algae. *Journal of Phycology*, 9:264–272, 1973.

[25] M.R. Droop. 25 years of algal growth kinetics: A personal view. *Botanica Marina*, XXVI:99–112, 1983.

[26] E.G. Foree and P.M. McCarty. Anaerobic decomposition of algae. *Environmental Science and Technology*, 4(10):842–849, 1970.

[27] L.G. Gassanova, Alexander I. Netrusov, V.V. Teplyakov, and M. Modigell. Fuel gases from organic wastes using membrane bioreactors. *Desalination*, 198:56–66, 2006.

[28] R.J. Geider and J. La Roche. Redfield revisited: Variability of c:n:p in marine microalgae and its biochemical basis. *European Journal of Phycology*, 37(1):1–17, 2002.

[29] C.G. Golueke and W.J. Oswald. Biological conversion of light energy to the chemical energy of methane. *Applied Microbiology*, 7(4):219–227, 1959.

[30] C.G. Golueke, W.J. Oswald, and H.B. Gotaas. Anaerobic digestion of algae. *Applied Microbiology*, 5(1):47–55, 1957.

[31] Chih-Hung Hsieh and Wen-Teng Wu. Cultivation of microalgae for oil production with a cultivation strategy of urea limitation. *Bioresource Technology*, 100(17):3921–3926, 2009.

[32] M. Huntley and D.G. Redalje. CO_2 mitigation and renewable oil from photosynthetic microbes: A new appraisal. *Mitigation and Adaptation for Global Change*, 12:573–608, 2007.

[33] A.M. Illman and A.H. Scragg S.W. Shales. Increase in chlorella strains calorific values when grown in low nitrogen medium. *Enzyme and Microbial Technology*, 27:631–635, 2000.

[34] R. Kleerebezem and M. Van Loosdrecht. Waste characterization for implementation in ADM1. *Water Science and Technology*, 54(4):167–174, 2006.

[35] I. Koster and G. Lettinga. The influence of ammonium-nitrogen on the specific activity of polletized methanogenic sludge. *Agricultural Wastes*, 9(3):205–216, 1984.

[36] Laurent Lardon, Arnaud Hélias, Bruno Sialve, Jean-Philippe Steyer, and Olivier Bernard. Life-cycle assessment of biodiesel production from microalgae. *Environmental Science and Technology*, 43(17):6475–6481, 2009.

[37] Zhi-Yuan Liu, Guang-Ce Wang, and Bai-Cheng Zhou. Effect of iron on growth and lipid accumulation in C*hlorella vulgaris*. *Bioresource Technology*, 99(11):4717–4722, 2008.

[38] G. Lyberatos and I. Skiadas. Modelling of anaerobic digestion - a review. *Global NEST Journal*, 1(2):63–76, 1999.

[39] F. Mairet, O. Bernard, M. Ras, L. Lardon, and J.-P. Steyer. A dynamic model for anaerobic digestion of microalgae. In *Proc 18th IFAC World Congress*, 2011.

[40] MathWorks. csaps: Cubic smoothing spline, 2011.

[41] Metcalf & Eddy, George Tchobanoglous, Franklin L. Burton, and H. David Stensel, editors. *Wastewater Engineering: Treatment and Reuse (Fourth Edition)*. McGraw Hill, New York, New York, 2003.

[42] J. Monod. The growth of bacterial cultures. *Annual Review of Microbiology*, 3:371–394, 1949.

[43] F.E. Mosey. Mathematical modelling of the anaerobic digestion process: Regulatory mechanisms for the formation of short-chain volatile acids from glucose. *Water Science and Technology*, 15:209–232, 1983.

[44] A.-L. Mouly. Première approche pour la modélisation du couplage d'une culture d'algues et d'un digesteur anaérobie. Technical report, University Lyon, INRIA, and Symbiose, 2009. M.Sc. Thesis.

[45] J.H. Mussgnug, V. Klassen, A. Schlüter, and O. Kruse. Microalgae as substrates for fermentative biogas production in a combined biorefinery concept. *Journal of Biotechnology*, 150(1):51–56, 2010.

[46] M. Myint and N. Nirmalakhandan. Evaluation of first-order, second-order, and surface-limiting reactions in anaerobic hydrolysis of cattle manure. *Environmental Engineering Science*, 23(6):970–980, 2006.

[47] G.C. Okpokwasili and C.O. Nweke. Microbial growth and substrate utilization kinetics. *African Journal of Biotechnology*, 5(4):305–317, 2005.

[48] Dirk De Pauw, Peter Vanrolleghem, Benoît Chachuat, and Olivier Bernard. A set of procedures to estimate model parameters on-line and off-line. Technical report, European Project TELEMAC, Ghent University, 2003.

[49] J. Pruvost, G. Van Vooren, B. Le Gouic, A. Couzinet-Mossion, and J. Legrand. Systematic investigation of biomass and lipid productivity by microalgae in photobioreactors for biodiesel application. *Bioresource Technology*, 102:150–158, 2011.

[50] M. Ras, L. Lardon, B. Sialve, N. Bernet, and J.-P. Steyer. Experiental study on a coupled process of production and anaerobic digestion of *chlorella vulgaris*. *Bioresource Technology*, 102(1):200–206, 2011.

[51] Bruno Sialve, Nicolas Bernet, and Olivier Bernard. Anaerobic digestion of microalgae as a necessary step to make microalgal biodiesel sustainable. *Biotechnology Advances*, 27:409–416, 2009.

[52] J. Steyer, O. Bernard, D. Batstone, and I. Angelidaki. Lessons learnt from 15 years of ICA in anaerobic digesters. *Water Science and Technology*, 53(4-5):25–33, 2006.

[53] A.F.M. Van Velsen. Adaptation of methanogenic sludge to high ammonia-nitrogen concentrations. *Water Research*, 13(10):995–999, 1979.

[54] E. Walter and L. Pronzato. Qualitative and quantitative experiment design for phenomenological models - a survey. *Automatica*, 26(2):195–213, 1990.

[55] H.W. Yen and D.E. Brune. Anaerobic co-digestion of algal sludge and waste paper to produce methane. *Bioresource Technology*, 98(1):130–134, 2007.

Appendix A

Nomenclature

A.1 Variables

A.1.1 Anaerobic Digester

Variable	Unit	Meaning
CO_2	$\left[\frac{\text{mol}}{\text{L}}\right]$	Carbon dioxide concentration
CO_3^{2-}	$\left[\frac{\text{mol}}{\text{L}}\right]$	Carbonate concentration
CH_4	$\left[\frac{\text{mol}}{\text{L}}\right]$	Methane concentration
D	$\left[\frac{1}{\text{day}}\right]$	Bioreactor dilution rate
F_{in}	$\left[\frac{\text{L}}{\text{day}}\right]$	Flowrate into bioreactor
F_{out}	$\left[\frac{\text{L}}{\text{day}}\right]$	Flowrate out of bioreactor
$[H^+]$	$\left[\frac{\text{mol}}{\text{L}}\right]$	Hydronium concentration
H_2	$\left[\frac{\text{mol}}{\text{L}}\right]$	Hydrogen concentration
HCO_3^-	$\left[\frac{\text{mol}}{\text{L}}\right]$	Bicarbonate concentration
I_i	[variable]	Inhibition factor associated with substrate i
IC	$\left[\frac{\text{mol}}{\text{L}}\right]$	Inorganic carbon (CO_2, HCO_3^-, CO_3^{2-}) concentration
IN	$\left[\frac{\text{mol}}{\text{L}}\right]$	Inorganic nitrogen ($NH_4^+ + NH_3$) concentration
NH_3	$\left[\frac{\text{mol}}{\text{L}}\right]$	Ammonia concentration
$[NH_4^+]$	$\left[\frac{\text{mol}}{\text{L}}\right]$	Ammonium concentration
$[OH^-]$	$\left[\frac{\text{mol}}{\text{L}}\right]$	Hydroxide concentration
P_{CO_2}	[atm]	Partial pressure of CO_2
pH	$[-]$	pH value
$\mathbf{q}()$	$\left[\frac{\text{concentration}}{\text{day}}\right]$	Generic gas production rate vector
q_{CH_4}	$\left[\frac{\text{mol}}{\text{day}}\right]$	Methane production rate
q_{CO_2}	$\left[\frac{\text{mol}}{\text{day}}\right]$	Carbon dioxide production rate
$\mathbf{r}()$	$\left[\frac{\text{concentration}}{\text{day}}\right]$	Generic reaction rate vector
S_1	$\left[\frac{\text{g COD}}{\text{L}}\right]$	Organic carbon (w/o inerts and proteins) substrate concentration
S_2	$\left[\frac{\text{g COD}}{\text{L}}\right]$	N-linked organic carbon substrate concentration
S_3	$\left[\frac{\text{g COD}}{\text{L}}\right]$	Volatile fatty acid concentration
S_4	$\left[\frac{\text{g COD}}{\text{L}}\right]$	Inert organic carbon (”reluctant”) substrate concentration
S_{cell}	$\left[\frac{\text{variable}}{\text{L}}\right]$	Droop limiting substrate concentration internal to biomass
S_i	[variable]	Concentration of substrate i
V_R	[L]	Liquid volume of bioreactor

Variable	Unit	Meaning
$\mathbf{X}$	$[\text{variable}]$	Generic state vector
$\mathbf{X}_{in}$	$[\text{variable}]$	Generic inlet state vector
X_1	$\left[\frac{\text{g COD}}{\text{L}}\right]$	Carbohydrate/lipid metabolizing acidogenic biomass concentration
X_2	$\left[\frac{\text{g COD}}{\text{L}}\right]$	Protein metabolizing acidogenic biomass concentration
X_3	$\left[\frac{\text{g COD}}{\text{L}}\right]$	VFA metabolizing methanogenic biomass concentration
X_i	$\left[\frac{\text{g COD}}{\text{L}}\right]$	Biomass concentration for substrate i
$\mathbf{X}_{in}$	$[\text{variable}]$	Generic inlet state vector
Z	$\left[\frac{\text{mol}}{\text{L}}\right]$	Non affected (cations-anions) concentration
$[Ca^{2+}]$	$\left[\frac{\text{mol}}{\text{L}}\right]$	Calcium ions concentration
$[Cl^{-}]$	$\left[\frac{\text{mol}}{\text{L}}\right]$	Chlorine ions concentration
$[HPO_4^{2-}]$	$\left[\frac{\text{mol}}{\text{L}}\right]$	Hydrogen phosphate concentration
$[H_2PO_4^{-}]$	$\left[\frac{\text{mol}}{\text{L}}\right]$	Dihydrogen phosphate concentration
$[H_3PO_4]$	$\left[\frac{\text{mol}}{\text{L}}\right]$	Phosphoric acid concentration
$[HSO_4^{-}]$	$\left[\frac{\text{mol}}{\text{L}}\right]$	Bisulfate concentration
$[H_2SO_4]$	$\left[\frac{\text{mol}}{\text{L}}\right]$	Sulfuric acid concentration
$[K^{+}]$	$\left[\frac{\text{mol}}{\text{L}}\right]$	Potassium ions concentration
$[Mg^{2+}]$	$\left[\frac{\text{mol}}{\text{L}}\right]$	Magnesium ions concentration
$[Na^{+}]$	$\left[\frac{\text{mol}}{\text{L}}\right]$	Sodium ions concentration
P	$\left[\frac{\text{mol}}{\text{L}}\right]$	Phosphorus concentration
$[PO_4^{3-}]$	$\left[\frac{\text{mol}}{\text{L}}\right]$	Phosphate concentration
S	$\left[\frac{\text{mol}}{\text{L}}\right]$	Sulfur concentration
$[SO_4^{2-}]$	$\left[\frac{\text{mol}}{\text{L}}\right]$	Sulfate concentration
μ_1	$\left[\frac{1}{\text{day}}\right]$	Calculated specific S_1 associated growth rate of carbohydrate/lipid metabolizing acidogenic bacteria
μ_2	$\left[\frac{1}{\text{day}}\right]$	Calculated specific S_2 associated growth rate of protein/DNA metabolizing acidogenic bacteria
μ_3	$\left[\frac{1}{\text{day}}\right]$	Calculated specific S_3 associated growth rate of VFA metabolizing methanogenic bacteria

A.1.2 Algal Photobioreactor

Variable	Unit	Meaning
I()	$[]$	Light intensity
IC	$\left[\frac{\text{mol}}{\text{L}}\right]$	Inorganic carbon (CO_2, HCO_3^-, CO_3^{2-}) concentration
IN	$\left[\frac{\text{mol nitrogen}}{\text{L}}\right]$	Inorganic nitrogen, algal substrate ($NH_4^+ + NH_3$)
IN_a	$\left[\frac{\text{mol nitrogen}}{\text{L}}\right]$	Algal internal nitrogen concentration in algal reactor
O_2	$\left[\frac{\text{mol } O_2}{\text{L}}\right]$	Dissolved oxygen concentration
X	$\left[\frac{\text{g carbon}}{\text{L}}\right]$	Algal biomass concentration in C
S_1	$\left[\frac{\text{g COD}}{\text{L}}\right]$	Organic carbon (w/o inerts and proteins) substrate concentration
S_2	$\left[\frac{\text{g COD}}{\text{L}}\right]$	N-linked organic carbon substrate concentration
S_3	$\left[\frac{\text{g COD}}{\text{L}}\right]$	Volatile fatty acid concentration
S_4	$\left[\frac{\text{g COD}}{\text{L}}\right]$	Inert organic carbon (”reluctant”) substrate concentration
X	$\left[\frac{\text{g COD}}{\text{L}}\right]$	Algal biomass concentration
z	$[\text{m}]$	depth coordinate in reactor

A.2 Parameters

A.2.1 Anaerobic Digestor Stoichiometry

Variable	Unit	Meaning
$\mathbf{p}$	[variable]	Generic parameter vector
Y_1	$\left[\frac{\text{g COD}}{\text{g COD}}\right]$	Fraction of the COD in algal biomass feed in the form of sugar/lipids
Y_2	$\left[\frac{\text{g COD}}{\text{g COD}}\right]$	Fraction of the COD in algal biomass feed in the form of proteins/DNA
Y_4	$\left[\frac{\text{g COD}}{\text{g COD}}\right]$	Fraction of the COD in algal biomass feed in the form of inerts
$\beta_{i,j}$	[variable]	Stoichiometric coefficient j of substrate/biomass pair i
β_1	$\left[\frac{\text{g COD}}{\text{g COD}}\right]$	Ratio of gCOD sugar/lipid consumed to gCOD sugar/lipid metabolizing acidogenic bacteria produced
β_2	$\left[\frac{\text{mol N}}{\text{g COD}}\right]$	Ratio of moles inorganic nitrogen consumed to gCOD sugar/lipid metabolizing acidogenic bacteria produced
β_3	$\left[\frac{\text{g COD}}{\text{g COD}}\right]$	Ratio of moles acetic acid (VFA) produced to gCOD sugar/lipid metabolizing acidogenic bacteria produced
β_4	$\left[\frac{\text{mol C}}{\text{g COD}}\right]$	Ratio of moles inorganic carbon consumed to gCOD sugar/lipid metabolizing acidogenic bacteria produced
β_5	$\left[\frac{\text{g COD}}{\text{g COD}}\right]$	Ratio of gCOD protein consumed to gCOD protein metabolizing acidogenic bacteria produced
β_6	$\left[\frac{\text{mol N}}{\text{g COD}}\right]$	Ratio of moles inorganic nitrogen produced to gCOD protein metabolizing acidogenic bacteria produced
β_7	$\left[\frac{\text{g COD}}{\text{g COD}}\right]$	Ratio of gCOD acetic acid (VFA) produced to gCOD protein metabolizing acidogenic bacteria produced
β_8	$\left[\frac{\text{mol C}}{\text{g COD}}\right]$	Ratio of moles inorganic carbon consumed to gCOD protein metabolizing acidogenic bacteria produced
β_9	$\left[\frac{\text{g COD}}{\text{g COD}}\right]$	Ratio of gCOD acetic acid (VFA) consumed to gCOD VFA metabolizing methanogenic bacteria produced
β_{10}	$\left[\frac{\text{mol N}}{\text{g COD}}\right]$	Ratio of moles inorganic nitrogen produced to gCOD VFA metabolizing methanogenic bacteria produced
β_{11}	$\left[\frac{\text{mol CH}_4}{\text{g COD}}\right]$	Ratio of moles methane (CH_4) produced to gCOD VFA metabolizing methanogenic bacteria produced
β_{12}	$\left[\frac{\text{mol C}}{\text{g COD}}\right]$	Ratio of moles inorganic carbon consumed to gCOD VFA metabolizing methanogenic bacteria produced

A.2.2 Anaerobic Digestor Kinetics

Variable	Unit	Meaning
f_b	$[-]$	Effluent bacteria dilution factor
H_{CO_2}	$\left[\frac{\text{mol}}{\text{m}^3\ \text{atm}}\right]$	Henry's law coefficient for CO_2
K_1	$\left[\frac{\text{g COD}}{\text{L}}\right]$	co_b associated half saturation constant of carbohydrate/lipid metabolizing acidogenic bacteria
K_2	$\left[\frac{\text{g COD}}{\text{L}}\right]$	cn_b associated half saturation constant of protein/DNA metabolizing acidogenic bacteria
K_3	$\left[\frac{\text{g COD}}{\text{L}}\right]$	vfa_b associated half saturation constant of VFA metabolizing methanogenic bacteria
$K_{3,I}$	$\left[\frac{\text{g COD}^2}{\text{L}^2}\right]$	vfa_b associated Haldane substrate inhibition constant of VFA metabolizing methanogenic bacteria
K_{ace}	$\left[\frac{\text{mol}}{\text{L}}\right]$	Acetic acid dissociation constant at 35 ^oC
K_{CO_2}	$\left[\frac{\text{mol}}{\text{L}}\right]$	Carbon dioxide dissolution equilibrium constant at 35 ^oC
K_{H_2O}	$\left[\frac{\text{mol}}{\text{L}}\right]$	Water acid dissociation constant at 35 ^oC
$K_{H_3PO_4}$	$\left[\frac{\text{mol}}{\text{L}}\right]$	Phosphoric acid dissociation constant at 35 ^oC
$K_{H_2PO_4^-}$	$\left[\frac{\text{mol}}{\text{L}}\right]$	Dihydrogen phosphate acid dissociation constant at 35 ^oC
$K_{HPO_4^{2-}}$	$\left[\frac{\text{mol}}{\text{L}}\right]$	Hydrogen phosphate acid dissociation constant at 35 ^oC
$K_{H_2SO_4}$	$\left[\frac{\text{mol}}{\text{L}}\right]$	S acid dissociation constant at 35 ^oC
$K_{HSO_4^-}$	$\left[\frac{\text{mol}}{\text{L}}\right]$	Bisulfate acid dissociation constant at 35 ^oC
$K_{HCO_3^-}$	$\left[\frac{\text{mol}}{\text{L}}\right]$	Bicarbonate acid dissociation constant at 35 ^oC
k_i	$\left[\frac{1}{\text{day}}\right]$	Disintegration coefficient of substrate i
K_i	$\left[\frac{\text{g COD}}{\text{L}}\right]$	Half-saturation coefficient of substrate/biomass combination i
$K_{i,I}$	[variable]	Inhibition coefficient for substrate i
k_La	$\left[\frac{\text{m}^3}{\text{day}}\right]$	Liquid gas mass transfer coefficient
K_{NH_3}	$\left[\frac{\text{mol N}}{\text{L}}\right]$	VFA metabolizing methanogenic bacteria ammonia inhibition constant
$K_{NH_4^+}$	$\left[\frac{\text{mol}}{\text{L}}\right]$	Ammonium acid dissociation constant at 35 ^oC
K_Q	$\left[\frac{\text{mol N}}{\text{L}}\right]$	Droop limiting cell quota
pH_{LL}	$[-]$	pH lower limit inhibition coefficient
pH_{UL}	$[-]$	pH upper limit inhibition coefficient

Variable	Unit	Meaning
$pH_{LL,AA}$	$[-]$	pH acetogenesis/acidogenesis lower limit inhibition coefficient
$pH_{UL,AA}$	$[-]$	pH acetogenesis/acidogenesis upper limit inhibition coefficient
$pH_{LL,M}$	$[-]$	pH methanogenesis lower limit inhibition coefficient
$pH_{UL,M}$	$[-]$	pH methanogenesis upper limit inhibition coefficient
ε	$\left[\frac{\text{g "element"}}{\text{L}}\right]$	Near zero value used to avoid numerical issues
$\bar{\mu}_i$	$\left[\frac{1}{\text{day}}\right]$	Maximum specific growth rate constant of substrate/biomass combination i
$\bar{\mu}_1$	$\left[\frac{1}{\text{day}}\right]$	Maximum specific S_1 associated growth rate constant of carbohydrate/lipid metabolizing acidogenic bacteria
$\bar{\mu}_2$	$\left[\frac{1}{\text{day}}\right]$	Maximum specific S_2 associated growth rate constant of protein/DNA metabolizing acidogenic bacteria
$\bar{\mu}_3$	$\left[\frac{1}{\text{day}}\right]$	Maximum specific S_3 associated growth rate constant of VFA metabolizing methanogenic bacteria
$\bar{\mu}_D$	$\left[\frac{1}{\text{day}}\right]$	Droop maximum specific growth rate constant

A.2.3 Algal Photobioreactor Stoichiometry

Variable	Unit	Meaning
α_1	$\left[\frac{\text{mol N}}{\text{g COD}}\right]$	
α_2	$\left[\frac{\text{mol N}}{\text{g COD}}\right]$	
α_3	$\left[\frac{\text{mol N}}{\text{g COD}}\right]$	
α_4	$\left[\frac{\text{g COD}}{\text{g COD}}\right]$	
K_Q	$\left[\frac{\text{mol N}}{\text{L}}\right]$	Droop limiting cell quota
$\bar{\mu}_D$	$\left[\frac{1}{\text{day}}\right]$	Droop maximum specific growth rate constant

A.2.4 Algal Photobioreactor Kinetics

Variable	Unit	Meaning
f_a	$[-]$	Effluent algae concentration factor of heterotrophic bacteria under aerobic conditions, 20^oC
K_{I1}	$\left[\frac{\text{W}}{\text{m}^2}\right]$	Haldane half saturation constant
K_{I2}	$\left[\frac{\text{W}^2}{\text{m}^4}\right]$	Haldane substrate inhibition constant
K_Q	$\left[\frac{\text{mol N}}{\text{L}}\right]$	Droop limiting cell quota
K_{IN}	$\left[\frac{\text{mol nitrogen}}{\text{L}}\right]$	Algal inorganic nitrogen uptake half saturation constant
K_3	$\left[\frac{\text{g COD}}{\text{L}}\right]$	vfa_a associated half saturation constant of heterotrophic bacteria
L	$[\text{m}]$	Average depth of microalgal pond
Q_0	$\left[\frac{\text{g nitrogen}}{\text{g carbon}}\right]$	Droop minimum algal internal nitrogen quota
Q_L	$\left[\frac{\text{g nitrogen}}{\text{g carbon}}\right]$	Limiting (maximum) algal internal nitrogen quota
$\bar{\mu}_D$	$\left[\frac{1}{\text{day}}\right]$	Droop maximum specific growth rate constant

Variable	Unit	Meaning
ε	$\left[\frac{\text{g "element"}}{\text{L}}\right]$	Near zero value used to avoid numerical issues
λ	$\left[\frac{1}{\text{m}}\right]$	Overall light absorption coefficient
λ_0	$\left[\frac{1}{\text{m}}\right]$	Base light absorption coefficient
λ_1	$\left[\frac{\text{L}}{\text{g nitrogen * m}}\right]$	Light absorption coefficient associated with algal nitrogen
λ_2	$\left[\frac{\text{L}}{\text{g carbon * m}}\right]$	Light absorption coefficient associated with algal biomass
λ_3	$\left[\frac{\text{L}}{\text{g COD * m}}\right]$	Light absorption coefficient associated with carbohydrate/lipid detritus
λ_4	$\left[\frac{\text{L}}{\text{g COD * m}}\right]$	Light absorption coefficient associated with protein/DNA detritus
λ_5	$\left[\frac{\text{L}}{\text{g COD * m}}\right]$	Light absorption coefficient associated with inerts
λ_6	$\left[\frac{\text{L}}{\text{g COD * m}}\right]$	Light absorption coefficient associated with heterotrophic bacteria
$\bar{\mu}_{a_1}$	$\left[\frac{1}{\text{day}}\right]$	Droop maximum specific growth rate constant associated with nitrogen based algal growth
μ_{a_1}	$\left[\frac{1}{\text{day}}\right]$	Calculated Droop specific growth rate associated with nitrogen based algal growth
$\bar{\mu}_{a_2}$	$\left[\frac{1}{\text{day}}\right]$	Heterotrophic algal maximum specific growth rate constant
μ_{a_2}	$\left[\frac{1}{\text{day}}\right]$	Calculated COD based heterotrophic algal specific growth rate
$\bar{\mu}_{h_{a1}}$	$\left[\frac{1}{\text{day}}\right]$	Maximum specific co_a associated growth rate constant of heterotrophic bacteria
$\mu_{h_{a1}}$	$\left[\frac{1}{\text{day}}\right]$	Constant specific co_a associated growth rate of heterotrophic bacteria
$\bar{\mu}_{h_{a2}}$	$\left[\frac{1}{\text{day}}\right]$	Maximum specific cn_a associated growth rate constant of heterotrophic bacteria
$\mu_{h_{a2}}$	$\left[\frac{1}{\text{day}}\right]$	Constant specific cn_a associated growth rate of heterotrophic bacteria
$\mu_{h_{a3}}$	$\left[\frac{1}{\text{day}}\right]$	Constant specific vfa_a associated growth rate of heterotrophic bacteria
$\bar{\rho}$	$\left[\frac{1}{\text{day}}\right]$	Maximum specific algal inorganic nitrogen uptake rate constant
ρ	$\left[\frac{1}{\text{day}}\right]$	Calculated specific algal inorganic nitrogen uptake rate

A.3 Other

Variable	Unit	Meaning
C	$[-]$	State to observation combination matrix
$\mathscr{C}$	$[-]$	Covariance matrix
$\mathscr{J}$	$[-]$	Objective function value
K	[variable]	Stoichiometric coefficient matrix
K_m	[variable]	Measured variable stoichiometric coefficient matrix
M_F	[variable]	Fisher information matrix
MW_{ace}	$\left[\frac{g}{mol}\right]$	Molar mass of acetate
N	$[-]$	Number of experimental data points
nc	$[-]$	Number of observation variables
np	$[-]$	Number of parameters
nr	$[-]$	Number of reactions
$\mathbf{q}_m$	$\left[\frac{conc.}{day}\right]$	Measured state gaseous rate vector
$\mathbf{r}_m$	$\left[\frac{conc.}{day}\right]$	Measured state reaction rate vector
$s()$	$[-]$	Sample standard deviation
U	[conc.]	PCA state integration vector
u	[conc.]	PCA state integration term from t_i to t_{i+1}
V	[conc.]	PCA reaction rate integration vector
v	[conc.]	PCA reaction rate integration term from t_i to t_{i+1}
W	[conc.]	PCA gaseous rate integration vector
w	[conc.]	PCA gaseous rate integration term from t_i to t_{i+1}
$y_i()$	[variable]	Model prediction of observation i
y_i^m	[variable]	Measured observation variable i
δ_i^{rel}	$[-]$	Relative 95% confidence interval of parameter i
λ_i	$[-]$	Eigenvalue i
μ	[variable]	Sample mean
ξ	[conc.]	Generic state vector
ξ^{in}	[conc.]	Generic state inlet vector
ξ_m	[conc.]	Generic measured state vector
ξ_m^{in}	[conc.]	Generic measured state inlet vector
ξ_{nm}	[conc.]	Generic non-measured state vector
Σ	$[-]$	Singular value matrix
$\omega_{i,j}$	$[-]$	Objective weight of variable i at time instant j
ρ	$\left[\frac{1}{day}\right]$	Calculated specific algal inorganic nitrogen uptake rate

Appendix B

Additional Relevant Tables

Table B.1: Two Reaction Set Trial #1 Optimal Parameter Combinations

1 Paramater Combinations					
$f(x,p)$	990.886	$f(x,p)$	1620.8	$f(x,p)$	3326.25
K_{co_b}	$1.589x10^{0} \pm 1.45x10^{-1}$	$\bar{\mu}_{vfa_b}$	$2.626x10^{-1} \pm 2.0x10^{-4}$	K_{nh_3}	$2.700x10^{-3} \pm 1.0x10^{-6}$
2 Paramater Combinations					
$f(x,p)$	984.791	$f(x,p)$	988.018	$f(x,p)$	990.703
K_{co_b}	$1.548x10^{0} \pm 1.41x10^{-1}$	K_{co_b}	$1.689x10^{0} \pm 2.05x10^{-1}$	K_{co_b}	$1.566x10^{0} \pm 1.88x10^{-1}$
$co_b(0)$	$8.916x10^{-1} \pm 8.65x10^{-2}$	$\bar{\mu}_{vfa_b}$	$1.954x10^{-1} \pm 6.1x10^{-3}$	$K_{vfa_{b1}}$	$1.478x10^{-1} \pm 1.21x10^{-2}$
3 Paramater Combinations					
$\mathbf{f(x,p)}$	**941.896**	$\mathbf{f(x,p)}$	**980.384**	$f(x,p)$	984.513
$\mathbf{K_{co_b}}$	$\mathbf{1.613x10^{0} \pm 1.74x10^{-1}}$	$\mathbf{K_{co_b}}$	$\mathbf{1.410x10^{0} \pm 1.92x10^{-1}}$	K_{co_b}	$1.587x10^{0} \pm 2.26x10^{-1}$
$\mathbf{K_{vfa_{b1}}}$	$\mathbf{8.546x10^{-2} \pm 1.712x10^{-2}}$	$\mathbf{K_{vfa_{b1}}}$	$\mathbf{1.374x10^{-1} \pm 1.36x10^{-2}}$	$\bar{\mu}_{vfa_b}$	$1.983x10^{-1} \pm 7.3x10^{-3}$
$\mathbf{K_{nh_3}}$	$\mathbf{5.135x10^{-4} \pm 1.109x10^{-4}}$	$\mathbf{co_b(0)}$	$\mathbf{8.409x10^{-1} \pm 9.15x10^{-2}}$	$co_b(0)$	$9.040x10^{-1} \pm 1.046x10^{-1}$
4 Paramater Combinations					
$\mathbf{f(x,p)}$	**934.645**				
$\mathbf{K_{co_b}}$	$\mathbf{1.544x10^{0} \pm 2.05x10^{-1}}$				
$\mathbf{K_{vfa_{b1}}}$	$\mathbf{8.480x10^{-2} \pm 1.715x10^{-2}}$				
$\mathbf{K_{nh_3}}$	$\mathbf{5.367x10^{-4} \pm 1.274x10^{-4}}$				
$\mathbf{co_b(0)}$	$\mathbf{9.404x10^{-1} \pm 9.99x10^{-2}}$				

Table B.2: Two Reaction Set Trial #2 Optimal Parameter Combinations

1 Paramater Combinations					
$f(x,p)$	990.886	$f(x,p)$	1620.8	$f(x,p)$	3326.25
K_{co_b}	$1.589x10^{0} \pm 1.45x10^{-1}$	$\bar{\mu}_{vfa_b}$	$2.626x10^{-1} \pm 2.0x10^{-4}$	K_{nh_3}	$2.700x10^{-3} \pm 1.0x10^{-6}$
2 Paramater Combinations					
$f(x,p)$	972.589	$f(x,p)$	984.768	$f(x,p)$	984.791
K_{co_b}	$1.873x10^{0} \pm 2.32x10^{-1}$	K_{co_b}	$1.701x10^{0} \pm 1.84x10^{-1}$	K_{co_b}	$1.548x10^{0} \pm 1.41x10^{-1}$
$K_{vfa_{b2}}$	$2.514x10^{0} \pm 1.129x10^{0}$	K_{nh_3}	$1.308x10^{-3} \pm 3.33x10^{-4}$	$co_b(0)$	$8.916x10^{-1} \pm 8.65x10^{-2}$
3 Paramater Combinations					
$\mathbf{f(x,p)}$	**941.896**	$f(x,p)$	944.63	$f(x,p)$	952.993
$\mathbf{K_{co_b}}$	$\mathbf{1.613x10^{0} \pm 1.74x10^{-1}}$	K_{co_b}	$1.843x10^{0} \pm 2.33x10^{-1}$	K_{co_b}	$1.851x10^{0} \pm 2.35x10^{-1}$
$\mathbf{K_{vfa_{b1}}}$	$\mathbf{8.546x10^{-2} \pm 1.712x10^{-2}}$	$K_{vfa_{b1}}$	$1.154x10^{-1} \pm 1.34x10^{-2}$	$\bar{\mu}_{vfa_b}$	$2.263x10^{-1} \pm 7.3x10^{-3}$
$\mathbf{K_{nh_3}}$	$\mathbf{5.135x10^{-4} \pm 1.109x10^{-4}}$	$K_{vfa_{b2}}$	$1.258x10^{0} \pm 3.80x10^{-1}$	$K_{vfa_{b2}}$	$9.018x10^{-1} \pm 3.58x10^{-1}$
4 Paramater Combinations					
$\mathbf{f(x,p)}$	**935.069**	$\mathbf{f(x,p)}$	**940.355**		
$\mathbf{K_{co_b}}$	$\mathbf{1.709x10^{0} \pm 2.35x10^{-1}}$	$\mathbf{K_{co_b}}$	$\mathbf{1.544x10^{0} \pm 2.04x10^{-1}}$		
$\mathbf{K_{vfa_{b1}}}$	$\mathbf{1.090x10^{-1} \pm 1.33x10^{-2}}$	$\mathbf{K_{vfa_{b1}}}$	$\mathbf{8.480x10^{-2} \pm 1.714x10^{-2}}$		
$\mathbf{K_{vfa_{b2}}}$	$\mathbf{1.307x10^{0} \pm 4.039x10^{-1}}$	$\mathbf{K_{nh_3}}$	$\mathbf{5.367x10^{-4} \pm 1.274x10^{-4}}$		
$\mathbf{co_b(0)}$	$\mathbf{8.429x10^{-1} \pm 8.97x10^{-2}}$	$\mathbf{co_b(0)}$	$\mathbf{9.404x10^{-1} \pm 9.99x10^{-2}}$		

Table B.3: Three Reaction Set Trial #1 Optimal Parameter Combinations

1 Paramater Combinations					
$f(x,p)$	1175.31	$f(x,p)$	1296.45	$f(x,p)$	1297.52
$\bar{\mu}_{cn_b}$	$3.311x10^{-2} \pm 2.51x10^{-3}$	$\bar{\mu}_{vfa_b}$	$2.335x10^{-1} \pm 5.4x10^{-3}$	$K_{vfa_{b1}}$	$8.682x10^{-2} \pm 6.89x10^{-3}$
2 Paramater Combinations					
$f(x,p)$	725.003	$f(x,p)$	1138.55	$f(x,p)$	1148.13
$\bar{\mu}_{co_b}$	$3.333x10^{-1} \pm 1.71x10^{-2}$	$\bar{\mu}_{cn_b}$	$3.376x10^{-2} \pm 2.48x10^{-3}$	$\bar{\mu}_{cn_b}$	$3.358x10^{-2} \pm 2.48x10^{-3}$
$\bar{\mu}_{cn_b}$	$3.689x10^{-2} \pm 2.65x10^{-3}$	$\bar{\mu}_{vfa_b}$	$1.805x10^{-1} \pm 6.87x10^{-3}$	$K_{vfa_{b1}}$	$1.796x10^{-1} \pm 1.45x10^{-2}$
3 Paramater Combinations					
$\mathbf{f(x,p)}$	**686.002**	$f(x,p)$	705.652	$f(x,p)$	722.088
$\bar{\mu}_{\mathbf{co_b}}$	$\mathbf{3.539x10^{-1} \pm 1.68x10^{-2}}$	$\bar{\mu}_{co_b}$	$3.453x10^{-1} \pm 1.69x10^{-2}$	$\bar{\mu}_{co_b}$	$3.361x10^{-1} \pm 1.72x10^{-2}$
$\bar{\mu}_{\mathbf{cn_b}}$	$\mathbf{3.461x10^{-2} \pm 2.11x10^{-3}}$	$\bar{\mu}_{cn_b}$	$3.500x10^{-2} \pm 2.22x10^{-3}$	$\bar{\mu}_{cn_b}$	$3.875x10^{-2} \pm 3.04x10^{-3}$
$\mathbf{K_{vfa_{b1}}}$	$\mathbf{1.155x10^{-1} \pm 9.8x10^{-3}}$	$\bar{\mu}_{vfa_b}$	$2.117x10^{-1} \pm 5.4x10^{-3}$	$c\#_b(0)$	$8.862x10^{-1} \pm 1.037x10^{-1}$
4 Paramater Combinations					
$\mathbf{f(x,p)}$	**649.701**	$\mathbf{f(x,p)}$	**681.441**		
$\bar{\mu}_{\mathbf{co_b}}$	$\mathbf{3.691x10^{-1} \pm 1.75x10^{-2}}$	$\bar{\mu}_{\mathbf{co_b}}$	$\mathbf{3.575x10^{-1} \pm 1.73x10^{-2}}$		
$\bar{\mu}_{\mathbf{cn_b}}$	$\mathbf{3.635x10^{-2} \pm 2.68x10^{-3}}$	$\bar{\mu}_{\mathbf{cn_b}}$	$\mathbf{3.767x10^{-2} \pm 3.22x10^{-3}}$		
$\mathbf{K_{vfa_{b1}}}$	$\mathbf{7.118x10^{-2} \pm 1.450x10^{-2}}$	$\mathbf{K_{vfa_{b1}}}$	$\mathbf{1.159x10^{-1} \pm 9.5x10^{-3}}$		
$\mathbf{K_{vfa_{b2}}}$	$\mathbf{1.978x10^{0} \pm 4.88x10^{-1}}$	$\mathbf{c\#_b(0)}$	$\mathbf{8.379x10^{-1} \pm 1.187x10^{-1}}$		

Table B.4: Three Reaction Set Trial #2 Optimal Parameter Combinations

1 Paramater Combinations					
$f(x,p)$	1122.53	$f(x,p)$	1175.31	$f(x,p)$	1296.45
K_{cn_b}	$5.112x10^{0} \pm 1.900x10^{0}$	$\bar{\mu}_{cn_b}$	$3.311x10^{-2} \pm 2.51x10^{-3}$	$\bar{\mu}_{vfa_b}$	$2.335x10^{-1} \pm 5.41x10^{-3}$
2 Paramater Combinations					
$f(x,p)$	722.472	$f(x,p)$	725.003	$f(x,p)$	849.249
$\bar{\mu}_{co_b}$	$3.256x10^{-1} \pm 1.66x10^{-2}$	$\bar{\mu}_{co_b}$	$3.333x10^{-1} \pm 1.71x10^{-2}$	$\bar{\mu}_{cn_b}$	$2.800x10^{0} \pm 1.252x10^{0}$
K_{cn_b}	$6.773x10^{0} \pm 1.127x10^{0}$	$\bar{\mu}_{cn_b}$	$3.689x10^{-2} \pm 2.65x10^{-3}$	K_{cn_b}	$3.000x10^{1} \pm 1.399x10^{1}$
3 Paramater Combinations					
$f(x,p)$	686.002	$f(x,p)$	689.31	$f(x,p)$	705.652
$\bar{\mu}_{co_b}$	$3.539x10^{-1} \pm 1.68x10^{-2}$	$\bar{\mu}_{co_b}$	$3.452x10^{-1} \pm 1.66x10^{-2}$	$\bar{\mu}_{co_b}$	$3.453x10^{-1} \pm 1.68910^{-2}$
$\bar{\mu}_{cn_b}$	$3.461x10^{-2} \pm 2.11x10^{-3}$	K_{cn_b}	$7.916x10^{0} \pm 1.431x10^{0}$	$\bar{\mu}_{cn_b}$	$3.500x10^{-2} \pm 2.22x10^{-3}$
$K_{vfa_{b1}}$	$1.155x10^{-1} \pm 9.8x10^{-3}$	$K_{vfa_{b1}}$	$1.201x10^{-1} \pm 9.8x10^{-3}$	$\bar{\mu}_{vfa_b}$	$2.117x10^{-1} \pm 5.4x10^{-3}$
4 Paramater Combinations					
$f(x,p)$	639.803	$f(x,p)$	640.642	$f(x,p)$	647.103
$\bar{\mu}_{co_b}$	$3.584x10^{-1} \pm 1.62x10^{-2}$	$\bar{\mu}_{co_b}$	$3.624x10^{-1} \pm 1.71x10^{-2}$	$\bar{\mu}_{co_b}$	$3.664x10^{-1} \pm 1.66x10^{-2}$
K_{cn_b}	$6.417x10^{0} \pm 1.163x10^{0}$	K_{cn_b}	$6.426x10^{0} \pm 1.159x10^{0}$	$\bar{\mu}_{cn_b}$	$3.656x10^{-2} \pm 2.74x10^{-3}$
$\bar{\mu}_{vfa_b}$	$1.574x10^{-1} \pm 7.4x10^{-3}$	$K_{vfa_{b1}}$	$7.055x10^{-2} \pm 1.374x10^{-2}$	$\bar{\mu}_{vfa_b}$	$1.608x10^{-1} \pm 8.4x10^{-3}$
$K_{vfa_{b1}}$	$3.717x10^{-2} \pm 1.473x10^{-2}$	$K_{vfa_{b2}}$	$1.759x10^{0} \pm 3.55x10^{-1}$	$K_{vfa_{b1}}$	$3.959x10^{-2} \pm 1.592x10^{-2}$
5 Paramater Combinations					
$\mathbf{f(x,p)}$	**613.985**	$\mathbf{f(x,p)}$	**616.651**		
$\bar{\mu}_{\mathbf{co_b}}$	$\mathbf{3.785x10^{-1} \pm 1.91x10^{-2}}$	$\bar{\mu}_{\mathbf{co_b}}$	$\mathbf{3.690x10^{-1} \pm 1.71x10^{-2}}$		
$\mathbf{K_{cn_b}}$	$\mathbf{6.426x10^{0} \pm 9.26x10^{-1}}$	$\mathbf{K_{cn_b}}$	$\mathbf{6.383x10^{0} \pm 9.48x10^{-1}}$		
$\mathbf{K_{vfa_{b1}}}$	$\mathbf{5.452x10^{-2} \pm 1.345x10^{-2}}$	$\bar{\mu}_{\mathbf{vfa_b}}$	$\mathbf{1.543x10^{-1} \pm 6.4x10^{-3}}$		
$\mathbf{K_{vfa_{b2}}}$	$\mathbf{1.547x10^{0} \pm 2.53x10^{-1}}$	$\mathbf{K_{vfa_{b1}}}$	$\mathbf{2.681x10^{-2} \pm 1.281x10^{-2}}$		
$\mathbf{c\#_b(0)}$	$\mathbf{7.216x10^{-1} \pm 4.99x10^{-2}}$	$\mathbf{c\#_b(0)}$	$\mathbf{7.44x10^{-1} \pm 4.94x10^{-2}}$		
6 Paramater Combinations					
$\mathbf{f(x,p)}$	**593.444**				
$\bar{\mu}_{\mathbf{co_b}}$	$\mathbf{3.945x10^{-1} \pm 2.25x10^{-2}}$				
$\mathbf{K_{cn_b}}$	$\mathbf{4.825x10^{0} \pm 7.62x10^{-1}}$				
$\mathbf{K_{vfa_{b1}}}$	$\mathbf{4.098x10^{-2} \pm 1.269x10^{-2}}$				
$\mathbf{K_{vfa_{b2}}}$	$\mathbf{1.326x10^{0} \pm 1.69x10^{-1}}$				
$\mathbf{c\#_b(0)}$	$\mathbf{4.076x10^{-1} \pm 1.057x10^{-1}}$				
$\mathbf{x_{\#_b}(0)}$	$\mathbf{4.466x10^{-1} \pm 2.043x10^{-1}}$				

Table B.5: Three Reaction Set Trial #3 Optimal Parameter Combinations

1 Paramater Combinations					
$f(x,p)$	818.507	$f(x,p)$	840.571	$f(x,p)$	878.621
$\bar{\mu}_{vfa_b}$	$2.293x10^{-1} \pm 4.6x10^{-3}$	$K_{vfa_{b1}}$	$9.056x10^{-2} \pm 6.75x10^{-3}$	$\bar{\mu}_{cn_b}$	$3.196x10^{-2} \pm 3.02x10^{-3}$
2 Paramater Combinations					
$f(x,p)$	196.645	$f(x,p)$	535.486	$f(x,p)$	562.114
$\bar{\mu}_{co_b}$	$5.006x10^{-1} \pm 1.20x10^{-2}$	$\bar{\mu}_{cn_b}$	$3.610x10^{-1} \pm 1.25x10^{-2}$	$\bar{\mu}_{cn_b}$	$3.495x10^{-1} \pm 1.34x10^{-2}$
$\bar{\mu}_{cn_b}$	$3.111x10^{-2} \pm 1.19x10^{-3}$	$K_{vfa_{b1}}$	$7.697x10^{-2} \pm 5.18x10^{-3}$	$\bar{\mu}_{vfa_b}$	$2.239x10^{-1} \pm 2.6x10^{-3}$
3 Paramater Combinations					
$f(x,p)$	176.407	$f(x,p)$	184.625	$f(x,p)$	193.78
$\bar{\mu}_{co_b}$	$5.083x10^{-1} \pm 1.10x10^{-2}$	$\bar{\mu}_{co_b}$	$5.046x10^{-1} \pm 1.14x10^{-2}$	$\bar{\mu}_{co_b}$	$5.030x10^{-1} \pm 1.19x10^{-2}$
$\bar{\mu}_{cn_b}$	$3.444x10^{-2} \pm 1.59x10^{-3}$	$\bar{\mu}_{cn_b}$	$3.339x10^{-2} \pm 1.45x10^{-3}$	$\bar{\mu}_{cn_b}$	$3.129x10^{-2} \pm 1.18x10^{-3}$
$K_{vfa_{b2}}$	$5.013x10^{0} \pm 7.39x10^{-1}$	$\bar{\mu}_{vfa_b}$	$1.912x10^{-1} \pm 2.5x10^{-3}$	$K_{nh_{3b}}$	$1.085x10^{-3} \pm 2.69x10^{-4}$
4 Paramater Combinations					
$\mathbf{f(x,p)}$	**147.888**	$f(x,p)$	159.494	$f(x,p)$	167.836
$\bar{\mu}_{\mathbf{co_b}}$	$\mathbf{5.133x10^{-1} \pm 9.9x10^{-3}}$	$\bar{\mu}_{co_b}$	$5.145x10^{-1} \pm 1.04x10^{-2}$	$\bar{\mu}_{co_b}$	$5.137x10^{-1} \pm 1.07x10^{-2}$
$\bar{\mu}_{\mathbf{cn_b}}$	$\mathbf{3.611x10^{-2} \pm 1.90x10^{-3}}$	$\bar{\mu}_{cn_b}$	$3.502x10^{-2} \pm 1.72x10^{-3}$	$\bar{\mu}_{cn_b}$	$3.471x10^{-2} \pm 1.67x10^{-3}$
$\bar{\mu}_{\mathbf{vfa_b}}$	$\mathbf{1.584x10^{-1} \pm 4.1x10^{-3}}$	$K_{vfa_{b1}}$	$1.021x10^{-1} \pm 1.00x10^{-2}$	$\bar{\mu}_{vfa_b}$	$2.296x10^{-1} \pm 1.07x10^{-2}$
$\mathbf{K_{vfa_{b1}}}$	$\mathbf{5.331x10^{-2} \pm 1.02x10^{-2}}$	$K_{vfa_{b2}}$	$2.698x10^{0} \pm 3.39x10^{-1}$	$K_{vfa_{b2}}$	$1.813x10^{0} \pm 4.35x10^{-1}$
5 Paramater Combinations					
$\mathbf{f(x,p)}$	**143.597**	$f(x,p)$	151.543		
$\bar{\mu}_{\mathbf{co_b}}$	$\mathbf{5.431x10^{-1} \pm 1.20x10^{-2}}$	$\bar{\mu}_{co_b}$	$5.214x10^{-1} \pm 1.03x10^{-2}$		
$\bar{\mu}_{\mathbf{cn_b}}$	$\mathbf{3.448x10^{-2} \pm 1.39x10^{-3}}$	$\bar{\mu}_{cn_b}$	$3.967x10^{-2} \pm 1.82x10^{-3}$		
$\bar{\mu}_{\mathbf{vfa_b}}$	$\mathbf{3.468x10^{-1} \pm 3.80x10^{-2}}$	$K_{vfa_{b1}}$	$8.300x10^{-2} \pm 1.05x10^{-2}$		
$\mathbf{K_{nh_{3b}}}$	$\mathbf{4.143x10^{-4} \pm 6.58x10^{-5}}$	$K_{vfa_{b2}}$	$2.121x10^{0} \pm 2.34x10^{-1}$		
$\mathbf{K_{vfa_{b2}}}$	$\mathbf{5.276x10^{-1} \pm 1.280x10^{-1}}$	$c\#_b(0)$	$7.799x10^{-1} \pm 4.11x10^{-2}$		
6 Paramater Combinations					
$\mathbf{f(x,p)}$	**132.874**				
$\bar{\mu}_{\mathbf{co_b}}$	$\mathbf{5.401x10^{-1} \pm 1.14x10^{-2}}$				
$\bar{\mu}_{\mathbf{cn_b}}$	$\mathbf{2.710x10^{-2} \pm 3.01x10^{-3}}$				
$\bar{\mu}_{\mathbf{vfa_b}}$	$\mathbf{3.525x10^{-1} \pm 3.19x10^{-2}}$				
$\mathbf{K_{nh_{3b}}}$	$\mathbf{2.603x10^{-4} \pm 5.95x10^{-5}}$				
$\mathbf{K_{vfa_{b2}}}$	$\mathbf{5.432x10^{-1} \pm 1.284x10^{-1}}$				
$\mathbf{c\#_b(0)}$	$\mathbf{1.488x10^{0} \pm 2.40x10^{-1}}$				

Table B.6: Three Reaction Set Trial #4 Optimal Parameter Combinations

1 Paramater Combinations					
$f(x,p)$	699.124	$f(x,p)$	710.221	$f(x,p)$	746.123
K_{cn_b}	$7.713x10^{-1} \pm 7.94x10^{-2}$	$\bar{\mu}_{cn_b}$	$3.669x10^{-1} \pm 8.43x10^{-3}$	$\bar{\mu}_{vfa_b}$	$2.213x10^{-1} \pm 3.1x10^{-3}$
2 Paramater Combinations					
$f(x,p)$	191.739	$f(x,p)$	439.557	$f(x,p)$	481.491
$\bar{\mu}_{co_b}$	$4.961x10^{-1} \pm 8.20x10^{-2}$	$\bar{\mu}_{co_b}$	$1.083x10^{-1} \pm 4.84x10^{-2}$	K_{co_b}	$1.234x10^{0} \pm 1.01x10^{-1}$
K_{cn_b}	$1.275x10^{1} \pm 9.4x10^{-1}$	$\bar{\mu}_{cn_b}$	$3.690x10^{-1} \pm 7.3x10^{-3}$	$\bar{\mu}_{cn_b}$	$3.671x10^{-1} \pm 7.3x10^{-3}$
3 Paramater Combinations					
$f(x,p)$	169.821	$f(x,p)$	178.278	$f(x,p)$	185.671
$\bar{\mu}_{co_b}$	$5.000x10^{-1} \pm 7.5x10^{-3}$	$\bar{\mu}_{co_b}$	$4.969x10^{-1} \pm 7.8x10^{-3}$	$\bar{\mu}_{co_b}$	$4.987x10^{-1} \pm 8.1x10^{-3}$
K_{cn_b}	$7.758x10^{0} \pm 7.74x10^{-1}$	K_{cn_b}	$8.780x10^{0} \pm 9.15x10^{-1}$	K_{cn_b}	$1.169x10^{1} \pm 9.76x10^{-1}$
$K_{vfa_{b2}}$	$4.528x10^{0} \pm 4.11x10^{-1}$	$\bar{\mu}_{vfa_b}$	$1.895x10^{-1} \pm 1.8x10^{-3}$	$K_{nh_{3b}}$	$8.430x10^{-4} \pm 1.312x10^{-4}$
4 Paramater Combinations					
$f(x,p)$	148.731	$f(x,p)$	158.661	$f(x,p)$	164.549
$\bar{\mu}_{co_b}$	$5.036x10^{-1} \pm 6.9x10^{-3}$	$\bar{\mu}_{co_b}$	$5.055x10^{-1} \pm 7.2x10^{-3}$	$\bar{\mu}_{co_b}$	$5.047x10^{-1} \pm 7.4x10^{-3}$
K_{cn_b}	$7.018x10^{0} \pm 6.71x10^{-1}$	K_{cn_b}	$7.758x10^{0} \pm 8.19x10^{-1}$	K_{cn_b}	$7.760x10^{0} \pm 8.01x10^{-1}$
$\bar{\mu}_{vfa_b}$	$1.607x10^{-1} \pm 2.7x10^{-3}$	$K_{vfa_{b1}}$	$1.118x10^{-1} \pm 7.0x10^{-3}$	$\bar{\mu}_{vfa_b}$	$2.222x10^{-1} \pm 5.3x10^{-3}$
$K_{vfa_{b1}}$	$6.471x10^{-2} \pm 7.31x10^{-3}$	$K_{vfa_{b2}}$	$2.836x10^{0} \pm 2.55x10^{-1}$	$K_{vfa_{b2}}$	$2.061x10^{0} \pm 3.67x10^{-1}$
5 Paramater Combinations					
$\mathbf{f(x,p)}$	**116.004**	$f(x,p)$	122.824	$f(x,p)$	127.551
$\bar{\mu}_{\mathbf{co_b}}$	$\mathbf{5.092x10^{-1} \pm 6.1x10^{-3}}$	$\bar{\mu}_{co_b}$	$5.125x10^{-1} \pm 6.4x10^{-3}$	$\bar{\mu}_{co_b}$	$5.128x10^{-1} \pm 6.6x10^{-3}$
$\mathbf{K_{cn_b}}$	$\mathbf{6.521x10^{0} \pm 5.22x10^{-1}}$	K_{cn_b}	$6.846x10^{0} \pm 5.79x10^{-1}$	K_{cn_b}	$6.951x10^{0} \pm 5.93x10^{-1}$
$\bar{\mu}_{\mathbf{vfa_b}}$	$\mathbf{1.594x10^{-1} \pm 1.8x10^{-3}}$	$K_{vfa_{b1}}$	$1.092x10^{-1} \pm 6.4x10^{-3}$	$\bar{\mu}_{vfa_b}$	$2.282x10^{-1} \pm 5.1x10^{-3}$
$\mathbf{K_{vfa_{b1}}}$	$\mathbf{6.392x10^{-2} \pm 6.49x10^{-3}}$	$K_{vfa_{b2}}$	$2.591x10^{0} \pm 1.87x10^{-1}$	$K_{vfa_{b2}}$	$1.717x10^{0} \pm 2.49x10^{-1}$
$\mathbf{k_{co_{2b}}}$	$\mathbf{3.747x10^{-1} \pm 8.57x10^{-2}}$	$k_{co_{2b}}$	$3.454x10^{-1} \pm 8.26x10^{-2}$	$k_{co_{2b}}$	$3.268x10^{-1} \pm 8.07x10^{-2}$
6 Paramater Combinations					
$\mathbf{f(x,p)}$	**95.601**	$\mathbf{f(x,p)}$	**109.458**		
$\bar{\mu}_{\mathbf{co_b}}$	$\mathbf{5.271x10^{-1} \pm 6.2x10^{-3}}$	$\bar{\mu}_{\mathbf{co_b}}$	$\mathbf{5.265x10^{-1} \pm 6.6x10^{-3}}$		
$\mathbf{K_{cn_b}}$	$\mathbf{7.128x10^{0} \pm 4.95x10^{-1}}$	$\mathbf{K_{cn_b}}$	$\mathbf{6.954x10^{0} \pm 4.79x10^{-1}}$		
$\mathbf{K_{vfa_{b1}}}$	$\mathbf{5.402x10^{-2} \pm 8.25x10^{-3}}$	$\bar{\mu}_{\mathbf{vfa_b}}$	$\mathbf{2.825x10^{-1} \pm 1.35x10^{-2}}$		
$\mathbf{K_{nh_{3b}}}$	$\mathbf{2.536x10^{-4} \pm 3.05x10^{-5}}$	$\mathbf{K_{nh_{3b}}}$	$\mathbf{3.127x10^{-4} \pm 4.35x10^{-5}}$		
$\mathbf{K_{vfa_{b2}}}$	$\mathbf{2.230x10^{0} \pm 1.30x10^{-1}}$	$\mathbf{K_{vfa_{b2}}}$	$\mathbf{9.175x10^{-1} \pm 1.220x10^{-1}}$		
$\mathbf{k_{co_{2b}}}$	$\mathbf{4.009x10^{-1} \pm 7.87x10^{-2}}$	$\mathbf{k_{co_{2b}}}$	$\mathbf{3.268x10^{-1} \pm 7.18x10^{-2}}$		

Table B.7: Three Reaction Set Trial #5 Optimal Parameter Combinations

1 Paramater Combinations					
$f(x,p)$	173.51	$f(x,p)$	173.587	$f(x,p)$	252.756
$\bar{\mu}_{cn_b}$	$3.120x10^{-2} \pm 2.20x10^{-3}$	K_{cn_b}	$1.065x10^{1} \pm 2.16x10^{0}$	pH_{LLAA}	$7.702x10^{0} \pm 4.6x10^{-2}$
2 Paramater Combinations					
$f(x,p)$	159.388	$f(x,p)$	163.084	$f(x,p)$	170.428
$\bar{\mu}_{co_b}$	$2.384x10^{-1} \pm 1.60x10^{-2}$	$\bar{\mu}_{co_b}$	$2.322x10^{-1} \pm 1.65x10^{-2}$	K_{cn_b}	$1.027x10^{1} \pm 1.99x10^{0}$
$\bar{\mu}_{cn_b}$	$3.092x10^{-2} \pm 2.06x10^{-3}$	K_{cn_b}	$1.153x10^{1} \pm 2.08x10^{0}$	$\bar{\mu}_{vfa_b}$	$1.829x10^{-1} \pm 8.1x10^{-3}$
3 Paramater Combinations					
$\mathbf{f(x,p)}$	**156.21**	$f(x,p)$	157.463	$f(x,p)$	158.285
$\bar{\mu}_{\mathbf{co_b}}$	$\mathbf{2.554x10^{-1} \pm 1.92x10^{-2}}$	$\bar{\mu}_{co_b}$	$2.524x10^{-1} \pm 1.90x10^{-2}$	$\bar{\mu}_{co_b}$	$2.347x10^{-1} \pm 1.60x10^{-2}$
$\bar{\mu}_{\mathbf{cn_b}}$	$\mathbf{3.403x10^{-2} \pm 2.47x10^{-3}}$	K_{cn_b}	$1.037x10^{1} \pm 1.66x10^{0}$	$\bar{\mu}_{cn_b}$	$3.160x10^{-2} \pm 2.18x10^{-3}$
$\mathbf{c\#_b(0)}$	$\mathbf{8.325x10^{-1} \pm 6.95x10^{-2}}$	$c\#_b(0)$	$7.807x10^{-1} \pm 6.64x10^{-2}$	$\bar{\mu}_{vfa_b}$	$1.913x10^{-1} \pm 7.3x10^{-3}$
4 Paramater Combinations					
$\mathbf{f(x,p)}$	**156.086**	$\mathbf{f(x,p)}$	**156.171**		
$\bar{\mu}_{\mathbf{co_b}}$	$\mathbf{2.522x10^{-1} \pm 2.04x10^{-2}}$	$\bar{\mu}_{\mathbf{co_b}}$	$\mathbf{2.538x10^{-1} \pm 2.04x10^{-2}}$		
$\bar{\mu}_{\mathbf{cn_b}}$	$\mathbf{3.395x10^{-2} \pm 2.48x10^{-3}}$	$\bar{\mu}_{\mathbf{cn_b}}$	$\mathbf{3.400x10^{-2} \pm 2.48x10^{-2}}$		
$\bar{\mu}_{\mathbf{vfa_b}}$	$\mathbf{1.968x10^{-1} \pm 8.1x10^{-3}}$	$\mathbf{K_{vfa_{b1}}}$	$\mathbf{1.534x10^{-1} \pm 1.58x10^{-2}}$		
$\mathbf{c\#_b(0)}$	$\mathbf{8.481x10^{-1} \pm 8.15x10^{-2}}$	$\mathbf{c\#_b(0)}$	$\mathbf{8.405x10^{-1} \pm 7.96x10^{-2}}$		

Table B.8: Three Reaction Set Trial #6 Optimal Parameter Combinations

1 Paramater Combinations					
$f(x,p)$	173.51	$f(x,p)$	173.587	$f(x,p)$	252.756
$\bar{\mu}_{cn_b}$	$3.120x10^{-2} \pm 2.20x10^{-3}$	K_{cn_b}	$1.065x10^{1} \pm 2.16x10^{0}$	pH_{LLAA}	$7.702x10^{0} \pm 4.6x10^{-2}$
2 Paramater Combinations					
$f(x,p)$	159.388	$f(x,p)$	163.084	$f(x,p)$	169.773
$\bar{\mu}_{co_b}$	$2.384x10^{-1} \pm 1.60x10^{-2}$	$\bar{\mu}_{co_b}$	$2.322x10^{-1} \pm 1.65x10^{-2}$	K_{cn_b}	$1.031x10^{1} \pm 1.96x10^{0}$
$\bar{\mu}_{cn_b}$	$3.092x10^{-2} \pm 2.06x10^{-3}$	K_{cn_b}	$1.153x10^{1} \pm 2.08x10^{0}$	$K_{vfa_{b2}}$	$1.061x10^{0} \pm 3.77x10^{-1}$
3 Paramater Combinations					
$f(x,p)$	155.353	$f(x,p)$	156.21	$f(x,p)$	157.463
$\bar{\mu}_{co_b}$	$2.696x10^{-1} \pm 2.44x10^{-2}$	$\bar{\mu}_{co_b}$	$2.554x10^{-1} \pm 1.92x10^{-2}$	$\bar{\mu}_{co_b}$	$2.524x10^{-1} \pm 1.90x10^{-2}$
$\bar{\mu}_{cn_b}$	$3.188x10^{-2} \pm 2.11x10^{-3}$	$\bar{\mu}_{cn_b}$	$3.403x10^{-2} \pm 2.47x10^{-3}$	K_{cn_b}	$1.037x10^{1} \pm 1.66x10^{0}$
$K_{nh_{3b}}$	$6.133x10^{-4} \pm 1.796x10^{-4}$	$c\#_b(0)$	$8.325x10^{-1} \pm 6.95x10^{-2}$	$c\#_b(0)$	$7.807x10^{-1} \pm 6.64x10^{-2}$
4 Paramater Combinations					
$f(x,p)$	152.357	$f(x,p)$	152.791	$f(x,p)$	154.613
$\bar{\mu}_{co_b}$	$2.652x10^{-1} \pm 2.20x10^{-2}$	$\bar{\mu}_{co_b}$	$3.294x10^{-1} \pm 3.07x10^{-2}$	$\bar{\mu}_{co_b}$	$2.993x10^{-1} \pm 3.63x10^{-2}$
K_{cn_b}	$7.914x10^{0} \pm 1.273x10^{0}$	$\bar{\mu}_{cn_b}$	$3.178x10^{-2} \pm 2.07x10^{-3}$	$\bar{\mu}_{cn_b}$	$3.195x10^{-2} \pm 2.09x10^{-3}$
$c\#_b(0)$	$5.606x10^{-1} \pm 8.16x10^{-2}$	$K_{vfa_{b1}}$	$1.054x10^{-1} \pm 1.89x10^{-2}$	$\bar{\mu}_{vfa_b}$	$2.120x10^{-1} \pm 1.17x10^{-2}$
$x_{\#_b}(0)$	$4.503x10^{-1} \pm 1.972x10^{-1}$	$K_{nh_{3b}}$	$3.226x10^{-4} \pm 8.23x10^{-5}$	$K_{nh_{3b}}$	$4.287x10^{-4} \pm 1.481x10^{-4}$
5 Paramater Combinations					
$\mathbf{f(x,p)}$	**146.58**	$f(x,p)$	149.866	$f(x,p)$	151.809
$\bar{\mu}_{\mathbf{co_b}}$	$\mathbf{3.596x10^{-1} \pm 2.71x10^{-2}}$	$\bar{\mu}_{co_b}$	$3.486x10^{-1} \pm 2.72x10^{-2}$	$\bar{\mu}_{co_b}$	$2.768x10^{-1} \pm 2.78x10^{-2}$
$\bar{\mu}_{\mathbf{cn_b}}$	$\mathbf{2.517x10^{-2} \pm 4.53x10^{-3}}$	$\bar{\mu}_{cn_b}$	$3.231x10^{-2} \pm 2.15x10^{-3}$	K_{cn_b}	$7.757x10^{0} \pm 1.242x10^{0}$
$\mathbf{K_{vfa_{b1}}}$	$\mathbf{7.570x10^{-2} \pm 1.728x10^{-2}}$	$K_{vfa_{b1}}$	$8.961x10^{-2} \pm 1.716x10^{-2}$	$K_{vfa_{b1}}$	$1.369x10^{-1} \pm 1.581x10^{-2}$
$\mathbf{K_{nh_{3b}}}$	$\mathbf{1.530x10^{-4} \pm 5.24x10^{-5}}$	$K_{nh_{3b}}$	$2.307x10^{-4} \pm 4.98x10^{-5}$	$c\#_b(0)$	$5.117x10^{-1} \pm 9.47x10^{-2}$
$\mathbf{c\#_b(0)}$	$\mathbf{1.488x10^{0} \pm 3.74x10^{-1}}$	$x_{\#_b}(0)$	$6.217x10^{-1} \pm 2.275x10^{-1}$	$c\#_b(0)$	$4.151x10^{-1} \pm 1.920x10^{-1}$
6 Paramater Combinations					
$\mathbf{f(x,p)}$	**141.96**	$\mathbf{f(x,p)}$	**148.346**		
$\bar{\mu}_{\mathbf{co_b}}$	$\mathbf{3.708x10^{-1} \pm 2.76x10^{-2}}$	$\bar{\mu}_{\mathbf{co_b}}$	$\mathbf{2.604x10^{-1} \pm 2.48x10^{-2}}$		
$\bar{\mu}_{\mathbf{cn_b}}$	$\mathbf{2.646x10^{-2} \pm 3.04x10^{-3}}$	$\mathbf{K_{cn_b}}$	$\mathbf{6.637x10^{0} \pm 1.075x10^{0}}$		
$\mathbf{K_{vfa_{b1}}}$	$\mathbf{4.887x10^{-2} \pm 1.740x10^{-2}}$	$\bar{\mu}_{\mathbf{vfa_b}}$	$\mathbf{1.528x10^{-1} \pm 1.68x10^{-2}}$		
$\mathbf{K_{nh_{3b}}}$	$\mathbf{1.563x10^{-4} \pm 3.64x10^{-5}}$	$\mathbf{K_{vfa_{b1}}}$	$\mathbf{5.806x10^{-2} \pm 2.625x10^{-2}}$		
$\mathbf{K_{vfa_{b2}}}$	$\mathbf{2.697x10^{0} \pm 8.87x10^{-1}}$	$\mathbf{c\#_b(0)}$	$\mathbf{4.330x10^{-1} \pm 8.44x10^{-2}}$		
$\mathbf{c\#_b(0)}$	$\mathbf{1.488x10^{0} \pm 2.25x10^{-1}}$	$\mathbf{x_{\#_b}(0)}$	$\mathbf{3.194x10^{-1} \pm 1.463x10^{-1}}$		

Appendix C

Analysis of Three Reaction Pathway Trials #5 and #6

Recall that initially it was hypothesized that the mismatch from the $TCOD_{in}$ and $TCOD_{out}$ would throw the fitting results and so weighting factors of 10.0 were added to the inorganic nitrogen, VFA, and % methane readings to offset this. It was decided to examine the impact of removing these weighting factors (i.e. give equal weighting to all experimental measurements). It should also be pointed out that these experiments were conducted before the steady state experiments chronologically and so the uniform adjustment of substrate and biomass initial values are still possible parameters.

The progression of Trial #5 is presented in Tab. B.7. In a similar vain to trials #1 - #4 a parameter from each of the rate laws was selected indicating that they are discernable within the experimental data. The results themselves are also reasonably close to the predictions of trial#1 and #2 for $\bar{\mu}_1$ (all predicting values in the 0.3 range) and trial #1 - #4 for $\bar{\mu}_2$ (all predicting values in the 0.03 range). The values for $\bar{\mu}_3$ and K_3 are slightly more erratic when compared to the results of the previous 4 trials but this has been found to be the case throughout testing (additional experimental design is required). Also of interest is the fact that only one kinetic constant from the methanogenic reaction was observed to fall within the 25% threshold (as opposed to 2 or more in all other trials). This is the result of removing the weighting factors which essentially raised the percieved uncertainty in the inorganic nitrogen, VFA, and % methane readings (weighting factors can be viewed as modifications to the base standard deviation within the normal distribution, increasing confidence in those measurments and therefore decreasing estimated parameter confidence for parameters associated with those measurements).

Having said this the value of $\bar{\mu}_2$ is on the lower side of the spectrum (refer back to Tab. 4.5), which is believed to be the cause of the constant model underestimation present in Fig. C.2. VFA prediction in Fig. C.1 also appears poor as compared to trials #1 - #4. It is believed that the mismatch in the TCOD and Biogas measurements resulted in the solver selecting suboptimal parameter points to minimize the error created by this offset. Still, it would appear the offset did not completely throw parameter estimations (as mentioned in the last paragraph) and the fits are not wildly off. The important thing would be to remove these sources of error from subsequent experiments to improve the parameter fitting process.

Similar to trial #1, a 50% threshold experiment was also run for the unweighted system to examine how the identification algorithm reacted (Trial #6). The progression of the identification run is presented in Tab. B.8. Once again we see the identification algorithm gravitating towards one of the two key kinetic parameters in each acidogenesis step along with an assortment of methanogenesis parameters. As has been seen before, the $\bar{\mu}_1$ and $\bar{\mu}_2$ are roughly consistent with the other trials, indicating the new weighting scheme does not completely alter the results (implying consistency). As in the 25% trial the $\bar{\mu}_2$ was found to

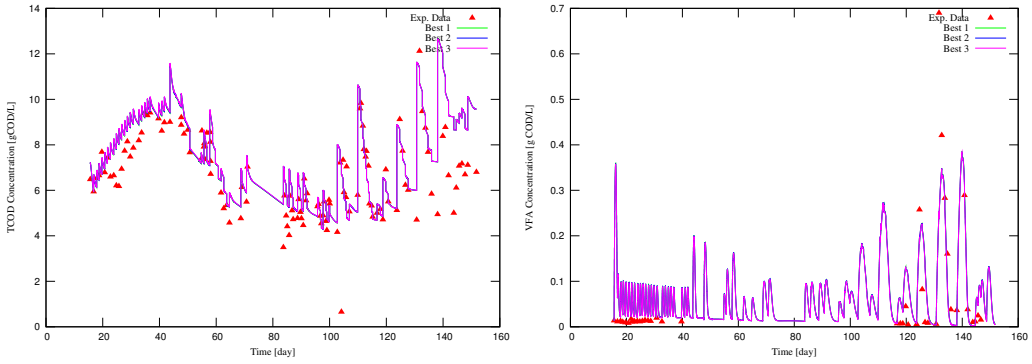

(a) Total COD (b) VFA

Figure C.1: Top 3 TCOD and VFA Prediction Results for Three Reaction Set Trial # 5

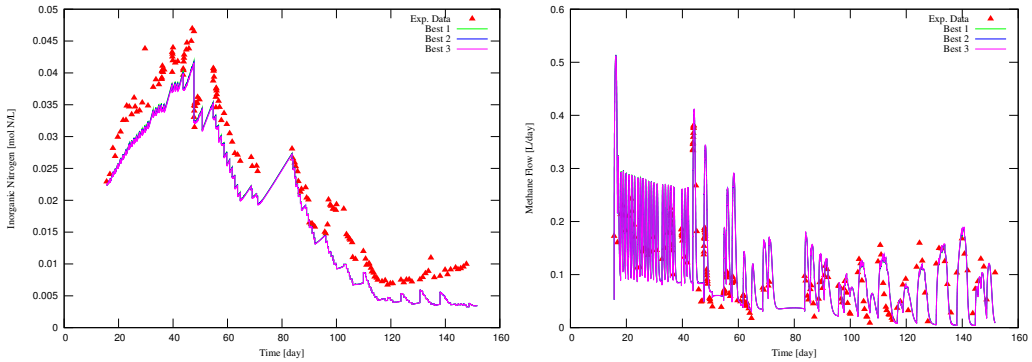

(a) Inorganic Nitrogen (b) Methane Flow

Figure C.2: Top 3 IN and Meth. Flow Prediction Results for Three Reaction Set Trial # 5

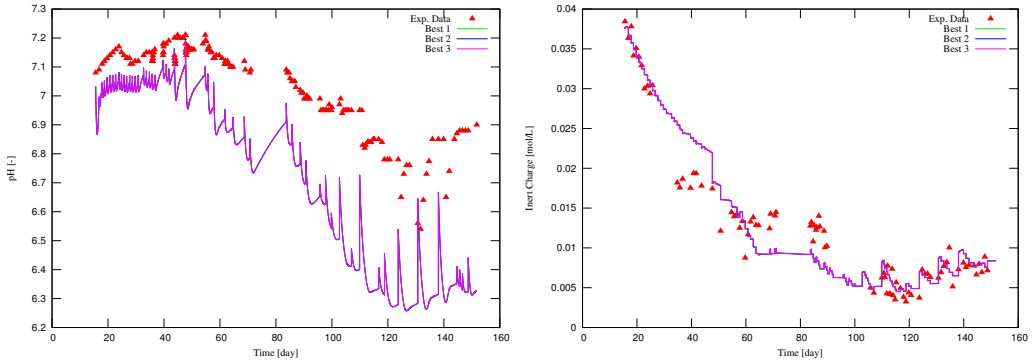

(a) pH (b) Inert Charge

Figure C.3: Top 3 pH and Inert Charge Prediction Results for Three Reaction Set Trial # 5

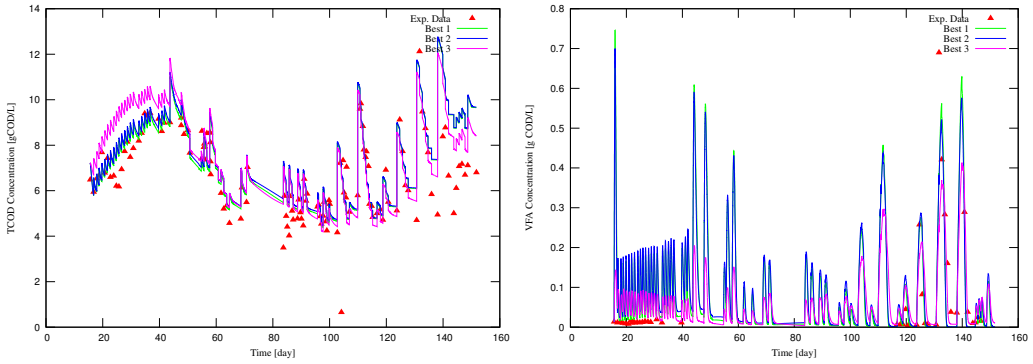

(a) Total COD (b) VFA

Figure C.4: Top 3 TCOD and VFA Prediction Results for Three Reaction Set Trial # 6

be slighter smaller with the reduced weighting, as compared with the previous trials (indicating that the known offset in the data appears to drive the solver to fit conflicting data sets, which push it away from other optimal fits). As would be expected, the increased tolerance resulted in additional methanogenic parameters and initial values falling within the threshold of the identification algorithm. This is consistent with all previous 50% threshold trials.

Fig. C.4 - C.6 give the model predictions for the top three combinations in trial #6. As in Trial #5 there appears to be slightly more offset in the inorganic nitrogen fits as compared to trials #1 - 4. Combination 3 is also interesting in that it would appear that manipulation of the starting substrate and biomass values pushes the estimate of K_2 closer to values seen in the weighted least square trials. The lower initial biomass would lead one to suspect that there would be significant inorganic nitrogen offset in the latter stages of the trial but it is hypothesized that the lower acidogen/acetogen and methanogen concentrations would also reduce inorganic nitrogen consumption, still resulting in a decent nitrogen fit. Other than this the fits are comparable to those observed in these previous trials.

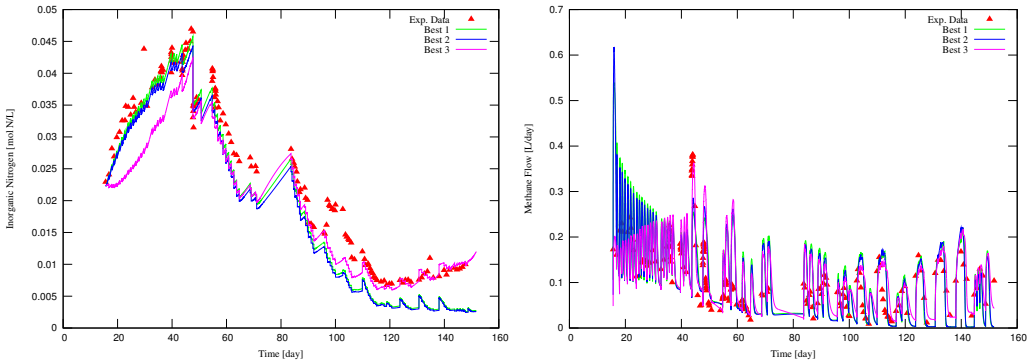

(a) Inorganic Nitrogen (b) Methane Flow

Figure C.5: Top 3 IN and Meth. Flow Prediction Results for Three Reaction Set Trial # 6

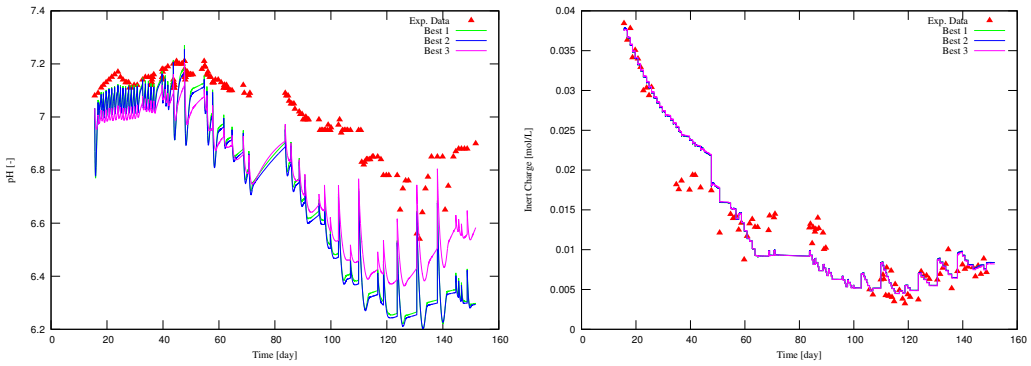

(a) pH (b) Inert Charge

Figure C.6: Top 3 pH and Inert Charge Prediction Results for Three Reaction Set Trial # 6

Appendix D

Source Code

four main scripts (with minor alterations where relevant for a given simulation) were used to generate the identification and optimality results presented in this thesis. Note that these files are meant to be used with the "`Differential Algebraic Equation Optimal Control`" (`DAEOC`) software package (part of the "`Simulation and Optimization Collection`" (`SOC`) package) developed by Dr. Benoît Chachuat. `SOC` is a software package written in `C++` and `Fortran` that acts as a general front end to standardize and simplify the formulation of dynamic optimization and control problems. The software does not contain any solvers but instead acts as a problem wrapper to standardize problem inputs and outputs so that multiple solvers may be plugged in and out with ease. Right now the software has confirmed operability for the nonlinear programming (NLP) solver packages: SLSQP, SIMANN, IPOPT, DAEPACK, NLPQL, NLPQLP, SNOPTA (SNOPTA used for this thesis); and the ODE/DAE solver packages: DASPK, DAEPACK (both DASPK and DAEPACK used for this thesis). The four main scripts scripts used, `main.cc`, `func.f`, `res.f`, and `NLP.f`; have been ommitted to conserve space but are available upon request. `main.cc` is a C++ file that builds all the required objects to formulate the dynamic optimization/ optimal control problem(s) and feed this information to the specified solvers. `main.cc` is also where one would build any user specific post-analysis tools. `func.f` a file containing the dynamic optimization/control objective control as well as any relevant constraints. `res.f` is a file containing the DAE equation set and facilitates the "dynamic" portion of problem formulation. Finally, `NLP.f` is an AE objective file used for generating optimal steady state predictions (a slightly modified `main.cc` file is required to facilitate this). `SOC` is currently not a publically available software package. For additional information and documentation please contact Dr. Benoît Chachuat (*b.chachuat@imperial.ac.uk*).

Appendix E

LBE-INRA Data Set

Table E.1: LBE-INRA Experimental Data (Part 1)

Date [D/M/Y]	Time	Time [Days]	Substrate	COD_{in} [gCOD/L]	V_{in} [L]	pH [-]
03/06/2009	16:30	0.0000	Pretreated Chlorella	3	0.100	7.35
04/06/2009	8:30	0.6667		0	0.010	7.30
05/06/2009	9:00	1.6875		0	0.020	7.27
06/06/2009	15:00	2.9375		0	0.000	7.36
08/06/2009	7:30	4.6250		0	0.010	7.37
09/06/2009	8:00	5.6458	Pretreated Chlorella	3	0.100	7.27
10/06/2009	9:30	6.7083		0	0.010	7.16
10/06/2009	19:00	7.1042		0	0.000	6.99
11/06/2009	9:00	7.6875		0	0.010	7.07
11/06/2009	12:30	7.8333		0	0.000	7.00
12/06/2009	8:30	8.6667		0	0.010	7.11
12/06/2009	13:45	8.8854		0	0.000	7.00
13/06/2009	9:00	9.6875	Pretreated Chlorella	3	0.100	6.69
15/06/2009	8:00	11.6458		0	0.010	7.06
15/06/2009	18:00	12.0625		0	0.000	7.09
16/06/2009	9:00	12.6875		0	0.010	7.10
16/06/2009	17:30	13.0417		0	0.000	7.03
17/06/2009	9:00	13.6875	Chlorella	1	0.040	6.99
17/06/2009	12:00	13.8125		0	0.005	
17/06/2009	18:00	14.0625		0	0.002	
18/06/2009	9:30	14.7083	Chlorella	1	0.040	7.07
18/06/2009	12:30	14.8333		0	0.000	
18/06/2009	16:15	14.9896		0	0.000	
19/06/2009	7:00	15.6042	Chlorella	1	0.040	7.08
20/06/2009	12:00	16.8125	Chlorella	1	0.040	7.09
21/06/2009	14:00	17.8958	Chlorella	1	0.040	7.11
22/06/2009	9:30	18.7083	Chlorella	1	0.040	7.12
22/06/2009	16:30	19.0000		0	0.000	
23/06/2009	9:00	19.6875	Chlorella	1	0.040	7.13
23/06/2009	16:30	20.0000		0	0.000	
24/06/2009	9:45	20.7188	Chlorella	1	0.040	7.14
25/06/2009	9:00	21.6875	Chlorella	1	0.040	7.15
25/06/2009	16:30	22.0000		0	0.001	
26/06/2009	9:30	22.7083	Chlorella	1	0.040	7.16
26/06/2009	16:00	22.9792		0	0.001	

Date [D/M/Y]	Time	Time [Days]	Substrate	COD_{in} [gCOD/L]	V_{in} [L]	pH [-]
27/06/2009	14:00	23.8958	Chlorella	1	0.040	7.17
28/06/2009	12:00	24.8125	Chlorella	1	0.040	7.15
29/06/2009	9:30	25.7083	Chlorella	1	0.040	7.14
29/06/2009	18:00	26.0625		0	0.001	
30/06/2009	8:00	26.6458	Chlorella	1	0.040	7.13
30/06/2009	17:30	27.0417		0	0.001	7.13
01/07/2009	9:45	27.7188	Chlorella	1	0.040	7.13
01/07/2009	16:45	28.0104		0	0.001	7.11
02/07/2009	9:00	28.6875	Chlorella	1	0.040	7.11
03/07/2009	9:00	29.6875	Chlorella	1	0.040	7.12
04/07/2009	11:30	30.7917	Chlorella	1	0.040	7.12
06/07/2009	9:30	32.7083	Chlorella	1	0.040	7.14
07/07/2009	9:30	33.7083	Chlorella	1	0.040	7.15
08/07/2009	11:30	34.7917	Chlorella	1	0.040	7.15
09/07/2009	10:00	35.7292	Chlorella	1	0.040	7.15
09/07/2009	11:00	35.7708		0	0.001	7.12
09/07/2009	12:00	35.8125		0	0.001	7.12
09/07/2009	13:30	35.8750		0	0.001	7.12
09/07/2009	14:55	35.9340		0	0.001	7.12
09/07/2009	16:17	35.9910		0	0.001	7.13
09/07/2009	17:31	36.0424		0	0.001	7.14
09/07/2009	18:50	36.0972		0	0.001	7.15
09/07/2009	21:00	36.1875		0	0.001	7.15
09/07/2009	23:00	36.2708		0	0.001	7.15
10/07/2009	9:45	36.7188	Chlorella	1	0.040	7.16
13/07/2009	8:30	39.6667	Chlorella	1	0.040	7.14
13/07/2009	9:00	39.6875		0	0.001	7.18
13/07/2009	10:30	39.7500		0	0.001	7.15
13/07/2009	11:45	39.8021		0	0.001	7.15
13/07/2009	14:15	39.9063		0	0.001	7.17
13/07/2009	16:00	39.9792		0	0.001	7.18
14/07/2009	12:00	40.8125	Chlorella	1	0.040	7.18
15/07/2009	10:00	41.7292	Chlorella	1	0.040	7.19
17/07/2009	9:30	43.7083	Chlorella	3	0.090	7.20
17/07/2009	10:15	43.7396		0	0.003	7.14
17/07/2009	11:15	43.7813		0	0.000	7.13
17/07/2009	12:15	43.8229		0	0.001	7.13
17/07/2009	13:15	43.8646		0	0.000	7.12
17/07/2009	14:15	43.9063		0	0.001	7.12
17/07/2009	15:15	43.9479		0	0.000	7.11
17/07/2009	16:15	43.9896		0	0.001	7.11

Date [D/M/Y]	Time	Time [Days]	Substrate	COD_{in} [gCOD/L]	V_{in} [L]	pH [-]
17/07/2009	17:15	44.0313		0	0.000	7.11
17/07/2009	18:15	44.0729		0	0.004	7.12
18/07/2009	12:30	44.8333		0	0.004	7.21
18/07/2009	19:15	45.1146		0	0.004	7.20
19/07/2009	12:00	45.8125		0	0.004	7.20
20/07/2009	9:00	46.6875		0	0.004	7.20
20/07/2009	17:30	47.0417		0	0.004	7.20
21/07/2009	8:30	47.6667	Chlorella	3	0.250	7.21
21/07/2009	9:00	47.6875		0	0.000	7.21
21/07/2009	10:00	47.7292		0	0.001	7.18
21/07/2009	11:30	47.7917		0	0.000	7.16
21/07/2009	12:00	47.8125		0	0.004	7.15
21/07/2009	14:00	47.8958		0	0.001	7.15
21/07/2009	15:15	47.9479		0	0.000	7.14
21/07/2009	16:00	47.9792		0	0.004	7.15
21/07/2009	17:30	48.0417		0	0.000	7.15
21/07/2009	18:30	48.0833		0	0.001	7.16
21/07/2009	19:30	48.1250		0	0.000	7.16
21/07/2009	20:15	48.1563		0	0.001	7.17
21/07/2009	21:15	48.1979		0	0.000	7.16
22/07/2009	8:30	48.6667		0	0.004	7.17
22/07/2009	10:00	48.7292		0	0.000	7.16
22/07/2009	11:30	48.7917		0	0.000	7.16
22/07/2009	13:45	48.8854		0	0.004	7.16
22/07/2009	15:15	48.9479		0	0.001	7.16
22/07/2009	16:45	49.0104		0	0.000	7.16
23/07/2009	9:30	49.7083		0	0.004	7.16
23/07/2009	12:30	49.8333		0	0.000	7.16
23/07/2009	16:30	50.0000		0	0.004	7.16
24/07/2009	9:30	50.7083		0	0.100	7.16
27/07/2009	14:10	53.9028		0	0.004	7.18
28/07/2009	10:00	54.7292	Chlorella	1	0.076	7.21
28/07/2009	11:40	54.7986		0	0.005	7.19
28/07/2009	14:15	54.9063		0	0.004	7.19
28/07/2009	16:15	54.9896		0	0.001	7.19
28/07/2009	18:00	55.0625		0	0.004	7.19
29/07/2009	9:00	55.6875	Chlorella	2	0.075	7.16
29/07/2009	10:30	55.7500		0	0.004	7.16
29/07/2009	12:00	55.8125		0	0.001	7.16
29/07/2009	13:40	55.8819		0	0.004	7.16
29/07/2009	15:40	55.9653		0	0.001	7.16

Date [D/M/Y]	Time	Time [Days]	Substrate	COD_{in} [gCOD/L]	V_{in} [L]	pH [-]
29/07/2009	17:40	56.0486		0	0.004	7.17
30/07/2009	9:30	56.7083		0	0.079	7.15
30/07/2009	18:30	57.0833		0	0.000	7.15
31/07/2009	10:00	57.7292	Chlorella	3	0.079	7.13
31/07/2009	12:00	57.8125		0	0.001	7.13
31/07/2009	13:45	57.8854		0	0.004	7.13
31/07/2009	15:30	57.9583		0	0.001	7.13
31/07/2009	16:45	58.0104		0	0.001	7.13
31/07/2009	18:00	58.0625		0	0.004	7.13
01/08/2009	10:00	58.7292	Water	0	0.075	7.14
02/08/2009	10:15	59.7396	Water	0	0.075	7.14
03/08/2009	11:15	60.7813	Water	0	0.075	7.13
04/08/2009	9:30	61.7083	Chlorella (Super-nate)	1	0.075	7.11
04/08/2009	11:15	61.7813		0	0.004	7.11
04/08/2009	12:30	61.8333		0	0.001	7.11
04/08/2009	14:45	61.9271		0	0.004	7.12
04/08/2009	17:30	62.0417		0	0.001	7.12
05/08/2009	9:00	62.6875	Chlorella	0	0.080	7.12
05/08/2009	9:15	62.6979		0	0.004	7.11
05/08/2009	10:30	62.7500		0	0.001	7.11
05/08/2009	12:15	62.8229		0	0.004	7.11
05/08/2009	14:15	62.9063		0	0.000	7.11
05/08/2009	17:15	63.0313		0	0.001	7.11
06/08/2009	9:30	63.7083	Water	0	0.080	7.10
06/08/2009	18:00	64.0625		0	0.004	7.10
07/08/2009	9:00	64.6875	Chlorella	1	0.075	7.10
11/08/2009	9:00	68.6875	Chlorella	2	0.062	7.12
11/08/2009	18:00	69.0625		0	0.062	7.09
13/08/2009	9:00	70.6875	Chlorella	2	0.062	7.08
13/08/2009	18:00	71.0625		0	0.062	7.09
26/08/2009	9:00	83.6875	Chlorella	2	0.062	7.09
26/08/2009	18:00	84.0625	Water	0	0.062	7.08
27/08/2009	9:00	84.6875	Water	0	0.062	7.08
27/08/2009	18:00	85.0625	Water	0	0.062	7.06
28/08/2009	10:00	85.7292	Chlorella	2	0.062	7.05
28/08/2009	17:00	86.0208	Water	0	0.062	7.05
29/08/2009	11:00	86.7708	Water	0	0.062	7.05
29/08/2009	20:00	87.1458	Water	0	0.062	7.03
31/08/2009	9:00	88.6875	Chlorella	2	0.062	7.02

Date [D/M/Y]	Time	Time [Days]	Substrate	COD_{in} [gCOD/L]	V_{in} [L]	pH [-]
31/08/2009	18:00	89.0625	Water	0	0.062	7.01
01/09/2009	9:30	89.7083	Water	0	0.062	7.01
01/09/2009	18:00	90.0625	Water	0	0.062	6.99
02/09/2009	9:30	90.7083	Chlorella	2	0.062	6.99
02/09/2009	18:00	91.0625		0	0.062	7.00
03/09/2009	9:00	91.6875		0	0.062	6.99
03/09/2009	18:00	92.0625		0	0.062	6.99
07/09/2009	10:00	95.7292	Chlorella	1	0.035	6.99
07/09/2009	18:50	96.0972		0	0.071	6.95
08/09/2009	10:00	96.7292		0	0.071	6.95
08/09/2009	18:30	97.0833		0	0.071	6.95
09/09/2009	9:30	97.7083	Chlorella	2	0.070	6.95
09/09/2009	17:50	98.0556		0	0.058	6.95
10/09/2009	9:30	98.7083		0	0.058	6.95
10/09/2009	17:15	99.0313		0	0.058	6.97
11/09/2009	11:35	99.7951	Chlorella	1	0.062	6.95
11/09/2009	17:15	100.0313		0	0.062	6.96
14/09/2009	9:30	102.7083	Chlorella	4	0.124	6.97
14/09/2009	19:00	103.1042		0	0.000	6.99
15/09/2009	9:00	103.6875		0	0.062	6.94
15/09/2009	20:15	104.1563		0	0.062	6.95
16/09/2009	10:30	104.7500		0	0.062	6.95
16/09/2009	18:00	105.0625		0	0.062	6.95
17/09/2009	11:00	105.7708		0	0.062	6.95
17/09/2009	16:15	105.9896		0	0.062	6.95
18/09/2009	16:00	106.9792	Chlorella	1	0.062	6.95
21/09/2009	14:00	109.8958	Chlorella	6	0.083	6.95
22/09/2009	9:30	110.7083		0	0.062	6.95
22/09/2009	17:00	111.0208		0	0.062	6.83
23/09/2009	10:00	111.7292		0	0.062	6.82
23/09/2009	18:00	112.0625		0	0.062	6.83
24/09/2009	9:30	112.7083		0	0.062	6.84
24/09/2009	16:30	113.0000		0	0.062	6.84
25/09/2009	9:15	113.6979		0	0.062	6.84
25/09/2009	17:00	114.0208		0	0.062	6.84
26/09/2009	12:00	114.8125		0	0.062	6.85
26/09/2009	20:45	115.1771		0	0.062	6.85
28/09/2009	10:00	116.7292	Chlorella	1	0.062	6.85
29/09/2009	14:00	117.8958		0	0.062	6.84
30/09/2009	11:00	118.7708	Chlorella	2	0.062	6.78
01/10/2009	12:00	119.8125		0	0.062	6.78

Date [D/M/Y]	Time	Time [Days]	Substrate	COD_{in} [gCOD/L]	V_{in} [L]	pH [-]
02/10/2009	9:00	120.6875		0	0.062	6.78
05/10/2009	9:15	123.6979	Chlorella	4	0.062	6.78
06/10/2009	9:45	124.7188		0	0.062	6.65
07/10/2009	9:15	125.6979		0	0.062	6.73
08/10/2009	9:30	126.7083		0	0.062	6.76
09/10/2009	9:30	127.7083		0	0.062	6.76
12/10/2009	9:00	130.6875	Chlorella	6	0.062	6.56
13/10/2009	9:00	131.6875		0	0.062	6.54
14/10/2009	9:00	132.6875		0	0.062	6.64
15/10/2009	11:00	133.7708		0	0.062	6.73
16/10/2009	9:00	134.6875		0	0.062	6.77
17/10/2009	15:00	135.9375		0	0.062	6.85
19/10/2009	18:00	138.0625	Chlorella	6	0.084	6.85
21/10/2009	14:00	139.8958		0	0.050	6.85
22/10/2009	12:00	140.8125		0	0.062	6.65
23/10/2009	14:45	141.9271		0	0.062	6.74
25/10/2009	11:00	143.7708		0	0.062	6.85
26/10/2009	8:00	144.6458	Chlorella	1	0.062	6.87
27/10/2009	8:00	145.6458	Chlorella	1	0.062	6.88
28/10/2009	8:00	146.6458	Chlorella	1	0.062	6.88
29/10/2009	10:00	147.7292		0	0.062	6.88
30/10/2009	9:30	148.7083	Chlorella	2	0.062	6.88
02/11/2009	10:30	151.7500	Senedesmus	1	0.062	6.90

Table E.2: LBE-INRA Experimental Data (Part 2)

Time [Days]	BioGas Accum [L]	% CH_4 [−]	Gas Flow [L/day] (calculated in MATLAB)	COD_{sol} [gCOD/L]	COD_{tot} [gCOD/L]
0.0000	0.0000	11.00	0.0847	0.185	4.783
0.6667	0.0515	17.91	0.0909	0.791	5.871
1.6875	0.1516	19.59	0.0761	0.602	5.562
2.9375	0.2107	21.99	0.0304		
4.6250	0.2365	15.25	0.0025	0.202	4.542
5.6458	0.2395	9.39	0.0210	0.194	4.434
6.7083	0.2915	11.48	0.0679	0.861	6.921
7.1042	0.3250	15.24	0.0894		
7.6875	0.3732	39.58	0.1505	0.782	6.502
7.8333	0.4085	39.70	0.1704		
8.6667	0.5682	40.60	0.2131	0.616	6.016
8.8854	0.6480	45.39	0.1983		
9.6875	0.7520	52.00	0.1218	0.438	5.858
11.6458	0.8931	62.68	0.0596	0.595	7.015
12.0625	0.9284	59.59	0.0609		
12.6875	0.9637	58.30	0.0585	0.387	6.977
13.0417	1.0027	56.46	0.0632		
13.6875	1.0064	26.56	0.1722	0.422	6.352
13.8125	1.0584	51.47	0.2086		
14.0625	1.1624	57.08	0.2565		
14.7083	1.2905	60.44	0.3238	0.474	5.264
14.8333	1.3611	58.02	0.3310		
14.9896	1.4409	57.48	0.3275		
15.6042	1.6061	61.37	0.2826	0.468	6.478
16.8125	1.9107	62.32	0.2587	0.49	5.940
17.8958	2.2170	63.18	0.3388	0.511	6.531
18.7083	2.5011	62.11	0.3703	0.549	6.649
19.0000	2.6812	63.44	0.3346		
19.6875	2.8112	66.92	0.2732	0.502	7.682
20.0000					
20.7188	3.1306	64.22	0.3283	0.423	6.783
21.6875	3.4481	65.10	0.3731	0.446	7.426
22.0000	3.6412	63.06	0.3483		
22.7083	3.7600	66.75	0.2892	0.433	6.593
22.9792	3.9327	64.05	0.2668		
23.8958	4.0738	65.54	0.1709	0.419	6.649
24.8125	4.2298	64.71	0.1753	0.357	6.207
25.7083	4.3839	62.22	0.2311	0.395	6.175

Time [Days]	BioGas Accum [L]	% CH_4 [−]	Gas Flow [L/day] (calculated in MATLAB)	COD_{sol} [gCOD/L]	COD_{tot} [gCOD/L]
26.0625	4.5362	63.72	0.2313		
26.6458	4.5807	62.06	0.2396	0.356	6.936
27.0417	4.7664	60.67	0.2410		
27.7188	4.8388	59.45	0.2313	0.335	7.730
28.0104	4.9818	61.83	0.2329		
28.6875	5.0858	59.59	0.2379	0.343	8.140
29.6875	5.3643	60.28	0.2842	0.354	7.474
30.7917	5.6763	61.06	0.2388	0.321	7.861
32.7083	6.0365	62.43	0.2078	0.487	8.187
33.7083	6.2816	63.51	0.2339	0.494	8.530
34.7917	6.5322	63.51	0.2790	0.507	9.390
35.7292	6.8008	63.80	0.3521	0.495	9.290
35.7708	6.8225	61.40	0.3540		
35.8125	6.8522	60.29	0.3541		
35.8750	6.8877	61.57	0.3493		
35.9340	6.9193	62.39	0.3391		
35.9910	6.9529	61.89	0.3240		
36.0424	6.9786	63.16	0.3070		
36.0972	6.9963	61.52	0.2869		
36.1875	7.0003	61.34	0.2542		
36.2708	7.0062	63.76	0.2273		
36.7188	7.0576	65.06	0.1538	0.516	9.410
39.6667	7.6046	63.20	0.2928	0.571	9.150
39.6875	7.6046	63.20	0.2952		
39.7500	7.6500	58.76	0.2999		
39.8021	7.6816	57.80	0.3001		
39.9063	7.7429	59.01	0.2902		
39.9792	7.7705	59.46	0.2772		
40.8125	7.8890	57.79	0.2294	0.513	8.610
41.7292	8.1615	64.85	0.1882	0.627	8.980
43.7083	8.5545	70.81	0.4722	0.617	9.000
43.7396	8.5664	70.81	0.4865	0.992	
43.7813	8.5782	68.87	0.5050		
43.8229	8.6158	64.36	0.5216		
43.8646	8.6454	66.74	0.5358		
43.9063	8.6770	66.74	0.5469		
43.9479	8.7086	68.10	0.5546		
43.9896	8.7422	67.60	0.5590		

Time [Days]	BioGas Accum [L]	% CH_4 [−]	Gas Flow [L/day] (calculated in MATLAB)	COD_{sol} [gCOD/L]	COD_{tot} [gCOD/L]
44.0313	8.7757	67.28	0.5606		
44.0729	8.7974	68.14	0.5599	0.884	
44.8333	9.1865	71.45	0.3768	0.373	
45.1146	9.2517	70.29	0.2591	0.401	
45.8125	9.3287	73.32	0.0981	0.326	
46.6875	9.4176	72.81	0.0668	0.329	
47.0417	9.4644	69.58	0.0719		
47.6667	9.4918	70.28	0.1965	0.7	8.870
47.6875	9.4918	70.28	0.2042	0.521	9.200
47.7292	9.4977	69.57	0.2193		
47.7917	9.5211	69.88	0.2396		
47.8125	9.5348	68.79	0.2455	0.507	
47.8958	9.5602	70.06	0.2625		
47.9479	9.5797	69.71	0.2675		
47.9792	9.5973	70.20	0.2684	0.402	
48.0417	9.6227	68.99	0.2653		
48.0833	9.6363	69.35	0.2601		
48.1250	9.6461	69.64	0.2530		
48.1563	9.6559	69.89	0.2468		
48.1979	9.6637	69.89	0.2381		
48.6667	9.7399	70.10	0.1557	0.263	8.480
48.7292	9.7457	70.43	0.1475		
48.7917	9.7536	70.35	0.1400		
48.8854	9.7672	69.72	0.1302	0.25	
48.9479	9.7711	69.87	0.1245		
49.0104	9.7848	69.45	0.1191		
49.7083	9.8454	69.32	0.0805	0.246	
49.8333	9.8571	69.47	0.0770		
50.0000	9.8825	69.47	0.0706	0.802	8.650
50.7083	9.9118	68.00	0.0580	0.944	7.660
53.9028	10.1247	69.00	0.0559	0.369	
54.7292	10.1560	69.00	0.0918	0.452	
54.7986	10.1618	66.98	0.0983	0.292	
54.9063	10.1950	65.08	0.1048	0.512	7.410
54.9896	10.2106	67.01	0.1063	0.348	8.620
55.0625	10.2263	66.12	0.1061		
55.6875	10.2458	65.40	0.1449	0.3	7.910
55.7500	10.2693	65.48	0.1525		

Time [Days]	BioGas Accum [L]	% CH_4 [−]	Gas Flow [L/day] (calculated in MATLAB)	COD_{sol} [gCOD/L]	COD_{tot} [gCOD/L]
55.8125	10.2907	66.16	0.1576	0.248	8.060
55.8819	10.3161	66.16	0.1593		
55.9653	10.3415	63.94	0.1556	0.636	7.940
56.0486	10.3689	66.27	0.1474	0.262	7.360
56.7083	10.4060	65.31	0.0989	0.373	8.520
57.0833	10.4626	66.77	0.0883		
57.7292	10.4841	67.87	0.1230	0.282	8.550
57.8125	10.5095	64.33	0.1335		
57.8854	10.5349	67.37	0.1406	0.292	8.550
57.9583	10.5564	65.77	0.1453	0.469	8.120
58.0104		65.51		0.461	7.280
58.0625		66.14		0.414	6.710
58.7292	10.6677	66.00	0.1309		
59.7396	10.7537	66.00	0.0775		
60.7813	10.8299	66.00	0.0745		
61.7083	10.8787	65.05	0.0925	0.466	5.890
61.7813	10.9178	66.45	0.0928		
61.8333	10.9256	66.46	0.0913		
61.9271	10.9393	68.77	0.0858		
62.0417	10.9568	65.54	0.0761		
62.6875	10.9686	65.65	0.0619	0.329	5.200
62.6979	10.9686	65.65	0.0624		
62.7500	10.9764	67.39	0.0649		
62.8229	10.9842	67.39	0.0677		
62.9063	10.9881	67.39	0.0697		
63.0313	11.0135	67.39	0.0694		
63.7083	11.0389	65.03	0.0552	0.294	5.340
64.0625	11.0682	64.89	0.0422		
64.6875	11.0760	65.00	0.0272	0.303	4.570
68.6875	11.2928	66.00	0.1134	0.331	4.760
69.0625	11.3729	66.00	0.1077	0.339	6.130
70.6875	11.4804	66.00	0.1195	0.283	5.490
71.0625	11.5663	66.00	0.1302	0.288	7.030
83.6875	12.5098	62.00	0.1564	0.36	3.490
84.0625	12.6172	63.00	0.1402	0.337	5.760
84.6875	12.6544	66.00	0.0905	0.321	4.880
85.0625	12.6973	66.00	0.0796	0.258	4.410
85.7292	12.7130	66.46	0.1091	0.261	4.020

Time [Days]	BioGas Accum [L]	% CH_4 [−]	Gas Flow [L/day] (calculated in MATLAB)	COD_{sol} [gCOD/L]	COD_{tot} [gCOD/L]
86.0208	12.8028	66.46	0.1202	0.284	5.750
86.7708	12.8634	66.46	0.0686	0.256	5.110
87.1458	12.8829	66.46	0.0309	0.253	4.720
88.6875	12.8927	66.46	0.0817	0.241	4.770
89.0625	12.9474	66.46	0.1292		5.600
89.7083	13.0646	66.30	0.1319	0.222	5.040
90.0625	13.0900	66.30	0.1125	0.222	4.760
90.7083	13.1310	66.30	0.1488	0.222	4.460
91.0625	13.2365	66.30	0.1757	0.294	6.510
91.6875	13.3302	66.30	0.1663	0.243	5.550
92.0625	13.3966	66.30	0.1436	0.188	5.860
95.7292	13.6916	64.30	0.1230	0.209	5.290
96.0972	13.7834	64.30	0.1219	0.28	5.390
96.7292	13.8264	64.30	0.0846	0.251	4.870
97.0833	13.8616	64.30	0.0739	0.214	4.540
97.7083	13.8694	65.50	0.1115	0.2	4.890
98.0556	13.9670	65.50	0.1325	0.288	5.500
98.7083	14.0315	65.50	0.0990	0.122	4.640
99.0313	14.0647	65.70	0.0696	0.135	4.240
99.7951	14.0667	66.00	0.0419	0.14	5.570
100.0313	14.1217	66.00	0.0388	0.142	5.410
102.7083	14.2336	66.30	0.1576	0.154	4.160
103.1042	14.3252	66.80	0.1923		
103.6875	14.4371	67.30	0.1803	0.221	7.210
104.1563	14.5205	68.00	0.1301	0.221	0.653
104.7500	14.5592	69.60	0.0703	0.16	7.330
105.0625	14.5877	68.00	0.0508	0.164	5.910
105.7708	14.6040	66.81	0.0308	0.148	5.690
105.9896	14.6162	66.00	0.0311	0.149	7.040
106.9792	14.6467	65.50	0.0133	0.131	5.060
109.8958	14.7871	64.90	0.1913	0.115	5.790
110.7083	14.9886	66.10	0.2354	0.16	9.590
111.0208	15.0741	66.10	0.2080	0.158	9.830
111.7292	15.1738	64.70	0.1287	0.126	8.830
112.0625	15.2206	64.70	0.0962	0.11	7.800
112.7083	15.2511	67.60	0.0572	0.112	7.470
113.0000	15.2837	67.60	0.0479	0.098	7.720
113.6979	15.2959	68.10	0.0366	0.094	7.070

Time [Days]	BioGas Accum [L]	% CH_4 [−]	Gas Flow [L/day] (calculated in MATLAB)	COD_{sol} [gCOD/L]	COD_{tot} [gCOD/L]
114.0208	15.3203	67.00	0.0356	0.078	5.410
114.8125	15.3366	66.95	0.0269	0.091	5.320
115.1771	15.3549	66.95	0.0211	0.08	4.830
116.7292	15.3814	65.80	0.0558	0.1	5.000
117.8958	15.4933	65.80	0.0746	0.081	5.170
118.7708	15.5279	68.00	0.1187	0.079	4.710
119.8125	15.7192	68.50	0.1326	0.104	6.910
120.6875	15.7843	67.00	0.0485	0.091	5.500
123.6979	15.9166	66.20	0.1730	0.09	5.120
124.7188	16.1669	66.50	0.2380	0.431	9.120
125.6979	16.3683	66.50	0.1879	0.241	7.730
126.7083	16.5230	67.49	0.0978	0.095	6.230
127.7083	16.5698	67.70	0.0169	0.067	6.010
130.6875	16.6899	67.80	0.1769	0.057	4.700
131.6875	16.9422	67.60	0.2198	0.931	12.120
132.6875	17.1131	67.60	0.2188	0.679	9.470
133.7708	17.3858	67.60	0.1834	0.49	8.740
134.6875	17.4855	67.40	0.1219	0.32	7.680
135.9375	17.6321	67.66	0.0412	0.078	5.840
138.0625	17.6667	67.60	0.1521	0.076	4.940
139.8958	18.1713	69.71	0.2395	0.808	8.380
140.8125	18.3179	69.40	0.2013	0.206	8.770
141.9271	18.5702	68.53	0.1558	0.11	6.650
143.7708	18.6984	69.39	0.0387	0.07	5.000
144.6458	18.7289	69.92	0.1039	0.079	6.110
145.6458	18.9121	67.84	0.1282	0.088	7.070
146.6458	18.9792	68.64	0.1876	0.089	7.170
147.7292	19.2926	67.00	0.1711	0.089	6.690
148.7083	19.3374	67.50	0.0776	0.073	7.110
151.7500	19.7424	68.00	0.1524	0.091	6.800

Table E.3: LBE-INRA Experimental Data (Part 3)

Time [Days]	VFA [gCOD/L]	IN [mol/L]	Z [mol/L]	Chlorine [mol/L]	NO_2 [mol/L]	NO_3 [mol/L]
0.0000		0.00421	0.06077	0.00015	0.01557	0
0.6667		0.00455	0.05860	0.00011	0.01477	0
1.6875		0.00582	0.05888	0.00019	0.01477	0
2.9375						
4.6250		0.00632	0.05779	0.00011	0.01471	0
5.6458		0.00632	0.05834	0.00014	0.01481	0
6.7083		0.00926	0.05546	0.00009	0.01369	0
7.1042						
7.6875		0.01014	0.05192	0.00014	0.01699	0
7.8333						
8.6667						
8.8854						
9.6875						
11.6458						
12.0625						
12.6875						
13.0417						
13.6875	0.01130	0.02511	0.04859	0.02836	0	0
13.8125						
14.0625						
14.7083	0.01130	0.01954	0.03646	0.02294	0	0.00014
14.8333						
14.9896						
15.6042	0.01347	0.02292	0.03843	0.02408	0	0
16.8125	0.01130	0.02408	0.03634	0.02293	0	0
17.8958	0.01238	0.02817	0.03780	0.02585	0	0
18.7083	0.01021	0.02691	0.03413	0.02140	0	0
19.0000						
19.6875	0.00913	0.02993	0.03506	0.02171	0	0
20.0000						
20.7188	0.00804	0.03074	0.03398	0.02109	0	0
21.6875	0.01717	0.03256	0.03292	0.02061	0	0
22.0000	0.01085					
22.7083	0.01238	0.03258	0.02999	0.01843	0	0
22.9792	0.01085	0.03483				
23.8958	0.01238	0.03468	0.03033	0.01837	0	0
24.8125	0.01130	0.03346	0.02937	0.01722	0	0
25.7083	0.01238	0.03608	0.03040	0.01776	0	0

Time [Days]	VFA [gCOD/L]	IN [mol/L]	Z [mol/L]	Chlorine [mol/L]	NO_2 [mol/L]	NO_3 [mol/L]
26.0625		0.03469				
26.6458	0.01444	0.03388				
27.0417						
27.7188	0.01336	0.03407				
28.0104						
28.6875	0.01238	0.03532				
29.6875		0.04380				
30.7917	0.01923	0.03484				
32.7083	0.01130	0.03776				
33.7083		0.03895				
34.7917		0.03818	0.01819	0.01241	0	0
35.7292		0.03902	0.01756	0.01170	0	0
35.7708		0.03902				
35.8125						
35.8750		0.03921				
35.9340		0.04030				
35.9910		0.04019				
36.0424		0.04039				
36.0972		0.04108				
36.1875						
36.2708		0.04010				
36.7188		0.04049	0.01865	0.01149	0	0
39.6667	0.01119	0.04325	0.01751	0.01212	0	0
39.6875		0.04010				
39.7500		0.04253				
39.8021		0.04297				
39.9063		0.04194				
39.9792		0.04397				
40.8125		0.04158	0.01937	0.01075	0	0
41.7292		0.04180	0.01935	0.01031	0	0
43.7083		0.03967	0.01779	0.01016	0	0
43.7396		0.04063				
43.7813						
43.8229		0.04039				
43.8646						
43.9063		0.04175				
43.9479						
43.9896		0.04233				

Time [Days]	VFA [gCOD/L]	IN [mol/L]	Z [mol/L]	Chlorine [mol/L]	NO_2 [mol/L]	NO_3 [mol/L]
44.0313						
44.0729		0.04283				
44.8333		0.04362				
45.1146		0.04472				
45.8125		0.04381				
46.6875		0.04498				
47.0417		0.04695				
47.6667		0.04651	0.01742	0.00960	0	0
47.6875		0.03304				
47.7292		0.03486				
47.7917						
47.8125		0.03404				
47.8958		0.03146				
47.9479						
47.9792		0.03527				
48.0417						
48.0833		0.03475				
48.1250						
48.1563		0.03516				
48.1979						
48.6667		0.03524				
48.7292						
48.7917						
48.8854		0.03531				
48.9479						
49.0104		0.03619				
49.7083		0.03581				
49.8333						
50.0000						
50.7083			0.01212	0.00689	0	0
53.9028						
54.7292		0.03876	0.01445	0.00762	0	0
54.7986		0.04072				
54.9063		0.04029				
54.9896		0.04051				
55.0625		0.03936				
55.6875		0.03620	0.01393	0.00700	0	0
55.7500		0.03456				

Time [Days]	VFA [gCOD/L]	IN [mol/L]	Z [mol/L]	Chlorine [mol/L]	NO_2 [mol/L]	NO_3 [mol/L]
55.8125		0.03749				
55.8819		0.03761				
55.9653		0.03719				
56.0486		0.03662				
56.7083		0.03558	0.01423	0.00649	0	0
57.0833		0.03461				
57.7292		0.03254	0.01249	0.00615	0	0
57.8125						
57.8854						
57.9583						
58.0104						
58.0625						
58.7292		0.03365	0.01335	0.00606	0	0
59.7396		0.03193	0.00874	0.00549	0	0
60.7813		0.03049	0.01170	0.00520	0	0
61.7083		0.02915	0.01328	0.00574	0	0
61.7813						
61.8333						
61.9271						
62.0417						
62.6875		0.02736	0.01381	0.00523	0	0
62.6979						
62.7500						
62.8229						
62.9063						
63.0313						
63.7083		0.02712	0.01284	0.00508	0	0
64.0625						
64.6875		0.02615	0.01282	0.00500	0	0
68.6875		0.02675	0.01242	0.00514	0	0
69.0625		0.02533	0.01426	0.00483	0	0
70.6875		0.02540	0.01404	0.00479	0	0
71.0625		0.02454	0.01448	0.00468	0	0
83.6875		0.02808	0.01276	0.00577	0	0
84.0625		0.02653	0.01322	0.00514	0	0
84.6875		0.02589	0.01078	0.00493	0	0
85.0625		0.02529	0.01280	0.00481	0	0
85.7292		0.02451	0.01224	0.00470	0	0

Time [Days]	VFA [gCOD/L]	IN [mol/L]	Z [mol/L]	Chlorine [mol/L]	NO_2 [mol/L]	NO_3 [mol/L]
86.0208		0.02297	0.01257	0.00441	0	0
86.7708		0.02130	0.01399	0.00396	0	0
87.1458		0.02175	0.01267	0.00615	0	0
88.6875		0.02200	0.01212	0.00424	0	0
89.0625		0.02039	0.01005	0.00397	0	0
89.7083		0.02008	0.01022	0.00395	0	0
90.0625		0.01648				
90.7083		0.01627				
91.0625		0.01632				
91.6875		0.01596				
92.0625		0.01582				
95.7292		0.01501				
96.0972		0.01476				
96.7292		0.01616				
97.0833		0.02009				
97.7083		0.01928				
98.0556		0.01909				
98.7083		0.01865				
99.0313		0.01864				
99.7951		0.01845				
100.0313		0.01935				
102.7083		0.01864				
103.1042						
103.6875		0.01464				
104.1563		0.01430				
104.7500		0.01396				
105.0625		0.01376				
105.7708		0.01337	0.00499	0.00239	0	0
105.9896		0.01103				
106.9792		0.01075	0.00434	0.00223	0	0
109.8958		0.01200	0.00623	0.00250	0	0
110.7083		0.01080	0.00683	0.00223	0	0
111.0208		0.00983	0.00630	0.00222	0	0
111.7292		0.00992	0.00426	0.00224	0	0
112.0625		0.01004	0.00774	0.00245	0	0
112.7083		0.00936	0.00421	0.00200	0	0
113.0000		0.00879	0.00419	0.00188	0	0
113.6979		0.00860	0.00734	0.00600	0	0

Time [Days]	VFA [gCOD/L]	IN [mol/L]	Z [mol/L]	Chlorine [mol/L]	NO_2 [mol/L]	NO_3 [mol/L]
114.0208		0.00799	0.00404	0.00203	0	0
114.8125		0.00780	0.00349	0.00174	0	0
115.1771		0.00749	0.00565	0.00170	0	0
116.7292	0.00696	0.00724	0.00491	0.00174	0	0
117.8958	0.00696	0.00740	0.00381	0.00194	0	0
118.7708	0.00696	0.00671	0.00323	0.00176	0	0
119.8125	0.04467	0.00693	0.00436	0.00188	0	0
120.6875	0.00434	0.00694	0.00404	0.00191	0	0
123.6979	0.00542	0.00749	0.00372	0.00216	0	0
124.7188	0.25739	0.00707	0.00725	0.00210	0	0
125.6979	0.08191	0.00752	0.00670	0.00210	0	0
126.7083	0.00958	0.00755	0.00675	0.00231	0	0
127.7083	0.00804	0.00722	0.00629	0.00256	0	0
130.6875	0.00587	0.00756	0.00622	0.00272	0	0
131.6875	0.68969	0.00790	0.00692	0.00255	0	0
132.6875	0.42090	0.00851	0.00770	0.00214	0	0
133.7708	0.28285	0.00886	0.00820	0.00299	0	0
134.6875	0.16023	0.01097	0.01002	0.00393	0	0
135.9375	0.03778	0.00788	0.00513	0.00281	0	0
138.0625	0.03606	0.00810	0.00728	0.00291	0	0
139.8958		0.00906	0.00811	0.00274	0	0
140.8125	0.28893	0.00834	0.00756	0.00276	0	0
141.9271	0.03798	0.00911	0.00784	0.00266	0	0
143.7708	0.00976	0.00942	0.00777	0.00272	0	0
144.6458	0.01130	0.00914	0.00662	0.00278	0	0
145.6458	0.02431	0.00929	0.00798	0.00266	0	0
146.6458	0.01519	0.00955	0.00693	0.00251	0	0
147.7292		0.00998	0.00886	0.00256	0	0
148.7083			0.00716	0.00238	0	0
151.7500						

Table E.4: LBE-INRA Experimental Data (Part 4)

Time [Days]	Phosphorus [mol/L]	Sulfur [mol/L]	Sodium [mol/L]	Potassium [mol/L]	Magnesium [mol/L]	Calcium [mol/L]
0.0000	0.000057	0.001029	0.06445	0.00347	0.002371	0.002951
0.6667	0.000038	0	0.06076	0.00347	0.002058	0.002019
1.6875	0.000038	0	0.06021	0.00358	0.002209	0.002409
2.9375						
4.6250	0.000041	0	0.05860	0.00385	0.002218	0.002589
5.6458	0.000026	0	0.05887	0.00400	0.002247	0.002678
6.7083	0	0	0.05459	0.00499	0.002281	0.001940
7.1042						
7.6875	0	0	0.05348	0.00498	0.002343	0.002328
7.8333						
8.6667						
8.8854						
9.6875						
11.6458						
12.0625						
12.6875						
13.0417						
13.6875	0.007797	0.000183	0.06083	0.00816	0.006698	0.002870
13.8125						
14.0625						
14.7083	0.002207	0.000118	0.04819	0.00694	0.001108	0.002790
14.8333						
14.9896						
15.6042	0.002693	0	0.05070	0.00781	0.001077	0.002857
16.8125	0.002686	0	0.04813	0.00791	0.000937	0.002618
17.8958	0.003235	0	0.05103	0.00894	0.001009	0.003190
18.7083	0.003035	0	0.04519	0.00841	0.000730	0.002447
19.0000						
19.6875	0.003330	0	0.04625	0.00914	0.000789	0.002343
20.0000						
20.7188	0.002944	0.000090	0.04498	0.00937	0.000472	0.002146
21.6875	0.003513	0	0.04376	0.00966	0.000611	0.002041
22.0000						
22.7083	0.004122	0	0.03958	0.00920	0.001356	0.001518
22.9792						
23.8958	0.003887	0	0.03972	0.00978	0.000967	0.001524
24.8125	0.003950	0	0.03737	0.00960	0.001041	0.001682
25.7083	0.005711	0	0.03844	0.01022	0.002551	0.001407

Time [Days]	Phosphorus [mol/L]	Sulfur [mol/L]	Sodium [mol/L]	Potassium [mol/L]	Magnesium [mol/L]	Calcium [mol/L]
26.0625						
26.6458						
27.0417						
27.7188						
28.0104						
28.6875						
29.6875						
30.7917						
32.7083						
33.7083						
34.7917	0.002720	0.001265	0.02701	0.01014	0	0
35.7292	0.002916	0.001244	0.02585	0.01021	0	0
35.7708						
35.8125						
35.8750						
35.9340						
35.9910						
36.0424						
36.0972						
36.1875						
36.2708						
36.7188	0.003880	0.001294	0.02566	0.01051	0.001152	0
39.6667	0.004045	0.003290	0.02828	0.01111	0.001386	0
39.6875						
39.7500						
39.8021						
39.9063						
39.9792						
40.8125	0.003701	0.000376	0.02352	0.01061	0.001137	0
41.7292	0.003962	0.000182	0.02254	0.01049	0.001467	0
43.7083	0.003643	0.001304	0.02271	0.01122	0.001059	0
43.7396						
43.7813						
43.8229						
43.8646						
43.9063						
43.9479						
43.9896						

Time [Days]	Phosphorus [mol/L]	Sulfur [mol/L]	Sodium [mol/L]	Potassium [mol/L]	Magnesium [mol/L]	Calcium [mol/L]
44.0313						
44.0729						
44.8333						
45.1146						
45.8125						
46.6875						
47.0417						
47.6667	0.004145	0.001349	0.02150	0.01191	0.001291	0
47.6875						
47.7292						
47.7917						
47.8125						
47.8958						
47.9479						
47.9792						
48.0417						
48.0833						
48.1250						
48.1563						
48.1979						
48.6667						
48.7292						
48.7917						
48.8854						
48.9479						
49.0104						
49.7083						
49.8333						
50.0000						
50.7083	0.003265	0.001166	0.01621	0.00997	0	0
53.9028						
54.7292	0.003618	0.001262	0.01685	0.01067	0.001278	0
54.7986						
54.9063						
54.9896						
55.0625						
55.6875	0.003537	0.001207	0.01561	0.01009	0.001445	0
55.7500						

Time [Days]	Phosphorus [mol/L]	Sulfur [mol/L]	Sodium [mol/L]	Potassium [mol/L]	Magnesium [mol/L]	Calcium [mol/L]
55.8125						
55.8819						
55.9653						
56.0486						
56.7083	0.003167	0.001163	0.01521	0.01012	0.001199	0
57.0833						
57.7292	0.003120	0.001107	0.01383	0.00916	0.001221	0
57.8125						
57.8854						
57.9583						
58.0104						
58.0625						
58.7292	0.003640	0.001147	0.01395	0.00970	0.001701	0
59.7396	0.003506	0.001087	0.01263	0.00894	0	0
60.7813	0.003178	0.001034	0.01165	0.00845	0.001762	0
61.7083	0.002202	0	0.01158	0.00812	0	0.001258
61.7813						
61.8333						
61.9271						
62.0417						
62.6875	0.001893	0	0.01079	0.00765	0	0.001681
62.6979						
62.7500						
62.8229						
62.9063						
63.0313						
63.7083	0.002055	0	0.01028	0.00739	0	0.001615
64.0625						
64.6875	0.001777	0	0.00983	0.00717	0	0.001694
68.6875	0.001893	0	0.00960	0.00738	0	0.001674
69.0625	0.001979	0	0.00950	0.00725	0.000822	0.001773
70.6875	0.002243	0	0.00902	0.00709	0.001129	0.001839
71.0625	0.002308	0	0.00903	0.00720	0.001290	0.001842
83.6875	0.003299	0.000400	0.00786	0.00809	0.001632	0.002442
84.0625	0.002329	0	0.00756	0.00766	0.001296	0.001946
84.6875	0.002230	0.001021	0.00721	0.00744	0.001367	0.001786
85.0625	0.002162	0	0.00695	0.00716	0.001438	0.001854
85.7292	0.002134	0	0.00669	0.00702	0.001298	0.001833

Time [Days]	Phosphorus [mol/L]	Sulfur [mol/L]	Sodium [mol/L]	Potassium [mol/L]	Magnesium [mol/L]	Calcium [mol/L]
86.0208	0.002068	0	0.00673	0.00675	0.001221	0.001998
86.7708	0.001958	0	0.00601	0.00607	0.001309	0.003013
87.1458	0.001942	0	0.00735	0.00718	0.001313	0.002202
88.6875	0.001999	0	0.00593	0.00622	0.001336	0.002172
89.0625	0.001891	0.000870	0.00590	0.00608	0.001176	0.002038
89.7083	0.001859	0.000862	0.00569	0.00595	0.001246	0.002180
90.0625						
90.7083						
91.0625						
91.6875						
92.0625						
95.7292						
96.0972						
96.7292						
97.0833						
97.7083						
98.0556						
98.7083						
99.0313						
99.7951						
100.0313						
102.7083						
103.1042						
103.6875						
104.1563						
104.7500						
105.0625						
105.7708	0.001086	0.000504	0.00324	0.00353	0	0.001647
105.9896						
106.9792	0.001084	0.000526	0.00298	0.00340	0	0.001450
109.8958	0.001239	0	0.00317	0.00385	0	0.001803
110.7083	0.001321	0.000730	0.00330	0.00404	0.000833	0.001773
111.0208	0.001124	0	0.00303	0.00370	0	0.001720
111.7292	0.001494	0.000785	0.00300	0.00373	0	0.001763
112.0625	0.001323	0	0.00312	0.00380	0.000806	0.001801
112.7083	0.001201	0.000712	0.00268	0.00342	0	0.001648
113.0000	0.001150	0.000666	0.00249	0.00309	0	0.001755
113.6979	0.001205	0.000685	0.00676	0.00416	0.000910	0.001870

Time [Days]	Phosphorus [mol/L]	Sulfur [mol/L]	Sodium [mol/L]	Potassium [mol/L]	Magnesium [mol/L]	Calcium [mol/L]
114.0208	0.001119	0.000505	0.00223	0.00282	0	0.001838
114.8125	0.001068	0.000644	0.00208	0.00268	0	0.001667
115.1771	0.001103	0.000598	0.00200	0.00270	0.000924	0.001807
116.7292	0.001030	0	0.00191	0.00253	0	0.001869
117.8958	0.001143	0.000657	0.00199	0.00274	0	0.002008
118.7708	0.000998	0.000582	0.00177	0.00253	0	0.001641
119.8125	0.001049	0.000618	0.00193	0.00282	0	0.002118
120.6875	0.001226	0.000622	0.00185	0.00281	0	0.002153
123.6979	0.000866	0.000486	0.00183	0.00312	0	0.001569
124.7188	0.001464	0.000481	0.00202	0.00349	0.000924	0.002476
125.6979	0.001501	0.000485	0.00191	0.00339	0.000865	0.002428
126.7083	0.001269	0	0.00186	0.00327	0.000819	0.002049
127.7083	0.001503	0	0.00186	0.00332	0.000915	0.001990
130.6875	0.001371	0.000619	0.00208	0.00348	0.000932	0.002277
131.6875	0.001692	0.000678	0.00204	0.00412	0.000917	0.002524
132.6875	0.001781	0	0.00179	0.00373	0.001001	0.002370
133.7708	0.001765	0	0.00191	0.00469	0.001058	0.002477
134.6875	0.002151	0	0.00246	0.00593	0.001318	0.003005
135.9375	0.001197	0.000647	0.00162	0.00402	0.000968	0.001716
138.0625	0.001370	0	0.00169	0.00411	0.000987	0.002219
139.8958	0.001909	0.000667	0.00201	0.00483	0.001171	0.002910
140.8125	0.001547	0.000526	0.00190	0.00464	0.001150	0.002321
141.9271	0.001269	0	0.00182	0.00441	0.001028	0.002003
143.7708	0.001350	0	0.00183	0.00440	0.000944	0.002178
144.6458	0.001209	0.000679	0.00189	0.00426	0.000960	0.002247
145.6458	0.001218	0	0.00169	0.00407	0.001022	0.002326
146.6458	0.001261	0.000711	0.00167	0.00404	0.001080	0.002436
147.7292	0.001352	0	0.00176	0.00416	0.001166	0.002593
148.7083	0.001156	0.000674	0.00168	0.00396	0.001062	0.002426
151.7500						

Table E.5: Least Squares Randomization Pattern

Time [Days]	IN Pattern	VFA Pattern	TCOD Pattern	% CH_4 Pattern	Gas Flow Pattern
15.6042	0	0	1	1	1
16.8125	1	1	1	0	0
17.8958	0	0	0	0	0
18.7083	0	1	1	0	0
19.0000	0	1	0	0	1
19.6875	1	1	0	1	0
20.0000	1	0	1	1	0
20.7188	1	1	1	0	0
21.6875	1	0	0	1	1
22.0000	1	1	0	0	1
22.7083	1	1	0	1	0
22.9792	0	1	0	0	0
23.8958	0	0	0	1	0
24.8125	0	0	1	1	1
25.7083	1	1	0	1	1
26.0625	0	0	1	1	0
26.6458	1	0	1	1	0
27.0417	1	1	0	1	0
27.7188	1	1	0	1	1
28.0104	1	0	0	1	1
28.6875	1	0	1	0	0
29.6875	0	0	0	0	1
30.7917	1	1	0	1	1
32.7083	1	1	1	1	1
33.7083	0	1	0	1	0
34.7917	0	0	0	1	0
35.7292	1	1	0	0	1
35.7708	1	0	1	1	0
35.8125	0	0	1	1	1
35.8750	0	1	0	1	1
35.9340	1	1	1	0	1
35.9910	0	1	1	1	0
36.0424	1	0	0	1	0
36.0972	1	1	0	0	1
36.1875	1	1	0	0	0
36.2708	0	0	0	0	1
36.7188	1	1	0	0	0
39.6667	0	0	0	1	1
39.6875	0	1	1	1	0

Time [Days]	IN Pattern	VFA Pattern	TCOD Pattern	% CH_4 Pattern	Gas Flow Pattern
39.7500	1	0	0	0	0
39.8021	0	1	0	0	0
39.9063	1	1	1	0	0
39.9792	1	1	1	0	1
40.8125	0	0	0	0	1
41.7292	1	1	1	0	0
43.7083	0	1	1	0	0
43.7396	1	1	0	1	1
43.7813	1	0	1	1	0
43.8229	0	1	1	1	0
43.8646	0	0	0	1	1
43.9063	1	0	0	1	1
43.9479	1	1	1	1	1
43.9896	1	1	1	1	1
44.0313	0	1	0	0	0
44.0729	0	1	0	1	0
44.8333	1	1	1	1	1
45.1146	1	0	1	0	1
45.8125	0	0	1	1	0
46.6875	1	1	1	1	1
47.0417	1	1	0	0	1
47.6667	0	0	0	0	1
47.6875	0	1	1	1	1
47.7292	0	0	1	0	1
47.7917	0	1	1	0	1
47.8125	0	1	1	0	1
47.8958	1	1	0	0	0
47.9479	1	0	1	1	1
47.9792	1	0	1	1	1
48.0417	1	1	0	0	0
48.0833	1	0	1	0	1
48.1250	0	0	0	1	0
48.1563	0	1	0	0	0
48.1979	1	1	1	0	1
48.6667	0	0	1	0	1
48.7292	0	1	1	0	0
48.7917	1	1	0	0	1
48.8854	0	1	1	0	0
48.9479	1	1	0	0	0

Time [Days]	IN Pattern	VFA Pattern	TCOD Pattern	% CH_4 Pattern	Gas Flow Pattern
49.0104	0	1	0	0	0
49.7083	0	1	1	0	1
49.8333	0	0	0	1	1
50.0000	1	1	0	0	1
50.7083	1	0	0	0	0
53.9028	0	1	1	1	0
54.7292	1	1	0	1	0
54.7986	0	0	1	1	1
54.9063	0	1	1	0	0
54.9896	1	1	1	1	0
55.0625	0	1	1	1	0
55.6875	1	0	0	1	1
55.7500	0	1	1	1	1
55.8125	1	1	0	0	1
55.8819	0	0	1	1	1
55.9653	0	1	1	0	1
56.0486	0	1	1	1	1
56.7083	0	1	1	1	0
57.0833	0	1	1	0	1
57.7292	0	0	1	0	1
57.8125	1	1	0	1	0
57.8854	0	1	1	0	1
57.9583	0	0	0	1	0
58.0104	0	1	1	0	0
58.0625	0	1	0	1	0
58.7292	1	0	0	1	0
59.7396	0	0	1	0	0
60.7813	1	0	1	0	1
61.7083	0	1	1	0	0
61.7813	0	0	0	0	1
61.8333	1	0	1	0	1
61.9271	1	1	1	1	0
62.0417	1	1	1	0	0
62.6875	0	0	0	0	1
62.6979	0	0	1	1	0
62.7500	1	0	0	0	1
62.8229	0	0	0	1	0
62.9063	0	0	1	1	0
63.0313	1	0	1	0	1

Time [Days]	IN Pattern	VFA Pattern	TCOD Pattern	% CH_4 Pattern	Gas Flow Pattern
63.7083	0	1	1	0	0
64.0625	1	0	0	0	0
64.6875	0	1	0	1	1
68.6875	0	0	0	1	0
69.0625	1	1	0	0	0
70.6875	0	1	0	0	1
71.0625	0	0	0	1	1
83.6875	0	0	1	0	1
84.0625	0	1	0	1	1
84.6875	0	1	1	1	0
85.0625	0	0	1	1	1
85.7292	1	1	1	1	0
86.0208	0	0	0	0	0
86.7708	1	1	0	0	0
87.1458	1	0	0	0	1
88.6875	1	0	1	0	1
89.0625	1	0	0	1	1
89.7083	0	0	0	0	1
90.0625	0	1	0	0	0
90.7083	0	1	0	1	1
91.0625	1	0	1	1	0
91.6875	1	1	1	0	1
92.0625	0	1	1	0	1
95.7292	0	1	0	1	1
96.0972	0	0	1	1	0
96.7292	0	1	0	0	0
97.0833	0	0	1	1	1
97.7083	1	0	1	0	0
98.0556	0	1	0	0	1
98.7083	1	0	1	0	1
99.0313	1	1	1	0	1
99.7951	1	1	0	0	0
100.0313	0	0	1	0	0
102.7083	1	0	0	0	1
103.1042	1	1	0	1	0
103.6875	0	1	1	1	1
104.1563	1	0	1	0	0
104.7500	0	1	0	1	0
105.0625	1	0	1	0	0

Time [Days]	IN Pattern	VFA Pattern	TCOD Pattern	% CH_4 Pattern	Gas Flow Pattern
105.7708	0	0	1	1	0
105.9896	1	1	1	0	0
106.9792	1	1	1	1	0
109.8958	1	1	1	0	0
110.7083	1	0	0	1	1
111.0208	1	1	1	0	1
111.7292	1	1	0	0	0
112.0625	1	0	0	0	0
112.7083	1	0	1	0	0
113.0000	0	0	1	1	0
113.6979	1	0	0	1	1
114.0208	0	0	1	1	1
114.8125	1	0	0	1	1
115.1771	1	1	1	1	0
116.7292	0	1	0	1	0
117.8958	1	0	1	1	1
118.7708	0	1	1	0	0
119.8125	1	0	0	0	1
120.6875	1	1	1	0	0
123.6979	0	1	1	0	1
124.7188	1	0	1	1	0
125.6979	1	0	0	1	1
126.7083	1	0	1	1	1
127.7083	1	0	0	0	1
130.6875	0	0	1	1	0
131.6875	0	1	0	0	1
132.6875	1	0	1	0	1
133.7708	0	1	1	1	0
134.6875	1	0	0	1	0
135.9375	0	1	0	0	1
138.0625	0	0	1	0	0
139.8958	1	0	0	1	0
140.8125	1	1	0	0	1
141.9271	1	1	0	0	0
143.7708	1	0	1	0	0
144.6458	0	1	1	0	1
145.6458	0	1	1	1	1
146.6458	1	1	1	0	0
147.7292	1	0	0	0	1
148.7083	0	1	0	0	0
151.7500	1	1	1	1	1